FUZZY LOGIC GUIDANCE SYSTEM DESIGN FOR GUIDED MISSILES

A THESIS SUBMITTED TO
THE GRADUATE SCHOOL OF NATURAL AND APPLIED SCIENCES
OF
THE MIDDLE EAST TECHNICAL UNIVERSITY

BY

A. ÖZGÜR VURAL

IN PARTIAL FULFILLMENT OF THE REQUIREMENTS FOR THE DEGREE
OF
MASTER OF SCIENCE
IN
THE DEPARTMENT OF MECHANICAL ENGINEERING

SEPTEMBER 2003

Approval of the Graduate School of Natural and Applied Sciences

Prof. Dr. Canan ÖZGEN
Director

I certify that this thesis satisfies all the requirements as a thesis for the degree of Master of Science

Prof. Dr. Kemal İDER
Head of the Department

This is to certify that we have read this thesis and that in our opinion it is fully adequate, in scope and quality, as a thesis for the degree of Master of Science.

Dr. Osman MERTTOPÇUOĞLU
Co.- Supervisor

Prof. Dr. Kemal ÖZGÖREN
Supervisor

Examining Committee Members

Prof. Dr. Samim ÜNLÜSOY _____

Prof. Dr. Kemal ÖZGÖREN _____

Prof. Dr. Tuna BALKAN _____

Dr. Osman MERTTOPÇUOĞLU _____

Prof. Dr. Kemal LEBLEBİCİOĞLU _____

ABSTRACT

FUZZY LOGIC GUIDANCE SYSTEM DESIGN FOR GUIDED MISSILES

VURAL, A. Özgür

M.S., Department of Mechanical Engineering

Supervisor: Prof. Dr. Kemal ÖZGÖREN

Co-Supervisor: Dr. Osman MERTTOPÇUOĞLU

September 2003, 110 pages

This thesis involves modeling, guidance, control, and flight simulations of a canard controlled guided missile.

The autopilot is designed by a pole placement technique. Designed autopilot is used with the guidance systems considered in the thesis.

Five different guidance methods are applied in the thesis, one of which is the famous proportional navigation guidance. The other four guidance methods are different fuzzy logic guidance systems designed considering different types of guidance inputs.

Simulations are done against five different target types and the performances of the five guidance methods are compared and discussed.

Keywords: Missile dynamics, flight simulation, guided missile, guidance and control, missile autopilot, pole placement, fuzzy logic guidance

ÖZ

GÜDÜMLÜ FÜZELER İÇİN BULANIK MANTIK GÜDÜM SİSTEMİ TASARIMI

VURAL, A. Özgür

Yüksek Lisans, Makina Mühendisliği Bölümü

Tez Yöneticisi: Prof. Dr. Kemal ÖZGÖREN

Ortak Tez Yöneticisi: Dr. Osman MERTTOPÇUOĞLU

Eylül 2003, 110 sayfa

Bu tez, ön kanatçık kontrollü bir füzenin modellenmesi, güdümü, kontrolü ve uçuş benzetimi konularını içermektedir.

Otopilot tasarımı bir kutup yerleştirme tekniği kullanılarak yapılmıştır. Tasarlanan otopilot tezde değerlendirilen güdüm sistemleriyle beraber kullanılmıştır.

Tezde, birisi ünlü güdüm yöntemi oransal güdüm olmak üzere beş farklı güdüm yöntemi uygulanmıştır. Oransal güdüm dışındaki dört güdüm yöntemi, farklı güdüm girdileri kullanılarak hazırlanan dört farklı bulanık mantık güdüm yöntemidir.

Benzetimler beş farklı hedef tipine karşı yapılmış ve sonucunda incelenen beş farklı güdüm yöntemi karşılaştırılmış ve tartışılmıştır.

Anahtar kelimeler: Füze dinamiği, uçuş benzetimi, güdümlü füze, güdüm ve kontrol, füze otopilotu, kutup yerleştirme, bulanık mantık güdüm yöntemi

To My Mother, Father and Sister,

Hülya, Hasan and Çiğdem

for their love, support and patience throughout my life...

ACKNOWLEDGEMENTS

I would like to express my sincere thanks and appreciation to my co-supervisor Dr. Osman MERTTOPÇUOĞLU for his support, guidance, understanding and suggestions during the preparation of this thesis.

I would also like to express my thanks to my supervisor Prof. Dr. Kemal ÖZGÖREN for his support, patience and understanding during the study.

My manager Ferda GÜLER is acknowledged for her patience and understanding throughout the study.

TABLE OF CONTENTS

ABSTRACT iii

ÖZ v

ACKNOWLEDGEMENTS viii

TABLE OF CONTENTS ix

LIST OF TABLES xiii

LIST OF FIGURES xiv

LIST OF SYMBOLS xviii

CHAPTER

1 INTRODUCTION 1

2 MATHEMATICAL MODEL OF THE MISSILE 5

2.1 Reference Frames 5

2.1.1 Euler Angles *7*

2.2 Equations of a Rigid Missile 9

2.2.1 Equations of the Mass Center Motion of The Missile *9*

2.2.2 Equations of the Angular Motion of The Missile *11*

2.3 External Forces and Moments Acting on the Missile Body 13

3 AUTOPILOT DESIGN 19

3.1 Simplified Missile Equations 20

3.2 External Forces and Moments 21

3.3 Pitch Autopilot Design 22

3.4 Yaw Autopilot Design 27

4 GUIDANCE DESIGN 30

4.1 Proportional Navigation Guidance 31
4.2 An Overview to Fuzzy Logic 33
4.2.1 Fuzzification *34*
4.2.2 Fuzzy rule-base *36*
4.2.3 Inference mechanism *37*
4.2.4 Defuzzification *38*
4.3 Fuzzy Logic Guidance 39
4.3.1 Fuzzy proportional guidance *45*
4.3.2 Fuzzy proportional derivative guidance *47*
4.3.3 Fuzzy proportional integral guidance *49*
4.3.4 Fuzzy proportional integral derivative guidance *51*
5 SIMULATIONS 55
5.1 Simulation Results for Target One 56
5.1.1 Position plots *57*
5.1.2 Acceleration plots *58*
5.1.3 Canard deflection plots *59*
5.1.4 Performance table *60*
5.2 Simulation Results for Target Two Variation One 60
5.2.1 Position plots *61*
5.2.2 Acceleration plots *62*
5.2.3 Canard deflection plots *63*
5.2.4 Performance table *64*
5.3 Simulation Results for Target Two Variation Two 64
5.3.1 Position plots *65*
5.3.2 Acceleration plots *66*
5.3.3 Canard deflection plots *67*
5.3.4 Performance table *68*
5.4 Simulation Results for Target Two Variation Three 68

5.4.1 Position plots *69*

5.4.2 Acceleration plots *70*

5.4.3 Canard deflection plots *71*

5.4.4 Performance table *72*

5.5 Simulation Results for Target Two Variation Four 72

5.5.1 Position plots *73*

5.5.2 Acceleration plots *74*

5.5.3 Canard deflection plots *75*

5.5.4 Performance table *76*

5.6 Simulation Results for Target Three Variation One 76

5.6.1 Position plots *77*

5.6.2 Acceleration plots *78*

5.6.3 Canard deflection plots *79*

5.6.4 Performance table *80*

5.7 Simulation Results for Target Three Variation Two 80

5.7.1 Position plots *81*

5.7.2 Acceleration plots *82*

5.7.3 Canard deflection plots *83*

5.7.4 Performance table *84*

5.8 Simulation Results for Target Four 84

5.8.1 Position plots *85*

5.8.2 Acceleration plots *86*

5.8.3 Canard deflection plots *87*

5.8.4 Performance table *88*

5.9 Simulation Results for Target Five 88

5.9.1 Position plots *89*

5.9.2 Acceleration plots *90*

5.9.3 Canard deflection plots *91*

5.9.4 Performance table *92*

6 CONCLUSION 93

7 REFERENCES 99

APPENDICES

A PROPERTIES OF THE MISSILE 103

A.1 Missile Geometry 103

A.2 Physical Properties of Missile 104

A.3 Velocity Profile 104

A.4 Saturation Limits of the Missile 105

B TARGET MODELS 106

B.1 Target One 106

B.2 Target Two 106

B.3 Target Three 107

B.4 Target Four 108

B.5 Target Five 109

C SEEKER BOX 110

LIST OF TABLES

TABLE

4.1 Fuzzy rule table example 37

4.2 Rule-base for FPG 45

4.3 Rule-base for FPDG 47

4.4 Rule-base for FPIG 49

4.5 Rule-base for FPIDG for input τ “m1” 51

4.6 Rule-base for FPIDG for input τ “z” 51

4.7 Rule-base for FPIDG for input τ “p1” 52

5.1 Performance table for target one 60

5.2 Performance table for target two with variation one 64

5.3 Performance table for target two with variation two 68

5.4 Performance table for target two with variation three 72

5.5 Performance table for target two with variation four 76

5.6 Performance table for target three with variation one 80

5.7 Performance table for target three with variation two 84

5.8 Performance table for target four 88

5.9 Performance table for target five 92

A.1 Missile velocity profile 105

B.1 Variations of target two 107

B.2 Parameter changes for target four 108

B.3 Z axes velocity profile for target five 109

LIST OF FIGURES

FIGURE

2.1 Earth Axes and Body Axes....6

2.2 Definition of α and β....17

3.1 Autopilot loop....19

3.2 Autopilot block diagram....25

4.1 Guidance Loop....30

4.2 Geometry of planar pursuit of PNG....31

4.3 Fuzzy logic controller architecture....33

4.4 Membership function examples....35

4.5 Min and product implication....39

4.6 PNG and Fuzzy guidance acceleration commands....40

4.7 Membership functions superimposed....42

4.8 Output membership functions for Fuzzy Guidance Systems....44

4.9 Input membership functions for FPG....45

4.10 Output surface for FPG....46

4.11 Input membership functions for $\ddot{\lambda}$ for FPDG....48

4.12 Output surface for FPDG....48

4.13 Input membership functions for τ for FPIG....50

4.14 Output surface for FPIG....50

4.15 Output surface for FPIDG at τ -0.01 rad....53

4.16 Output surface for FPIDG at τ 0 rad. 53

4.17 Output surface for FPIDG at τ 0.01 rad. 54

5.1 Block diagram of the model formed 55

5.2 X vs. Y for target one 57

5.3 X vs. Z for target one 57

5.4 Ayref vs. t for target one 58

5.5 Azref vs. t for target one 58

5.6 Rudder command vs. t for target one 59

5.7 Elevator command vs. t for target one 59

5.8 X vs. Y for target two with variation one 61

5.9 X vs. Z for target two with variation one 61

5.10 Ayref vs. t for target two with variation one 62

5.11 Azref vs. t for target two with variation one 62

5.12 Rudder command vs. t for target two with variation one 63

5.13 Elevator command vs. t for target two with variation one 63

5.14 X vs. Y for target two with variation two 65

5.15 X vs. Z for target two with variation two 65

5.16 Ayref vs. t for target two with variation two 66

5.17 Azref vs. t for target two with variation two 66

5.18 Rudder command vs. t for target two with variation two 67

5.19 Elevator command vs. t for target two with variation two 67

5.20 X vs. Y for target two with variation three 69

5.21 X vs. Z for target two with variation three 69

5.22 Ayref vs. t for target two with variation three 70

5.23 Azref vs. t for target two with variation three 70
5.24 Rudder command vs. t for target two with variation three 71
5.25 Elevator command vs. t for target two with variation three 71
5.26 X vs. Y for target two with variation four 73
5.27 X vs. Z for target two with variation four 73
5.28 Ayref vs. t for target two with variation four 74
5.29 Azref vs. t for target two with variation four 74
5.30 Rudder command vs. t for target two with variation four 75
5.31 Elevator command vs. t for target two with variation four 75
5.32 X vs. Y for target three with variation one 77
5.33 X vs. Z for target three with variation one 77
5.34 Ayref vs. t for target three with variation one 78
5.35 Azref vs. t for target three with variation one 78
5.36 Rudder command vs. t for target three with variation one 79
5.37 Elevator command vs. t for target three with variation one 79
5.38 X vs. Y for target three with variation two 81
5.39 X vs. Z for target three with variation two 81
5.40 Ayref vs. t for target three with variation two 82
5.41 Azref vs. t for target three with variation two 82
5.42 Rudder command vs. t for target three with variation two 83
5.43 Elevator command vs. t for target three with variation two 83
5.44 X vs. Y for target four 85
5.45 X vs. Z for target four 85
5.46 Ayref vs. t for target four 86

5.47 Azref vs. t for target four 86

5.48 Rudder command vs. t for target four 87

5.49 Elevator command vs. t for target four 87

5.50 X vs. Y for target five 89

5.51 X vs. Z for target five 89

5.52 Ayref vs. t for target five 90

5.53 Azref vs. t for target five 90

5.54 Rudder command vs. t for target five 91

5.55 Elevator command vs. t for target five 91

LIST OF SYMBOLS

a^*	reference acceleration input in the body frame
a_z^*	reference acceleration input in z direction in the body frame
a	realized acceleration in the body frame
a_n	normal acceleration command which is perpendicular to the missile velocity vector
an	acceleration of target four
a_{ref}	reference acceleration command
a_z	realized acceleration in z direction in the body frame
A	maximum cross sectional area of the missile
Ayref	reference acceleration command in y axis in the body frame
Azref	reference acceleration command in z axis in the body frame
c	speed of the sound
$\hat{C}^{(e,b)}$	transformation matrix from the body frame to the earth frame
C_i	aerodynamic force and moment coefficients
d	missile diameter

$\vec{F}$	net force vector acting on the missile body
$\overline{F}$	column matrix representation of the net force vector of the missile
F	a fuzzy set named F
F_{ax}, F_{ay}, F_{az}	components of force occurring due to aerodynamic effects acting on the missile in the body frame
F_X, F_Y, F_Z	components of net force acting on the missile body in the body frame
FPDG	fuzzy proportional derivative guidance
FPG	fuzzy proportional guidance
FPIG	fuzzy proportional integral guidance
FPIDG	fuzzy proportional integral derivative guidance
g	gravitational acceleration of the earth
$\overline{g}$	column matrix representation of the gravitational acceleration of the earth
g_x, g_y, g_z	gravitational acceleration components in the body frame
h	altitude of the missile
$\vec{H}$	angular momentum vector of the missile
$\overline{H}$	column matrix representation of the angular momentum vector of the missile
$\hat{I}_C$	inertia matrix of the missile mass center
$\breve{I}_C$	inertia tensor of the missile mass center
I_X, I_Y, I_Z, I_{XY}, I_{XZ}, I_{YZ}	inertia of the missile about the subscripted axes

ka	acceleration gain for target four
K_p, K_i, K_q, K_r, K_δ	autopilot gains
L, M, N	components of moment occurring due to aerodynamic effects acting on the missile in the body frame
L_{ref}	reference missile cross sectional length for aerodynamic calculations
L_T, M_T, N_T	components of moment occurring due to thrust in the body frame
LOS	line of sight
m	mass of the missile
$\vec{M}$	net moment vector acting on the missile body
$\bar{M}$	column matrix representation of the net moment vector
M	Mach number
M_X, M_Y, M_Z	components of net moment acting on the missile in the body frame
N	navigation constant
$p_{1,2,3,4}$	located poles of the characteristic equation
p, q, r	components of angular velocity in the body frame with respect to the earth frame
PNG	proportional navigation guidance
Q_d	dynamic pressure
$\bar{r}$	column matrix representation of a vector

$\bar{r}^{(b)}$	column matrix representation of a vector in the body frame
$\bar{r}^{(e)}$	column matrix representation of a vector in the earth frame
$\hat{R}_i(\theta_k)$	elementary rotation matrix along i^{th} axis by θ_k
R	universal gas constant
R_i	i^{th} rule in the rule-base
S_{ref}	reference missile cross sectional area for aerodynamic calculations
T	temperature
T_0	temperature at sea level
T_x, T_y, T_z	components of the thrust force acting on the missile in the body frame
TOF	time of flight
u, v, w	velocity components of the missile in the body frame
u	an element in the universe of discourse
U	universe of discourse
utarg	speed of target four
vart2	variation parameter for target two
vart3	variation parameter for target three
$\vec{V}_T$	total velocity vector of the missile
$\bar{V}_T$	column matrix representation of the total velocity vector of the missile

V_c	closing velocity of the missile to the target
V_M	missile velocity
V_T	magnitude of the total velocity of the missile
V_T	target velocity
$w_{n1,n2}$	desired natural frequencies for the characteristic equation
X_b, Y_b, Z_b	axes of the body fixed reference frame
X_e, Y_e, Z_e	axes of the earth fixed reference frame
X_t, Y_t, Z_t	coordinates of the target in the earth frame

Greek Letters

α	angle of attack
β	side slip angle
δ_a	aileron deflection
δ_e	elevator deflection
δ_r	rudder deflection
ΔV	cumulative velocity increment
γ	specific heat ratio
$\xi_{1,2}$	desired damping ratios for the characteristic equation
λ	line of sight angle
μ_F	membership function of the fuzzy set *F*
φ , θ , ψ	Euler angles
$\vec{\omega}$	angular velocity vector of the missile

$\bar{\omega}$	column matrix representation of angular velocity vector of the missile
ρ	density of the air
ρ_0	air density at sea level
σ_M	angle between a reference and missile velocity vector
σ_T	angle between a reference and target velocity vector
τ	angle between line of sight and missile velocity vector

CHAPTER 1

INTRODUCTION

There are many types of controllers whose design require complex mathematical models and a lot of labour work to do. At the end of the design, they are said to satisfy the parameters that they are designed to. But any perfect model used at the design stage is at most a model and involves lack of knowledge on the real system to be controlled, which can not be included in the model. So the resulting controller can not give the exact result expected from it, but gives a result which is satisfactory enough.

Fuzzy logic is a controller strategy which does not require a precise model of the system to be controlled, but requires experience on controlling the system. Thus, knowledge from an experienced operator of a control system can be used as a rule-base for the fuzzy logic controller and it can replace the human operator who is in charge of controlling the system. So, a fuzzy logic controller is in a sense like a human in the loop controller, which emulates a human's decision making in the control process.

Because of the mathematical simplicity, and applicability of the fuzzy logic on the systems that the designers have experience in, fuzzy logic controllers found a large area of application. Their area of application comprises simple systems such as water level control of a tank, and complex systems such as the control of a stability augmentation system of an aircraft.

Some examples on the applications of fuzzy logic on flight control are; using fuzzy logic controller and genetic algorithms as a hybrid controller for inner loop stability augmentation of aircraft [1], using fuzzy logic controller and neural networks as a hybrid controller for aircraft antilock brake system [2], and missile control using fuzzy logic with learning capabilities of cerebellar model arithmetic computer neural networks [3].

In this thesis, effectiveness of the fuzzy logic controller is analysed and discussed as a guidance system of a canard controlled missile (see APPENDIX A for missile properties). Four kinds of fuzzy logic guidance systems are designed and the evaluated results through a fuzzy logic guidance system are compared with the famous and widely used guidance law, known as proportional navigation guidance law.

Some examples on the applications of fuzzy logic as a missile guidance law are; evaluating the performances of the famous guidance laws proportional navigation guidance and augmented proportional navigation guidance with fuzzy logic [4], design of a fuzzy logic based optimal guidance law for homing missiles [5], design

of fuzzy logic guidance law against high speed target [6], windshear recovery using fuzzy logic guidance and control [7], adaptive fuzzy gain scheduled guidance system design where fuzzy logic is used as a part of a hybrid guidance system [8], guidance law design by adaptive fuzzy sliding mode control [9]. In most of the given examples, performance of the designed guidance law is compared with the performance of proportional navigation guidance law.

The fuzzy logic guidance system considerations given above considers LOS rate, seeker angle, intercept point angle estimate, target acceleration, missile velocity, closing velocity, missile altitude, and time to go as input parameters to fuzzy logic. In this thesis a new information, the derivative of line of sight rate is considered as an input, and the seeker angle information is used for locating the relative position of the target with respect to the missile velocity vector. All the information considered as inputs to the fuzzy logic are combined in different combinations and the contributions of each information to the missile performance are inspected. Thus, this study makes a contribution to the literature by the information used and by the way that it handles the information.

CHAPTER 2 describes the mathematical model of the missile used to evaluate the simulation results for the applied guidance systems. The equations of motion for a rigid missile are derived and obtained in this chapter.

CHAPTER 3 describes the design of an autopilot, which is used in the simulations together with the guidance systems considered. In this chapter, the necessary

assumptions are made for linearising the equations of motion, and a pole placement technique is used to design the autopilot.

CHAPTER 4 describes the design of the fuzzy logic guidance systems. In this chapter the relevant inputs, selection of input ranges, rule-base formation and membership function selection procedures are described and resulting fuzzy logic guidance systems are introduced.

CHAPTER 5 includes the results of the simulations done by using the designed fuzzy logic guidance systems and proportional navigation guidance law. The simulations are performed against five types of targets and some variations of them. The results are given in plots and tabulated form.

In CHAPTER 6 the results of the simulations, the performances of the guidance methods are discussed and compared.

Information on the missile, target models and the method for evaluating the seeker information are given in the Appendix.

CHAPTER 2

MATHEMATICAL MODEL OF THE MISSILE

The evaluation of missile behavior requires mathematical modeling of the forces acting on the missile body. As more factors that contribute the forces acting on the model are considered, the obtained mathematical model behaves closer to a missile. In this thesis assumptions that reduce the non-linearity of the real missile and simplify the model are introduced as required, and the model is kept as intensive as possible to represent the real missile. The missile under consideration is given in APPENDIX A. Equations of motion of a rigid missile are composed of a set of nonlinear first order differential equations which are defined in the reference frames described below.

2.1 Reference Frames

In this thesis, two reference frames are used to describe the motion of the missile, which are both right handed and orthogonal. Namely, they are the body fixed reference frame and the earth fixed reference frame. Body fixed reference frame is fixed on the missile body. The earth fixed reference frame is fixed on the earth and

can be assumed inertial because the range of the missile is short compared with the radius of the earth and the motion of the missile is much faster compared with the motion of the earth. The axes on the earth fixed reference frame are X_e, Y_e, and Z_e. Z_e points downwards to the center of the earth, X_e point to the initial firing direction of the missile, and Y_e is defined by the orthogonal right hand rule. The axes on the body fixed reference frame are X_b, Y_b, and Z_b. Their origin is at the missile's center of mass. The reference frames and their axes are shown in Figure 2.1.

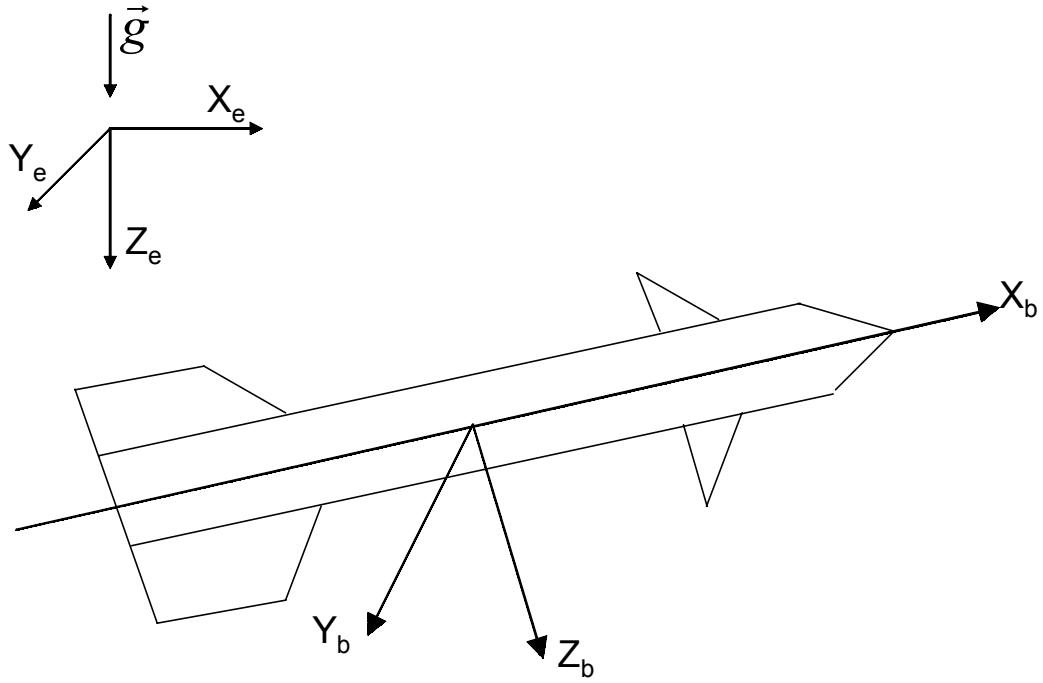

Figure 2.1 Earth Axes and Body Axes

A vector $\vec{r}$ can be expressed by different column matrices in different coordinate frames. The expressions of the same vector in two different coordinate frames can be related to each other by means of the transformation matrix as,

$$\overline{r}^{(e)} = \hat{C}^{(e,b)} \cdot \overline{r}^{(b)} \tag{2.1}$$

The matrix $\hat{C}^{(e,b)}$ is an orthogonal transformation matrix which transforms from body fixed reference frame to earth fixed reference frame. The following properties hold for the transformation matrix,

$$\hat{C}^{(e,b)} = \hat{C}^{(b,e)^{-1}} = \hat{C}^{(b,e)^{T}} \tag{2.2}$$

$\hat{C}^{(e,b)}$ is also named as direction cosine matrix, and in general it is expressed using Euler Angles.

2.1.1 Euler Angles

Transformation between two reference frames can be expressed by successively using the basic rotation matrices that describe rotations about the relevant coordinate axes. In this thesis, and generally in flight mechanics applications, the 3-2-1 transformation sequence is used.

The Euler angles of the 3-2-1 sequence are denoted as, ψ: "yaw angle", θ: "pitch angle", φ: "roll angle". The basic rotation matrices using these Euler angles can be written as,

$$\hat{R}_3(\psi) = \begin{pmatrix} c\psi & -s\psi & 0 \\ s\psi & c\psi & 0 \\ 0 & 0 & 1 \end{pmatrix} \tag{2.3}$$

$$\hat{R}_2(\theta) = \begin{pmatrix} c\theta & 0 & s\theta \\ 0 & 1 & 0 \\ -s\theta & 0 & c\theta \end{pmatrix} \tag{2.4}$$

$$\hat{R}_1(\varphi) = \begin{pmatrix} 1 & 0 & 0 \\ 0 & c\varphi & -s\varphi \\ 0 & s\varphi & c\varphi \end{pmatrix} \tag{2.5}$$

Using the above rotation matrices, the overall transformation matrix can be generated as,

$$\hat{C}^{(e,b)} = \hat{R}_3(\psi) \cdot \hat{R}_2(\theta) \cdot \hat{R}_1(\varphi) \tag{2.6}$$

$$\hat{C}^{(e,b)} = \begin{pmatrix} c\theta c\psi & s\varphi s\theta c\psi - c\varphi s\psi & c\varphi s\theta c\psi + s\varphi s\psi \\ c\theta s\psi & s\varphi s\theta s\psi + c\varphi c\psi & c\varphi s\theta s\psi - s\varphi c\psi \\ -s\theta & s\varphi c\theta & c\varphi c\theta \end{pmatrix} \tag{2.7}$$

2.2 Equations of a Rigid Missile

The equations of motion can be derived from the Newton's Second Law of Motion for rigid bodies. The translational and rotational equations can be written as,

$$\vec{F} = m \cdot \frac{d}{dt}(\vec{V}_T)\Big|_I \tag{2.8}$$

$$\vec{M} = \frac{d}{dt}(\vec{H})\Big|_I \tag{2.9}$$

In these equations, $\vec{F}$ and $\vec{M}$ are the net force and moment acting on the missile body. $\vec{V}_T$ is the mass center velocity and m is the mass of the missile. $\vec{H}$ is the angular momentum of the missile about its mass center, which can be evaluated as $\vec{H} = \breve{I}_C \cdot \vec{\omega}$ where $\breve{I}_C$ is the inertia tensor and $\vec{\omega}$ is the angular velocity vector. $\Big|_I$ indicates that the differentiation is done in an inertial frame.

2.2.1 Equations of the Mass Center Motion of The Missile

Equation (2.8) can be written in the body axes as,

$$\vec{F} = m \cdot \left\{ \frac{d}{dt}(\vec{V}_T)\Big|_B + \vec{\omega} \times \vec{V}_T \right\} \tag{2.10}$$

where $\big|_B$ indicates that the differentiation is done in the body frame. The vectors in (2.10) are expressed in the body frame as,

$$\bar{\omega} = \begin{pmatrix} p \\ q \\ r \end{pmatrix} \tag{2.11}$$

$$\bar{V}_T = \begin{pmatrix} u \\ v \\ w \end{pmatrix} \tag{2.12}$$

$$\bar{F} = \begin{pmatrix} F_X \\ F_Y \\ F_Z \end{pmatrix} \tag{2.13}$$

Using the equations (2.10), (2.11), (2.12), and (2.13), missile body accelerations can be written as,

$$\dot{u} = \frac{F_X}{m} - w \cdot q + v \cdot r \tag{2.14}$$

$$\dot{v} = \frac{F_Y}{m} - u \cdot r + w \cdot p \tag{2.15}$$

$$\dot{w} = \frac{F_Z}{m} - v \cdot p + u \cdot q \tag{2.16}$$

Integrating the equations (2.14), (2.15), and (2.16) simultaneously, the body translational velocities u, v, and w can be evaluated. Using the transformation matrix (2.7), and the body frame components of the translational velocity, the

translational velocity of the missile in the earth fixed reference frame can be evaluated as,

$$\begin{pmatrix} \dot{X}_e \\ \dot{Y}_e \\ \dot{Z}_e \end{pmatrix} = \hat{C}^{(e,b)} \cdot \begin{pmatrix} u \\ v \\ w \end{pmatrix} \tag{2.17}$$

Integrating the velocity components along the earth axes, the coordinates X_e, Y_e, Z_e, of the mass center of the missile in the earth fixed frame can be determined.

2.2.2 Equations of the Angular Motion of The Missile

The inertia matrix of the missile body about its mass center is expressed in the body fixed frame as,

$$\hat{I}_C = \begin{pmatrix} I_X & -I_{XY} & -I_{XZ} \\ -I_{XY} & I_Y & -I_{YZ} \\ -I_{XZ} & -I_{YZ} & I_Z \end{pmatrix} \tag{2.18}$$

Since the missile under consideration is symmetric, I_{XY}, I_{XZ}, I_{YZ} are zero. Thus, the inertia matrix simplifies to,

$$\hat{I}_C = \begin{pmatrix} I_X & 0 & 0 \\ 0 & I_Y & 0 \\ 0 & 0 & I_Z \end{pmatrix} \tag{2.19}$$

Equation (2.9) can be written in the body axes as,

$$\vec{H} = \breve{I}_C \cdot \left\{ \frac{d}{dt}(\vec{\omega}) \Big|_B \right\} + \vec{\omega} \times \breve{I}_C \cdot \vec{\omega} \tag{2.20}$$

The moment vector is expressed in the body frame as,

$$\bar{M} = \begin{pmatrix} M_X \\ M_Y \\ M_Z \end{pmatrix} \tag{2.21}$$

Using the equations (2.11), (2.19), (2.20), and (2.21), missile body angular accelerations can be written as,

$$\dot{p} = \frac{M_X}{I_X} \tag{2.22}$$

$$\dot{q} = \frac{M_Y}{I_Y} + r \cdot p \cdot \frac{(I_Y - I_X)}{I_Y} \tag{2.23}$$

$$\dot{r} = \frac{M_Z}{I_Y} + p \cdot q \cdot \frac{(I_X - I_Y)}{I_Y} \tag{2.24}$$

Integrating the equations (2.22), (2.23), and (2.24) simultaneously, the angular velocity components p, q, r can be evaluated.

On the other hand, the rates of the Euler angles are related to p, q, r as follows [17],

$$\dot{\psi} = \frac{(q \cdot \sin\varphi + r \cdot \cos\varphi)}{\cos\theta} \tag{2.25}$$

$$\dot{\theta} = q \cdot \cos\varphi - r \cdot \sin\varphi \tag{2.26}$$

$$\dot{\varphi} = (q \cdot \sin\varphi + r \cdot \cos\varphi) \cdot \tan\theta + p \tag{2.27}$$

Integrating the Euler angle rates, the angular position of the missile body in the earth fixed frame can be determined.

2.3 External Forces and Moments Acting on the Missile Body

External forces and moments acting on the missile body are due motor thrust, aerodynamic forces, and gravitational forces due to the earth's gravitational acceleration. The forces and moments acting on the missile body can be written as,

$$\bar{F} = \begin{pmatrix} F_{ax} + m \cdot g_x + T_x \\ F_{ay} + m \cdot g_y + T_y \\ F_{az} + m \cdot g_z + T_z \end{pmatrix} \tag{2.28}$$

$$\bar{M} = \begin{pmatrix} L + L_T \\ M + M_T \\ N + N_T \end{pmatrix} \tag{2.29}$$

In the above equations, F_{ax}, F_{ay}, F_{az} and L, M, N are the force and the moment component that occur due to aerodynamic effects. g_x, g_y, and g_z are the components of the gravitational acceleration in the body axes. T_x, T_y, T_z and L_T, M_T, N_T are the

force and moment components that occur due to the motor thrust. In this thesis, missile under consideration does not have a thrust data, and for simplicity and adjustability of the model an equivalent velocity profile is used, which is formed by assuming that the effects of the forces caused by axial thrust and axial drag result in an axial velocity profile given in APPENDIX A. The gravity components can be written as,

$$\begin{pmatrix} g_x \\ g_y \\ g_z \end{pmatrix} = \hat{C}^{(b,e)} \cdot \begin{pmatrix} 0 \\ 0 \\ g \end{pmatrix} \tag{2.30}$$

Aerodynamic forces and moments can be expressed as,

$$\begin{pmatrix} F_{ax} \\ F_{ay} \\ F_{az} \end{pmatrix} = Q_d \cdot A \cdot \begin{pmatrix} C_x \\ C_y \\ C_z \end{pmatrix} \tag{2.31}$$

$$\begin{pmatrix} L \\ M \\ N \end{pmatrix} = Q_d \cdot A \cdot d \cdot \begin{pmatrix} C_l \\ C_m \\ C_n \end{pmatrix} \tag{2.32}$$

In the above equations Q_d is the dynamic pressure, A is the maximum cross sectional area of the missile, and d is the corresponding diameter. The C_i terms are the dimensionless aerodynamic force and moment coefficients. Namely,

C_x : Axial force coefficient

C_y : Side force coefficient

C_z : Normal force coefficient

C_l : Rolling moment coefficient

C_m : Pitching moment coefficient

C_n : Yawing moment coefficient

Dynamic pressure is defined as,

$$Q_d = \frac{1}{2} \cdot \rho \cdot V_T^{\,2} \tag{2.33}$$

where

$$V_T = \sqrt{\left(u^2 + v^2 + w^2\right)} \tag{2.34}$$

ρ is the density of air and changes with altitude as,

$$\rho = \begin{cases} \rho_0 . (1 - 0.00002256.\,h)^{4.256} & \text{for } h \le 10000\text{m.} \\ 0.412.\,e^{-0.000151.(h-10000)} & \text{for } h > 10000\text{m.} \end{cases} \tag{2.35}$$

ρ_0 is the density of the air at sea level and it is equal to 1.223 kg/m^3.

The aerodynamic force and moment coefficients are functions of many parameters, but they are basically dependent on Mach number, which is a dimensionless number defined as,

$$M = \frac{V_T}{c} \tag{2.36}$$

where c is the speed of sound defined as,

$$c = \sqrt{(\gamma \cdot R \cdot T)} \tag{2.37}$$

In the above equation, γ is the specific heat ratio of the air, which is equal to 1.4, R is the universal gas constant, which is equal to 287 J/kg.K, and T is the ambient temperature, which changes with altitude as,

$$T = \begin{cases} T_0 \cdot (1 - 0.00002256 \cdot h) & \text{for } h \le 10000\text{m} \\ 0.7744 \cdot T_0 & \text{for } h > 10000\text{m} \end{cases} \tag{2.38}$$

where T_0 is the temperature at sea level and is equal to 293 K.

During the flight of the missile, some angles are introduced to describe the motion of the missile. These angles are the angle of attack (α), and the side slip angle (β). They are defined as,

$$\alpha = \arctan\left(\frac{w}{u}\right) \tag{2.39}$$

$$\beta = \arcsin\left(\frac{v}{V_T}\right) \tag{2.40}$$

Figure 2.2 also depicts α and β.

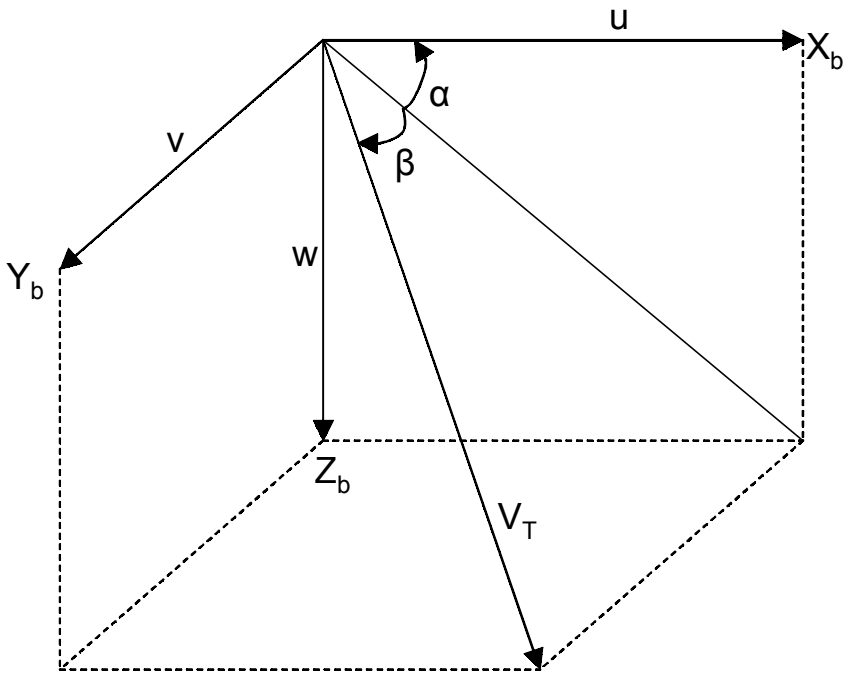

Figure 2.2 Definition of α and β

An aerodynamic coefficient C_i is a function of many flight parameters as,

$$C_i = C_i(M, \alpha, \beta, \delta_a, \delta_e, \delta_r, p, q, r, \dot{\alpha}, \dot{\beta}) \tag{2.41}$$

In this thesis, the aerodynamic coefficients are kept as nonlinear functions of Mach, α, β, δ_e and δ_r and all other flight parameters are taken at the trim value of zero. Missile DATCOM is used for the calculation of the aerodynamic coefficients [18]. In order to use the aerodynamic coefficients in the autopilot design studies, they need to be expressed linearly. So, they are linearised as,

$$C_x = C_{x0} \tag{2.42}$$

$$C_y = C_{y\beta} \cdot \beta + C_{y\delta} \cdot \delta_r + C_{yr} \cdot r \cdot \frac{d}{2 \cdot V_T} \tag{2.43}$$

$$C_z = C_{z\alpha} \cdot \alpha + C_{z\delta} \cdot \delta_e + C_{zq} \cdot q \cdot \frac{d}{2 \cdot V_T} \tag{2.44}$$

$$C_l = C_{l\delta} \cdot \delta_a + C_{lp} \cdot p \cdot \frac{d}{2 \cdot V_T} \tag{2.45}$$

$$C_m = C_{m\alpha} \cdot \alpha + C_{m\delta} \cdot \delta_e + C_{mq} \cdot q \cdot \frac{d}{2 \cdot V_T} \tag{2.46}$$

$$C_n = C_{n\beta} \cdot \beta + C_{n\delta} \cdot \delta_r + C_{nr} \cdot r \cdot \frac{d}{2 \cdot V_T} \tag{2.47}$$

CHAPTER 3

AUTOPILOT DESIGN

There are many kinds of autopilots in use. The autopilot considered in this thesis is an acceleration autopilot, which takes a reference acceleration signal as input and outputs the canard deflection. The autopilot working loop is shown in Figure 3.1.

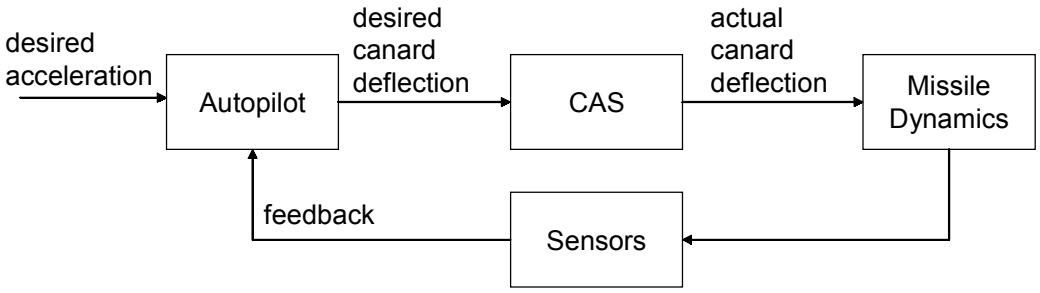

Figure 3.1 Autopilot loop

In this thesis a pitch autopilot and a yaw autopilot are designed for testing the designed guidance system. A roll autopilot design is not considered, but it is assumed that the missile has a fast enough roll autopilot so that it does not make a roll motion throughout the flight.

3.1 Simplified Missile Equations

Since the missile has no roll motion, the equations are simplified. All p and φ terms are taken as zero. Thus, the translational and angular acceleration equations become,

$$\dot{v} = \frac{F_Y}{m} - u \cdot r \tag{3.1}$$

$$\dot{w} = \frac{F_Z}{m} + u \cdot q \tag{3.2}$$

$$\dot{q} = \frac{M_Y}{I_Y} \tag{3.3}$$

$$\dot{r} = \frac{M_Z}{I_Y} \tag{3.4}$$

The Euler angle rates simplify to,

$$\dot{\psi} = \frac{r}{\cos\theta} \tag{3.5}$$

$$\dot{\theta} = q \tag{3.6}$$

The transformation matrix reduces to,

$$\hat{C}^{(e,b)} = \begin{pmatrix} c\theta c\psi & -s\psi & s\theta c\psi \\ c\theta s\psi & c\psi & s\theta s\psi \\ -s\theta & 0 & c\theta \end{pmatrix} \tag{3.7}$$

Further simplifications are needed for the model. Since u is much larger than both v and w, $u \cong V_T$, and the values of the angles α and β are expected to be small, they can be approximated as,

$$\alpha = \frac{w}{u} \tag{3.8}$$

$$\beta = \frac{v}{u} \tag{3.9}$$

Replacing F_Z/m with a_z, F_Y/m with a_y, and solving equations (3.1), (3.2), (3.8), and (3.9) simultaneously a_y and a_z can be evaluated as,

$$a_y = u \cdot (\dot{\beta} + r) \tag{3.10}$$

$$a_z = u \cdot (\dot{\alpha} - q) \tag{3.11}$$

3.2 External Forces and Moments

Remembering the assumptions that the missile has already got a roll autopilot, and the forces due to thrust and drag are included in a given "u" velocity profile, the remaining external forces and moments can be written as,

$$F_y = F_{ay} + m \cdot g_y \tag{3.12}$$

$$F_z = F_{az} + m \cdot g_z \tag{3.13}$$

$$M_Y = M \tag{3.14}$$

$$M_Z = N \tag{3.15}$$

Taking the gravitational effects as external disturbances, all external forces and moments occur due to aerodynamic effects in the model. Replacing the aerodynamic terms with the parameters described in CHAPTER 2, and substituting them into the equations (3.3), (3.4), (3.10), and (3.11) they become,

$$\dot{q} = Q_d \cdot A \cdot d \cdot \left(C_{m\alpha} \cdot \alpha + C_{m\delta} \cdot \delta_e + C_{mq} \cdot q \cdot \frac{d}{2 \cdot V_T} \right) / I_y \tag{3.16}$$

$$\dot{r} = Q_d \cdot A \cdot d \cdot \left(C_{n\beta} \cdot \beta + C_{n\delta} \cdot \delta_r + C_{nr} \cdot r \cdot \frac{d}{2 \cdot V_T} \right) / I_y \tag{3.17}$$

$$\dot{\alpha} = q + Q_d \cdot A \cdot \left(C_{z\alpha} \cdot \alpha + C_{z\delta} \cdot \delta_e + C_{zq} \cdot q \cdot \frac{d}{2 \cdot V_T} \right) / (m \cdot u) \tag{3.18}$$

$$\dot{\beta} = -r + Q_d \cdot A \cdot \left(C_{y\beta} \cdot \beta + Cy \cdot \delta_r + C_{yr} \cdot r \cdot \frac{d}{2 \cdot V_T} \right) / (m \cdot u) \tag{3.19}$$

3.3 Pitch Autopilot Design

The pitch autopilot will control the missile so that it obeys the acceleration command in the pitch plane, which is the x-z plane of the body frame. For notational convenience, it is appropriate to introduce the following symbols,

$$Z_{\alpha} = \frac{Q_d \cdot A}{m} \cdot C_{z\alpha} \tag{3.20}$$

$$Z_{\delta} = \frac{Q_d \cdot A}{m} \cdot C_{z\delta} \tag{3.21}$$

$$Z_q = \frac{Q_d \cdot A}{m} \cdot \left(\frac{d}{2 \cdot V_T} \right) \cdot C_{zq} \tag{3.22}$$

$$M_{\alpha} = \frac{Q_d \cdot A \cdot d}{I_y} \cdot C_{m\alpha} \tag{3.23}$$

$$M_{\delta} = \frac{Q_d \cdot A \cdot d}{I_y} \cdot C_{m\delta} \tag{3.24}$$

$$M_q = \frac{Q_d \cdot A \cdot d}{I_y} \cdot \left(\frac{d}{2 \cdot V_T} \right) \cdot C_{mq} \tag{3.25}$$

Using these symbols, the equations (3.16), and (3.18) can be rewritten as,

$$\dot{\alpha} = \frac{Z_{\alpha}}{u} \cdot \alpha + \left(\frac{Z_q}{u} + 1 \right) \cdot q + \frac{Z_{\delta}}{u} \cdot \delta_e \tag{3.26}$$

$$\dot{q} = M_{\alpha} \cdot \alpha + M_q \cdot q + M_{\delta} \cdot \delta_e \tag{3.27}$$

Equations (3.11), and (3.26) lead to,

$$a_z = Z_{\alpha} \cdot \alpha + Z_q \cdot q + Z_{\delta} \cdot \delta_e \tag{3.28}$$

Equation (3.28) can be solved for α, and it can be differentiated in order to obtain the following equations,

$$\alpha = \frac{1}{Z_\alpha} \cdot \left(a_z - Z_q \cdot q - Z_\delta \cdot \delta_e \right) \tag{3.29}$$

$$\dot{a}_z = Z_\alpha \cdot \dot{\alpha} + Z_q \cdot \dot{q} + Z_\delta \cdot \dot{\delta}_e \tag{3.30}$$

Solving equations (3.26), (3.27), (3.29), and (3.30) simultaneously for $\dot{a}_z$ and $\dot{q}$, the equations for them are obtained as,

$$\begin{aligned} \dot{a}_z = & \left(\frac{Z_\alpha}{u} + \frac{Z_q \cdot M_\alpha}{Z_\alpha} \right) \cdot a_z + \left(Z_\alpha + Z_q \cdot M_q - \frac{{Z_q}^2 \cdot M_\alpha}{Z_\alpha} \right) \cdot q \\ & + \left(Z_q \cdot M_\delta - \frac{Z_\delta \cdot Z_q \cdot M_\alpha}{Z_\alpha} \right) \cdot \delta_e + Z_\delta \cdot \dot{\delta}_e \end{aligned} \tag{3.31}$$

$$\dot{q} = \frac{M_\alpha}{Z_\alpha} \cdot a_z + \left(M_q - \frac{Z_q \cdot M_\alpha}{Z_\alpha} \right) \cdot q + \left(M_\delta - \frac{Z_\delta \cdot M_\alpha}{Z_\alpha} \right) \cdot \delta_e \tag{3.32}$$

Taking the laplace transforms of the equations (3.31) and (3.32), they can be solved to give the transfer functions,

$$a_z(s) = \frac{Z_\delta \cdot s^2 + \left(Z_q \cdot M_\delta - M_q \cdot Z_\delta \right) \cdot s + \left(M_\delta \cdot Z_\alpha - Z_\delta \cdot M_\alpha \right)}{s^2 - \left(M_q + \frac{Z_\alpha}{u} \right) \cdot s + \left(\frac{Z_\alpha}{u} \cdot M_q - M_\alpha \cdot \left(\frac{Z_q}{u} + 1 \right) \right)} \delta_e(s) \tag{3.33}$$

$$q(s) = \frac{M_\delta \cdot s + \left(\frac{Z_\delta \cdot M_\alpha}{u} - \frac{M_\delta \cdot Z_\alpha}{u} \right)}{s^2 - \left(M_q + \frac{Z_\alpha}{u} \right) \cdot s + \left(\frac{Z_\alpha}{u} \cdot M_q - M_\alpha \cdot \left(\frac{Z_q}{u} + 1 \right) \right)} \delta_e(s) \tag{3.34}$$

For the sake of brevity, these equations can be represented as follows,

$$a_z(s) = \frac{N_{11} \cdot s^2 + N_{12} \cdot s + N_{13}}{s^2 + D_2 \cdot s + D_3} \delta_e(s) \tag{3.35}$$

$$q(s) = \frac{N_{22} \cdot s + N_{23}}{s^2 + D_2 \cdot s + D_3} \delta_e(s) \tag{3.36}$$

This system can be controlled by means of an autopilot presented in Figure 3.2, which is similar to the one in [16].

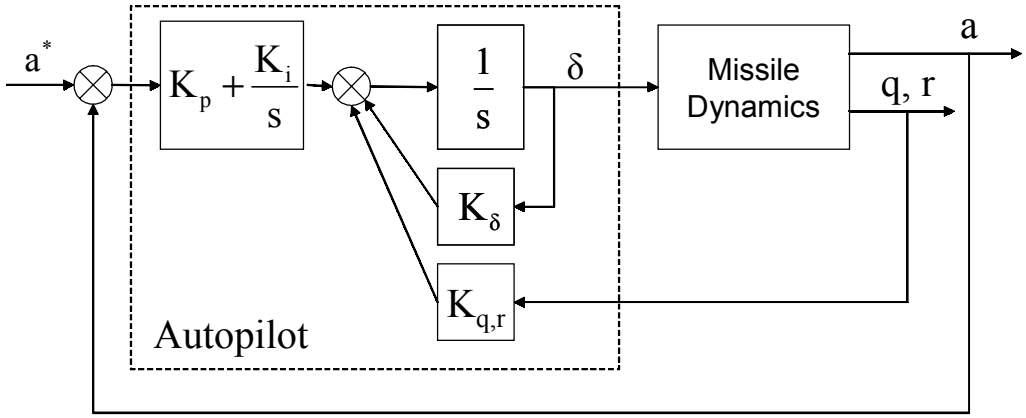

Figure 3.2 Autopilot block diagram

Applying block diagram algebra, the transfer function of the autopilot can be solved as,

$$\frac{a_z(s)}{a_z^*(s)} = \frac{K_p \cdot N_{11} \cdot s^3 + (K_i \cdot N_{11} + K_p \cdot N_{12}) \cdot s^2 + (K_i \cdot N_{12} + K_p \cdot N_{13}) \cdot s + K_i \cdot N_{13}}{s^4 + (D_2 - K_\delta + K_p \cdot N_{11}) \cdot s^3 + (K_p \cdot N_{12} + D_3 + K_i \cdot N_{11} - K_\delta \cdot D_2 - K_q \cdot N_{22}) \cdot s^2 + (-K_\delta \cdot D_3 + K_p \cdot N_{13} - K_q \cdot N_{23} + K_i \cdot N_{12}) \cdot s + K_i \cdot N_{13}} \tag{3.37}$$

or

$$\frac{a_z(s)}{a_z^*(s)} = \frac{\Delta_n(s)}{\Delta_d(s)} \tag{3.38}$$

In order to get stable system with a fast response guaranteed by the pole locations, let the characteristic polynomial be,

$$\begin{aligned}\Delta_d(s) &= \left(s^2 + 2\xi_1 w_{n1} + {w_{n1}}^2\right)\cdot\left(s^2 + 2\xi_2 w_{n2} + {w_{n2}}^2\right) \\ &= s^4 + 2\left(\xi_1 w_{n1} + \xi_2 w_{n2}\right)s^3 + \left({w_{n1}}^2 + {w_{n2}}^2 + 4\xi_1\xi_2 w_{n1} w_{n2}\right) \\ &\quad + 2w_{n1}w_{n2}\left(\xi_1 w_{n2} + \xi_2 w_{n1}\right)s + {w_{n1}}^2 \cdot {w_{n2}}^2\end{aligned} \tag{3.39}$$

or for simplicity,

$$\Delta_d(s) = s^4 + E_1 \cdot s^3 + E_2 \cdot s^2 + E_3 \cdot s + E_4 \tag{3.40}$$

With the above characteristic equation, the poles are placed to,

$$p_{1,2} = -w_{n1}\left(\xi_1 \pm j\sqrt{1-{\xi_1}^2}\right) \tag{3.41}$$

$$p_{3,4} = -w_{n2}\left(\xi_2 \pm j\sqrt{1-{\xi_2}^2}\right) \tag{3.42}$$

Equating the denominator of (3.37) to (3.39), the autopilot gains can be evaluated as,

$$K_p = \frac{E_3 - N_{12}\frac{E_4}{N_{13}} - D_3E_1 + D_2D_3 + \frac{N_{23}}{N_{22}}\left(\frac{E_4N_{11}}{N_{13}} + D_3 + D_2E_1 - {D_2}^2 - E_2\right)}{N_{13} - D_3N_{11} - \frac{N_{23}}{N_{22}}\left(N_{12} - D_2N_{11}\right)} \tag{3.43}$$

$$K_i = \frac{E_4}{N_{13}} \tag{3.44}$$

$$K_\delta = N_{11}K_p - E_1 + D_2 \tag{3.45}$$

$$K_q = K_p\frac{N_{12} - D_2N_{11}}{N_{22}} + \frac{1}{N_{22}}\left(\frac{E_4N_{11}}{N_{13}} + D_3 + D_2E_1 - {D_2}^2 - E_2\right) \tag{3.46}$$

3.4 Yaw Autopilot Design

Yaw autopilot will control the missile so that it obeys the acceleration command in the yaw plane, which is the x-y plane in body frame. For notational convenience, it is appropriate to introduce the following symbols,

$$Y_\beta = \frac{Q_d \cdot A}{m} \cdot C_{y\beta} \tag{3.47}$$

$$Y_\delta = \frac{Q_d \cdot A}{m} \cdot C_{y\delta} \tag{3.48}$$

$$Y_r = \frac{Q_d \cdot A}{m} \cdot \left(\frac{d}{2 \cdot V_T}\right) \cdot C_{yr} \tag{3.49}$$

$$N_\beta = \frac{Q_d \cdot A \cdot d}{I_y} \cdot C_{n\beta} \tag{3.50}$$

$$N_\delta = \frac{Q_d \cdot A \cdot d}{I_y} \cdot C_{n\delta} \tag{3.51}$$

$$N_r = \frac{Q_d \cdot A \cdot d}{I_y} \cdot \left(\frac{d}{2 \cdot V_T} \right) \cdot C_{nr} \tag{3.52}$$

Using these symbols, the equations (3.17), and (3.19) can be rewritten as,

$$\dot{\beta} = \frac{Y_\beta}{u} \cdot \beta + \left(\frac{Y_r}{u} - 1 \right) \cdot r + \frac{Y_\delta}{u} \cdot \delta_r \tag{3.53}$$

$$\dot{r} = N_\beta \cdot \beta + N_r \cdot r + N_\delta \cdot \delta_r \tag{3.54}$$

Equations (3.10), and (3.53) lead to,

$$a_y = Y_\beta \cdot \beta + Y_r \cdot r - Y_\delta \cdot \delta_r \tag{3.55}$$

Equation (3.55) can be solved for β, and it can be differentiated in order to obtain the following equations,

$$\beta = \frac{1}{Y_\beta} \cdot \left(a_y + Y_\delta \cdot \delta_r - Y_r \cdot r \right) \tag{3.56}$$

$$\dot{a}_y = Y_\beta \cdot \dot{\beta} + Y_r \cdot \dot{r} - Y_\delta \cdot \dot{\delta}_r \tag{3.57}$$

Solving equations (3.53), (3.54), (3.56), and (3.57) simultaneously for $\dot{a}_y$ and $\dot{r}$ the equations for them are obtained as,

$$\dot{a}_y = \left(\frac{Y_\beta}{u} + \frac{Y_r \cdot N_\beta}{Y_\beta} \right) \cdot a_y + \left(Y_r \cdot N_r - Y_\beta - \frac{Y_r^{\,2} \cdot N_\beta}{Y_\beta} \right) \cdot \dot{r} + \left(\frac{2 \cdot Y_\beta \cdot Y_\delta}{u} + \frac{Y_r \cdot N_\beta \cdot Y_\delta}{Y_\beta} \right) \cdot \delta_r - Y_\delta \cdot \dot{\delta}_r \tag{3.58}$$

$$\dot{r} = \frac{N_\beta}{Y_\beta} \cdot a_y + \left(N_r - \frac{Y_r \cdot N_\beta}{Y_\beta} \right) \cdot \dot{r} + \left(\frac{N_\beta \cdot Y_\delta}{Y_\beta} + N_\delta \right) \cdot \delta_r \tag{3.59}$$

Taking the laplace transforms of the equations (3.58) and (3.59), they can be solved to give the transfer functions,

$$a_y(s) = \frac{Y_\delta \cdot s^2 + \left(Y_r \cdot N_\delta - N_r \cdot Y_\delta \right) \cdot s + \left(N_\beta \cdot Y_\delta - Y_\beta \cdot N_\delta \right)}{s^2 - \left(N_r + \frac{Y_\beta}{u} \right) \cdot s + \left(\frac{Y_\beta}{u} \cdot N_r - N_\beta \cdot \left(\frac{Y_r}{u} - 1 \right) \right)} \delta_r(s) \tag{3.60}$$

$$r(s) = \frac{N_\delta \cdot s + \left(\frac{N_\beta \cdot Y_\delta}{u} - \frac{Y_\beta \cdot N_\delta}{u} \right)}{s^2 - \left(N_r + \frac{Y_\beta}{u} \right) \cdot s + \left(\frac{Y_\beta}{u} \cdot N_r - N_\beta \cdot \left(\frac{Y_r}{u} - 1 \right) \right)} \delta_r(s) \tag{3.61}$$

The autopilot used for the pitch autopilot is used for the yaw autopilot as well, and the associated pole placement is done in the same way.

CHAPTER 4

GUIDANCE DESIGN

Guidance is the unit that drives the missile. Getting information about the missile and the target, guidance decides what to do to get to the target. Figure 4.1 depicts the guidance loop of the missile. A good guidance system is the system that can hit different types of targets, with minimum control effort, at minimum time, through the minimum flight path.

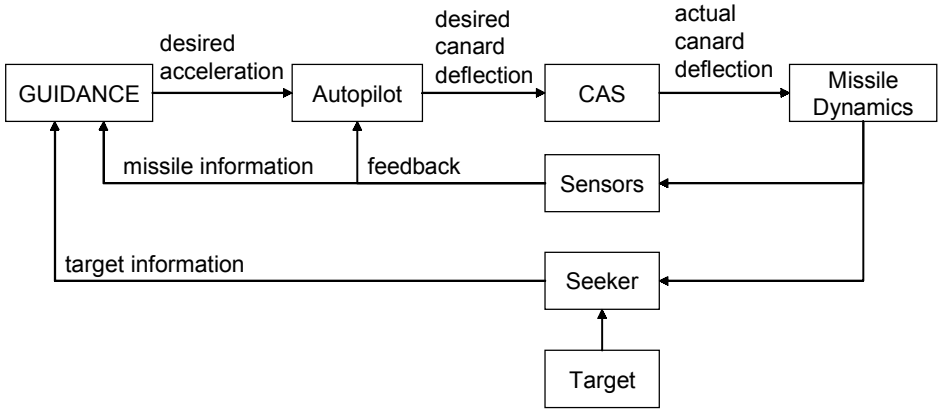

Figure 4.1 Guidance Loop

There are many types of targets such as stationary targets, constant speed targets, accelerating targets, highly maneuvering targets. Guidance design highly depends

on the intended target type and mission of the missile. In this thesis, a canard controlled, surface to air missile is considered, and guidance is done separately in pitch and yaw planes. Fuzzy logic guidance is designed to fill in the guidance box in the Figure 4.1. The aim of the designed fuzzy guidance is to make improvements on the well known and commonly used guidance system named Proportional Navigation Guidance (PNG).

4.1 Proportional Navigation Guidance

Many of the currently operational guided missiles employ proportional navigation guidance as the guidance law. In this strategy, the missile turning rate is controlled to be proportional to the turn rate of the line of sight (LOS) from the missile to the target. For an aerodynamically controlled missile, the PNG law may be considered as the optimal pursuit strategy in the sense of minimizing the terminal miss distance [11]. The geometry of the planar pursuit for the PNG is shown in Figure 4.2.

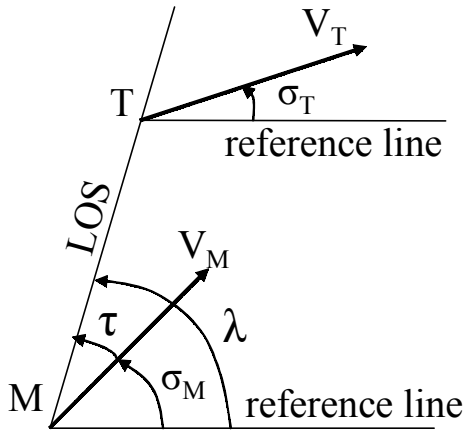

Figure 4.2 Geometry of planar pursuit of PNG

In Figure 4.2 consider T as the target and M as the missile in a plane moving with constant speeds V_T and V_M, respectively, which is the assumption made during the evaluation of the PNG law. The line MT from the missile to the target is the LOS which is inclined at an angle λ with respect to the reference line. λ is also known as LOS angle. The missile velocity V_M makes an angle σ_M with the reference line. The PNG law is defined as [12], [13], [14], [15],

$$a_n = N \cdot \dot{\lambda} \cdot V_c \tag{4.1}$$

where a_n is the commanded normal acceleration, and V_c is the closing velocity of the missile to the target. Since the term V_c can not be known during the flight of a missile, it is estimated as V_M, which is the total velocity of the missile. The term N is the navigation constant and is usually set to a reasonable value between 2 and 4, based on experience [15]. In this thesis N is selected to be 3, which is a general choice.

4.2 An Overview to Fuzzy Logic

Before going on to the fuzzy logic guidance design, for convenience, some of the basic concepts of fuzzy logic are summarized, [10]. The fuzzy logic controller architecture is shown in Figure 4.3.

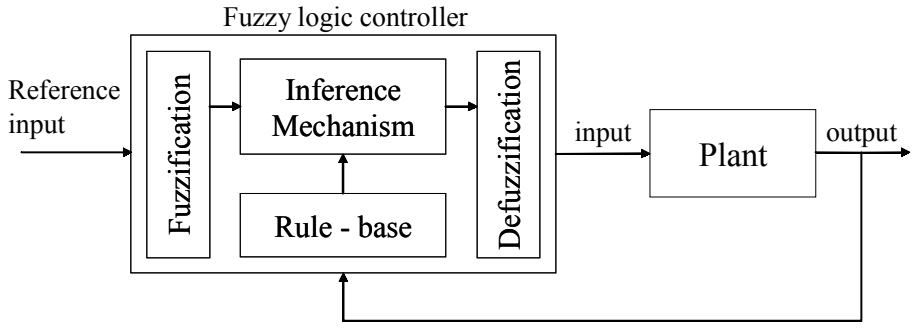

Figure 4.3 Fuzzy logic controller architecture

As it is depicted in the Figure 4.3, a fuzzy logic controller is composed of four elements,

- *A fuzzification interface,* which converts controller inputs into information that the inference mechanism can easily use.
- *A rule-base,* which contains the expert's description on how to achieve a good control.
- *An inference mechanism,* which emulates the expert's decision making in applying knowledge to control the plant.
- *A defuzzification interface,* which converts the conclusions of the inference mechanism into the outputs of the controller.

4.2.1 Fuzzification

In this step, the fuzzy logic controller takes input variables and maps them to membership function values in particular fuzzy sets. Understanding the process requires knowing the definitions of fuzzy set and membership function.

The fuzzy sets are defined as,

$$F = \{u \in U \mid \mu_F(u) \in [0,1]\} \tag{4.2}$$

where μ_F is called the membership function of the fuzzy set F, u is an element in the universe of discourse U, which is the input domain of the fuzzy set F. Membership function performs a mapping,

$$\mu_F : U \to [0,1], u \to \mu_F(u) \tag{4.3}$$

from the universe of discourse U into the fuzzy set F. A membership value of zero indicates that the element is not a member of the set F. A membership value of one indicates that the element is fully a member of the set. A value between zero and one indicates that a fuzzy relation exists between the element and the fuzzy set. A membership function can have any shape, that is, any mathematical expression that satisfies with the definition of a function, [10]. Some of the common membership functions are shown in Figure 4.4.

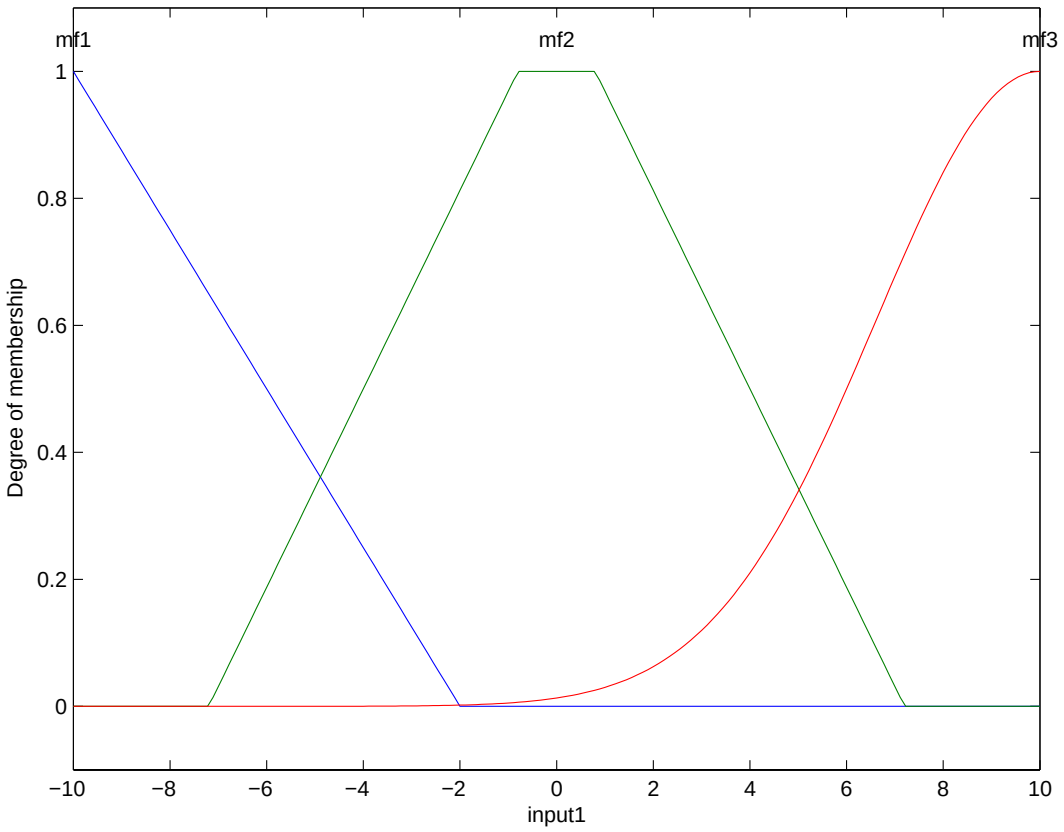

Figure 4.4 Membership function examples

The horizontal axis of the Figure 4.4 represents an input named input1, and the vertical axis represents the degree of membership, which is the membership function value. Plotted membership functions cover different range of values of input1. There are three membership functions shown, which are triangular, trapezoidal, and Gaussian, those belong to the fuzzy sets mf1, mf2, and mf3, respectively. The fuzzy sets mf1, mf2 and mf3 could also be named as “negative”, “zero” and “positive”, respectively.

4.2.2 Fuzzy rule-base

The rule-base is composed of a set of rules, which are linguistic combinations of the inputs to produce the outputs. The rules are simple if-then statements formed by the expert's description such as,

If x is A_1 and y is B_1 then z is C_1

Where x and y are the input variables and A_1 and B_1 are the input fuzzy sets, and z is an output variable with the output fuzzy set C_1. This rule could also be written in a linguistically more descriptive way such as,

If "error" is "negative-small" and "change-in-error" is "negative-large" then "force" is "positive-large"

For a two input, one output system, rule-base formed by linguistic descriptions like the above rule can be tabulated as in Table 4.1.

Table 4.1 Fuzzy rule table example

"force" z		"change-in-error" y				
		-2	-1	0	1	2
"error" x	-1	2	2	1	0	-1
	0	2	1	0	-1	-2
	1	1	0	-1	-2	-2

where "force" is the output, "error" and "change-in-error" are the inputs and terms like "-2", "0" and "1" are linguistic descriptions of fuzzy sets.

4.2.3 Inference mechanism

Inference mechanism is the mechanism that evaluates each fired rule of the fuzzy controller. Consider a rule R_1,

R_1: If x is A_1 and y is B_1 then z is C_1

R_1 can be defined as a fuzzy set implication as,

$$\mu_{R_1} = \left[\mu_{A_1}(x) \text{ and } \mu_{B_1}(y)\right] \rightarrow \mu_{C_1}(z) \tag{4.4}$$

R_1 is considered to be a fired rule if $\mu_{A_1}(x) > 0$ and $\mu_{B_1}(y) > 0$. The evaluation of the rule R_1 requires the evaluation of the implication $z = \mu_{A_1}(x)$ and $\mu_{B_1}(y)$, to give z as an input to the output membership function $\mu_{C_1}(z)$ of the fuzzy set C_1. The implication to be evaluated is connected by a statement "and". There are two common methods for evaluating the statement "and", which are correlation-min and correlation-product. They can respectively be written as,

$$\left[\mu_{A_1}(x) \text{ and } \mu_{B_1}(y)\right] = \min\left\{\mu_{A_1}(x), \mu_{B_1}(y)\right\} \tag{4.5}$$

$$\left[\mu_{A_1}(x) \text{ and } \mu_{B_1}(y)\right] = \mu_{A_1}(x) \cdot \mu_{B_1}(y) \tag{4.6}$$

where equation (4.5) returns the minimum of $\mu_{A_1}(x)$ or $\mu_{B_1}(y)$, and the equation (4.6) returns the algebraic product $\mu_{A_1}(x) \cdot \mu_{B_1}(y)$. The process is done for each fired rule.

4.2.4 Defuzzification

Defuzzification is the process of evaluating the outputs of the inference mechanism. Most commonly used defuzzification method is the center of gravity (COG) defuzzification. Defuzzification depends on the implication used. Figure 4.5 shows the effect of the used implication on the output membership functions.

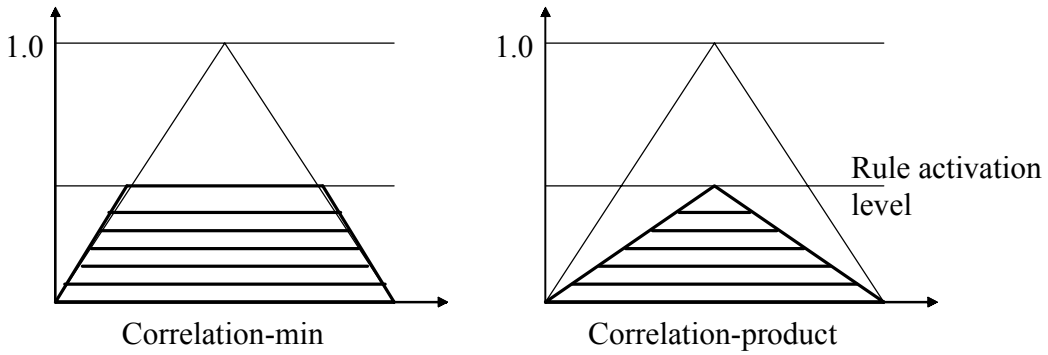

Figure 4.5 Min and product implication

Correlation-min simply results with a "chop off the top" while correlation-product results in the "shrinking" of the triangular membership function. COG defuzzification is defined as,

$$\text{COG} = \frac{\int y \cdot \mu_F(y)\, dy}{\int \mu_F(y)\, dy} \tag{4.7}$$

which is simply the moment of area of the fired rule outputs about the origin, divided by the total area of the fired rule outputs. The area used here is the shaded area in the Figure 4.5.

4.3 Fuzzy Logic Guidance

Fuzzy Logic Guidance is basically the implementation of the fuzzy logic controller to activate the guidance in the missile. The linguistic values and the decision

making process through a rule-base of a fuzzy controller is utilized to generate the reference acceleration that the autopilot requires.

In this chapter, four different types of fuzzy logic guidance are designed. They are fuzzy proportional guidance (FPG), fuzzy proportional derivative guidance (FPDG), fuzzy proportional-integral guidance (FPIG), and fuzzy proportional-integral-derivative guidance (FPIDG). They are named for the inputs they take. The FPG takes the LOS rate ($\dot{\lambda}$) as input. FPDG guidance takes $\dot{\lambda}$ and the derivative of the LOS rate ($\ddot{\lambda}$) as input. FPIG takes $\dot{\lambda}$ and angle between LOS and missile velocity vector (τ) as input. FPIDG guidance takes $\dot{\lambda}$, $\ddot{\lambda}$, and τ as input.

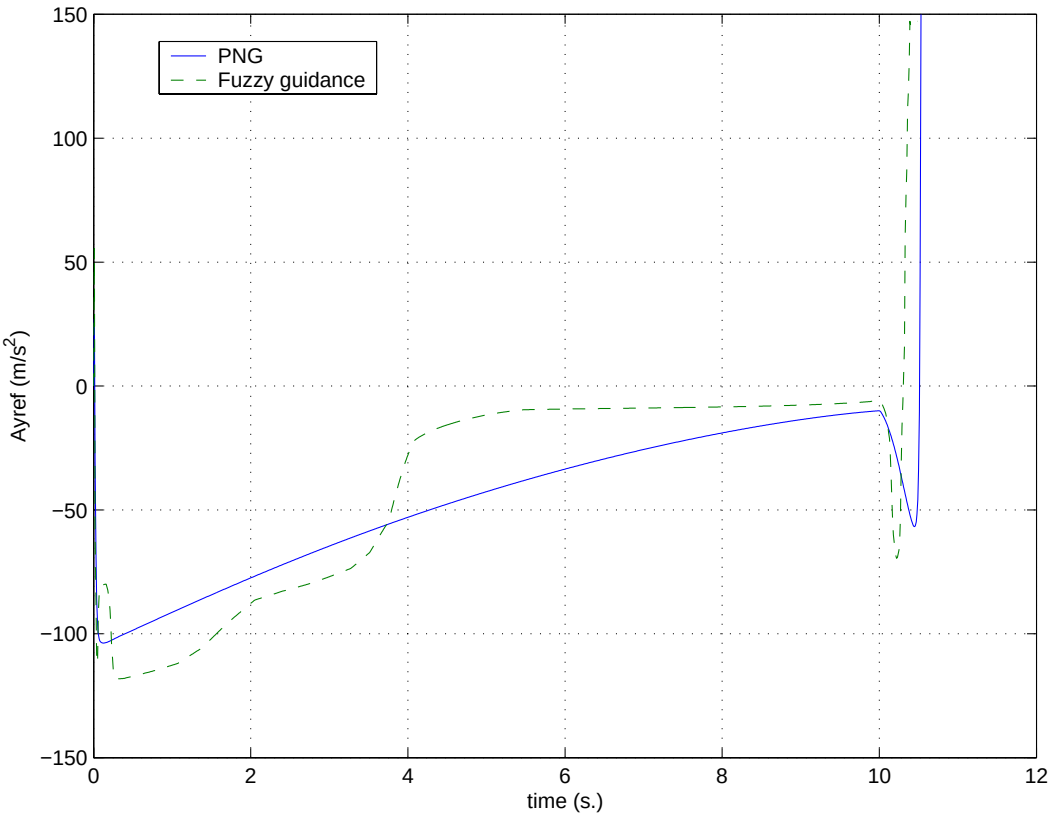

Figure 4.6 PNG and Fuzzy guidance acceleration commands

As one of the cases of the simulations given in CHAPTER 5, Figure 4.6 shows the reference accelerations commanded by PNG and one of the fuzzy logic guidance systems. They are the acceleration commands generated for a target traveling at a constant speed, which is known as a classical PNG target. Details of this simulation are given in CHAPTER 5. As it is seen in Figure 4.6, PNG gives an initial high acceleration command which decreases linearly with $\dot{\lambda}$. That is the characteristic of PNG. If a guidance system is designed which turns the missile to the target with a high initial command kept constant for some time and then lowers the command, it will be advantageous for further acceleration demands caused by possible high maneuvers of the target. The behavior of the fuzzy guidance in Figure 4.6 is similar to the explained behavior. In order to evaluate that behavior, acceleration outputs of the designed fuzzy logic guidance systems must be as high as possible. Without altering the rule-base, that can be done by generating the highest possible fuzzification result for the defuzzification process. For this reason, correlation-min "and" implication is selected, which generates a higher implication result than correlation-product. Consider Figure 4.7.

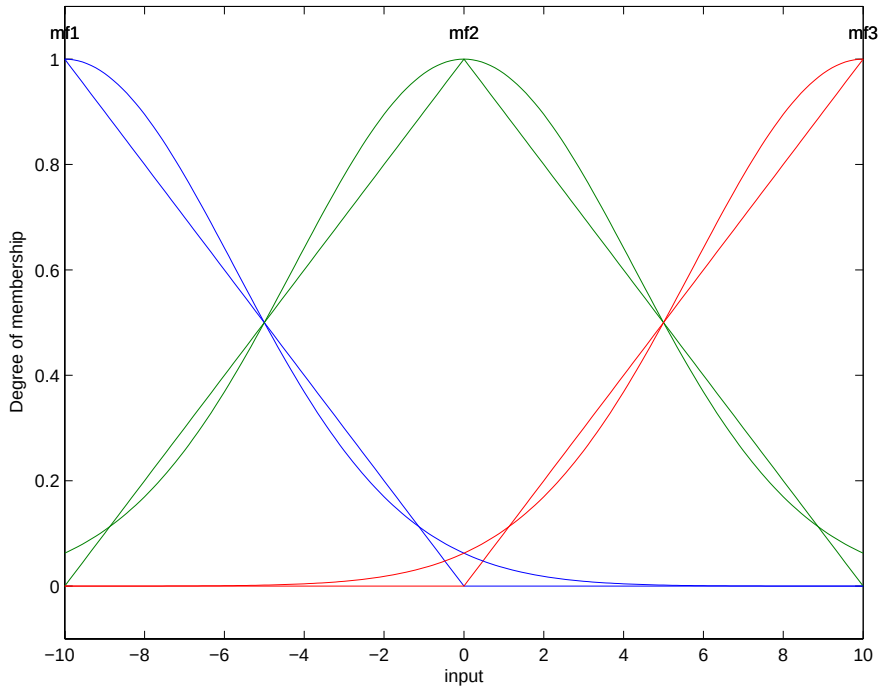

Figure 4.7 Membership functions superimposed

In the Figure 4.7 uniformly distributed Gaussian and triangular membership functions are superimposed. Gaussian membership function gives a higher membership value for the values about the center, and provides more overlap which causes more rules to be fired. Thus, the acceleration output is increased without manipulating the rule-base. For this reason, in the designed fuzzy guidance systems, correlation-min is used for implication "and", and Gaussian membership function is used for input variables. Deciding the ranges of the input membership functions is also essentially important. The input ranges of the input membership functions are decided through a trial and error process which is done by running simulations and tuning the input range. The input range is tuned in order to give a non-oscillatory control response and in order to maximize the acceleration output.

Ranges of the input variables are initially selected from the values in the simulations that use PNG. They are finalized after tuning in the simulations that use fuzzy logic guidance.

All of the designed fuzzy guidance systems use the same linguistic descriptions. They are,

"m4" : stands for minus 4

"m3" : stands for minus 3

"m2" : stands for minus 2

"m1" : stands for minus 1

"z" : stands for zero

"p1" : stands for plus 1

"p2" : stands for plus 2

"p3" : stands for plus 3

"p4" : stands for plus 4

Output membership functions for all of the designed fuzzy logic guidance systems are the same. They are shown in Figure 4.8.

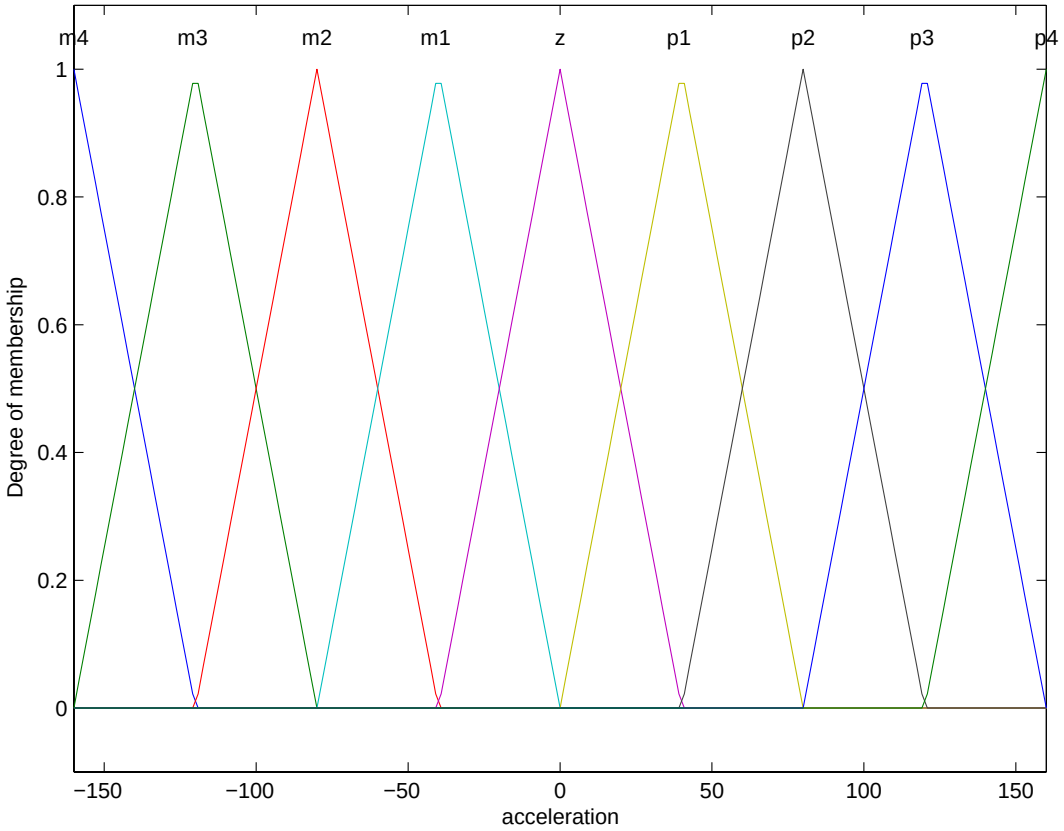

Figure 4.8 Output membership functions for Fuzzy Guidance Systems

Triangular membership functions are used for output fuzzy sets, since the use of Gaussian membership functions in the output fuzzy sets does not have an advantage on increasing the output acceleration commands.

4.3.1 Fuzzy proportional guidance

FPG takes $\dot{\lambda}$ as input, just like PNG does. Rule-base for the FPG is tabulated as,

Table 4.2 Rule-base for FPG

Acceleration	$\dot{\lambda}$								
	m4	m3	m2	m1	z	p1	p2	p3	p4
	m4	m3	m2	m1	z	p1	p2	p3	p4

As $\dot{\lambda}$ gets bigger or smaller, acceleration output gets bigger or smaller. $\dot{\lambda}$ is implied through the membership functions shown in Figure 4.9.

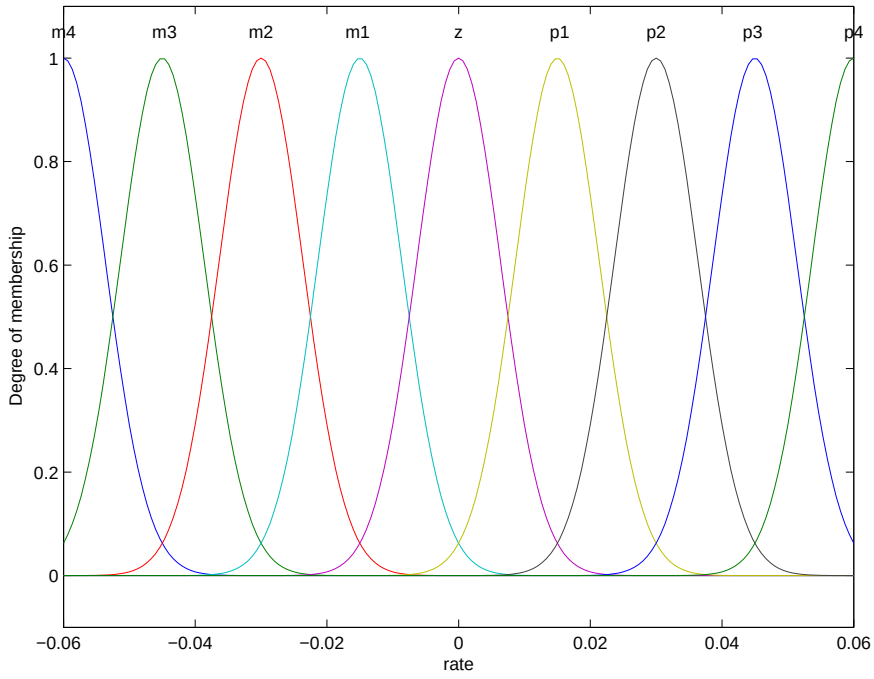

Figure 4.9 Input membership functions for FPG

The acceleration output of the FPG can be plotted with respect to its input as in Figure 4.10.

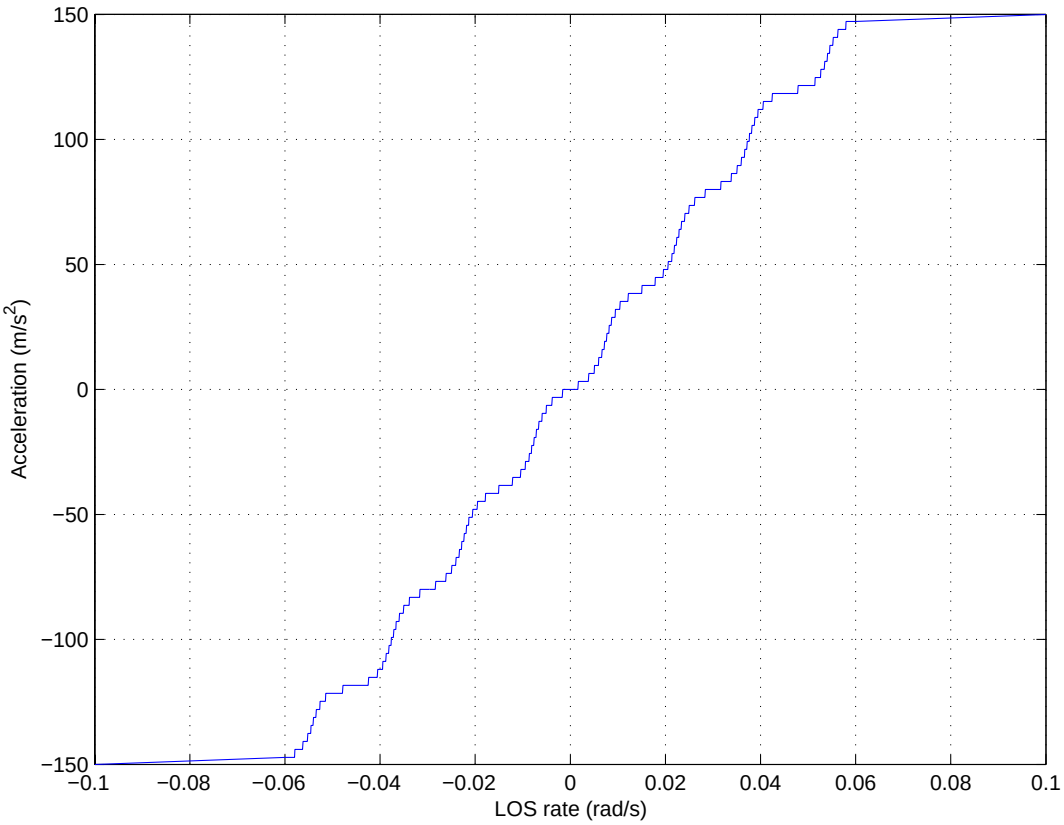

Figure 4.10 Output surface for FPG

The output surface can be considered as a look-up table of output value for the FPG.

4.3.2 Fuzzy proportional derivative guidance

FPDG takes $\dot{\lambda}$ and $\ddot{\lambda}$ as inputs. PNG law only uses $\dot{\lambda}$ information in order to generate acceleration output. It does not use the deceleration or acceleration information of the LOS rate. By using the acceleration and deceleration information, FPDG applies "greater" acceleration output if the target is accelerating, and "smaller" acceleration output if the target is decelerating. The rule-base of the FPDG is tabulated as,

Table 4.3 Rule-base for FPDG

Acceleration		$\dot{\lambda}$								
		m4	m3	m2	m1	z	p1	p2	p3	p4
$\ddot{\lambda}$	m1	m4	m4	m3	m2	z	p1	p1	p2	p3
	z	m4	m3	m2	m1	z	p1	p2	p3	p4
	p1	m3	m2	m1	m1	z	p2	p3	p4	p4

The membership functions for $\dot{\lambda}$ input of FPDG are the same as those for the FPG shown in Figure 4.9. The membership functions for $\ddot{\lambda}$ input are shown in Figure 4.11.

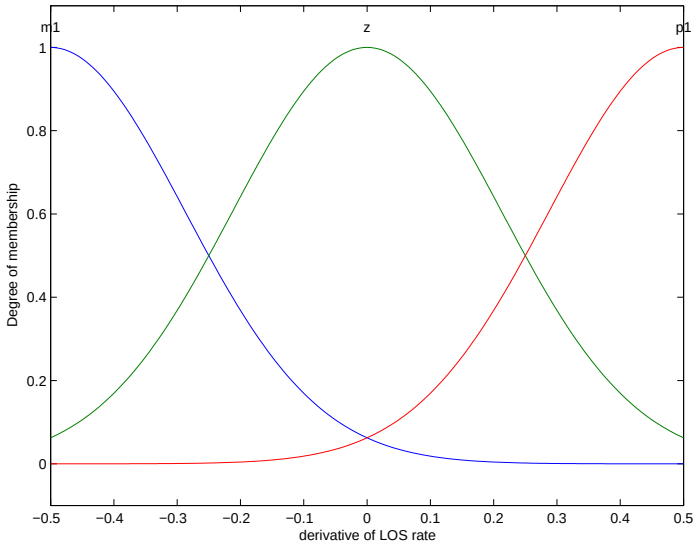

Figure 4.11 Input membership functions for $\ddot{\lambda}$ for FPDG

The acceleration output of the FPDG can be plotted with respect to its inputs as in Figure 4.12, which can be considered as a look-up table for FPDG.

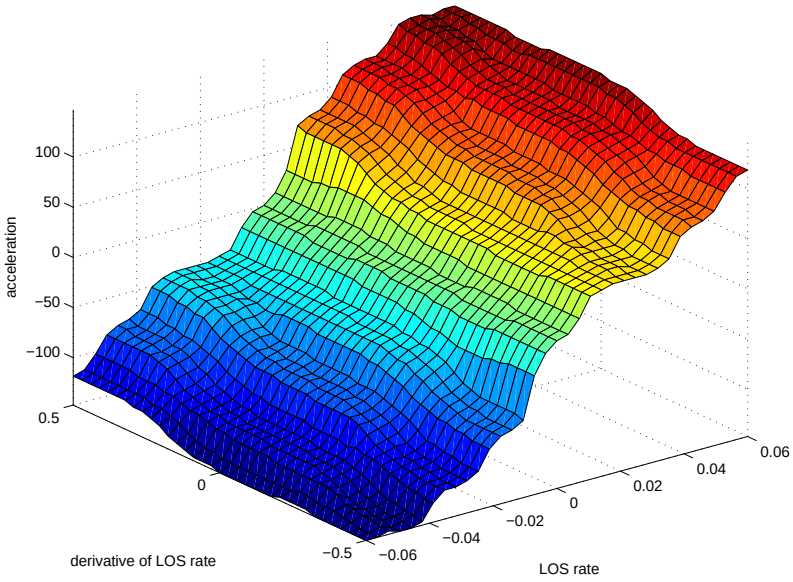

Figure 4.12 Output surface for FPDG

4.3.3 Fuzzy proportional integral guidance

FPIG takes $\dot{\lambda}$ and τ as input. τ gives the relative position information of the target. As PNG does, fuzzy guidance also heads the missile to the rendezvous point where the impact would occur. If the target is on the right and is moving towards left, FPIG does not make any modifications, because it can not know how close the σ_M direction to the intercept point is. But, if the target is on the right and is moving towards left, FPIG applies "greater" acceleration output to head the missile to the rendezvous point, since obviously σ_M direction is looking at far behind the intercept point. The rule-base of the FPIG is tabulated as,

Table 4.4 Rule-base for FPIG

Acceleration		$\dot{\lambda}$								
		m4	m3	m2	m1	z	p1	p2	p3	p4
τ	m1	m4	m4	m3	m2	z	p1	p2	p3	p4
	z	m4	m3	m2	m1	z	p1	p2	p3	p4
	p1	m4	m3	m2	m1	z	p2	p3	p4	p4

The membership functions for $\dot{\lambda}$ of the FPIG are the same as those for the FPG and FPDG shown in Figure 4.9. The membership functions for τ input are shown in Figure 4.13.

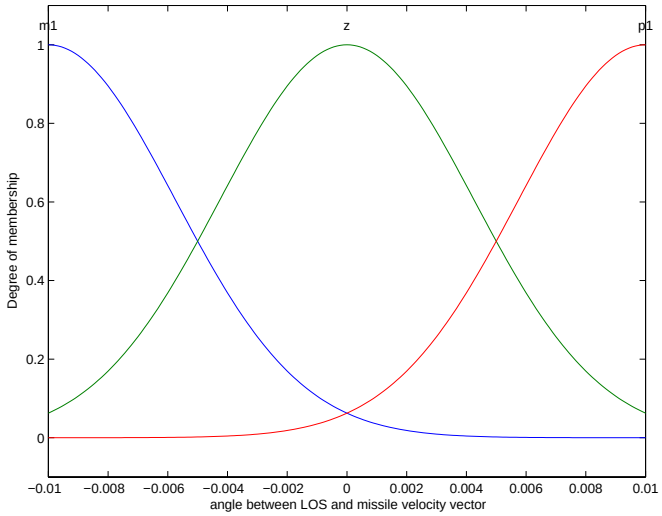

Figure 4.13 Input membership functions for τ for FPIG

The acceleration output of the FPDG can be plotted with respect to its inputs as in Figure 4.14, which can be considered as a look-up table for FPDG.

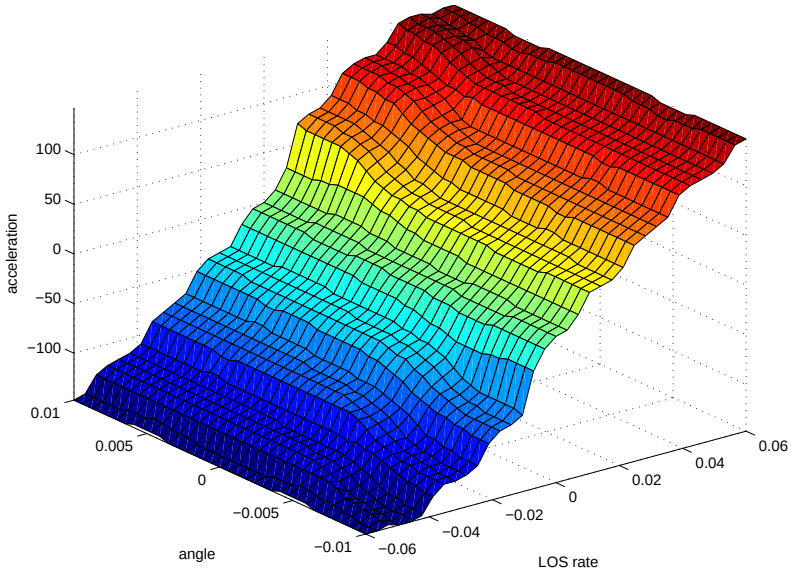

Figure 4.14 Output surface for FPIG

4.3.4 Fuzzy proportional integral derivative guidance

FPIDG takes $\dot{\lambda}$, $\ddot{\lambda}$, and τ as inputs. FPIDG uses all the information that the previously designed fuzzy guidance systems in this chapter uses. FPIDG combines these information to give an acceleration output command. The rule-base of the FPIDG is a three dimensional table. So it can not be given in a single table. It is divided into three tables for input τ values of "m1", "z" and "p1", which are tabulated in Table 4.5, Table 4.6, and Table 4.7, respectively.

Table 4.5 Rule-base for FPIDG for input τ "m1"

Acceleration		$\dot{\lambda}$								
		m4	m3	m2	m1	z	p1	p2	p3	p4
$\ddot{\lambda}$	m1	m4	m4	m4	m3	z	p1	p1	p2	p3
	z	m4	m4	m3	m2	z	p1	p2	p3	p4
	p1	m4	m3	m2	m1	z	p2	p3	p4	p4

Table 4.6 Rule-base for FPIDG for input τ "z"

Acceleration		$\dot{\lambda}$								
		m4	m3	m2	m1	z	p1	p2	p3	p4
$\ddot{\lambda}$	m1	m4	m4	m3	m2	z	p1	p1	p2	p3
	z	m4	m3	m2	m1	z	p1	p2	p3	p4
	p1	m3	m2	m1	m1	z	p2	p3	p4	p4

Table 4.7 Rule-base for FPIDG for input τ "p1"

Acceleration		$\dot{\lambda}$								
		m4	m3	m2	m1	z	p1	p2	p3	p4
$\ddot{\lambda}$	m1	m4	m4	m3	m2	z	p1	p2	p3	p4
	z	m4	m3	m2	m1	z	p2	p3	p4	p4
	p1	m3	m2	m1	m1	z	p3	p4	p4	p4

The membership functions for $\dot{\lambda}$ input of FPIDG are the same as those for the fuzzy guidance systems FPG, FPDG, and FPIG, and they are as shown in Figure 4.9. The membership functions for $\ddot{\lambda}$ input are the same as those for FPDG and they are shown in Figure 4.11. The membership functions for τ input are the same as those for FPIG and they are shown in Figure 4.13.

FPIDG has three inputs and one output, so it can be defined in four dimensional space, but for visualization in three dimensional space, some slices at certain τ input values can be taken. The output surfaces for τ input values at -0.01 radians, 0 radians, and 0.01 radians are plotted in Figure 4.15, Figure 4.16, and Figure 4.17, respectively.

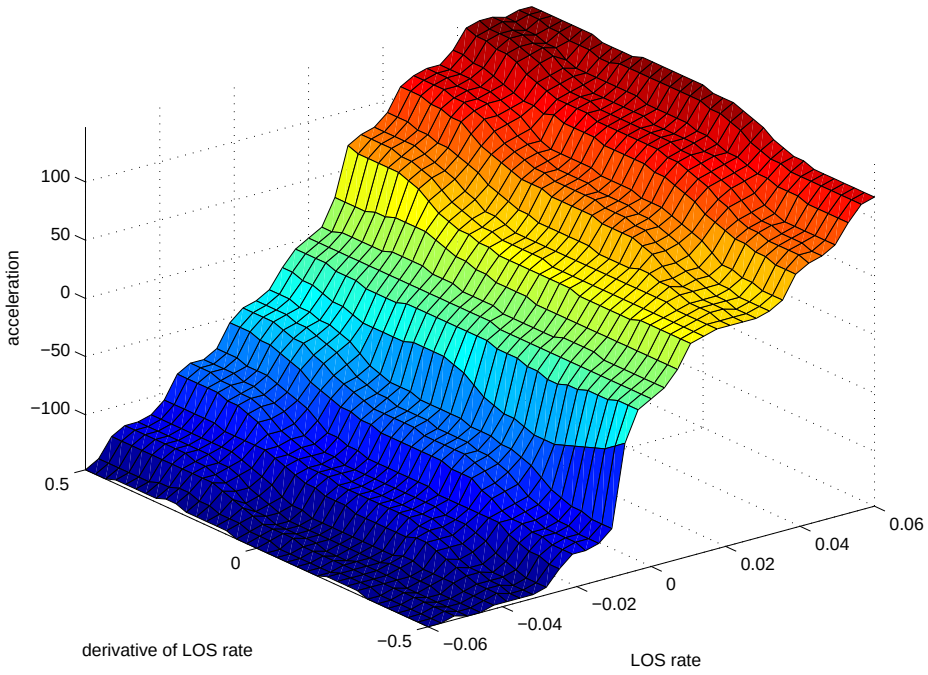

Figure 4.15 Output surface for FPIDG at τ -0.01 rad.

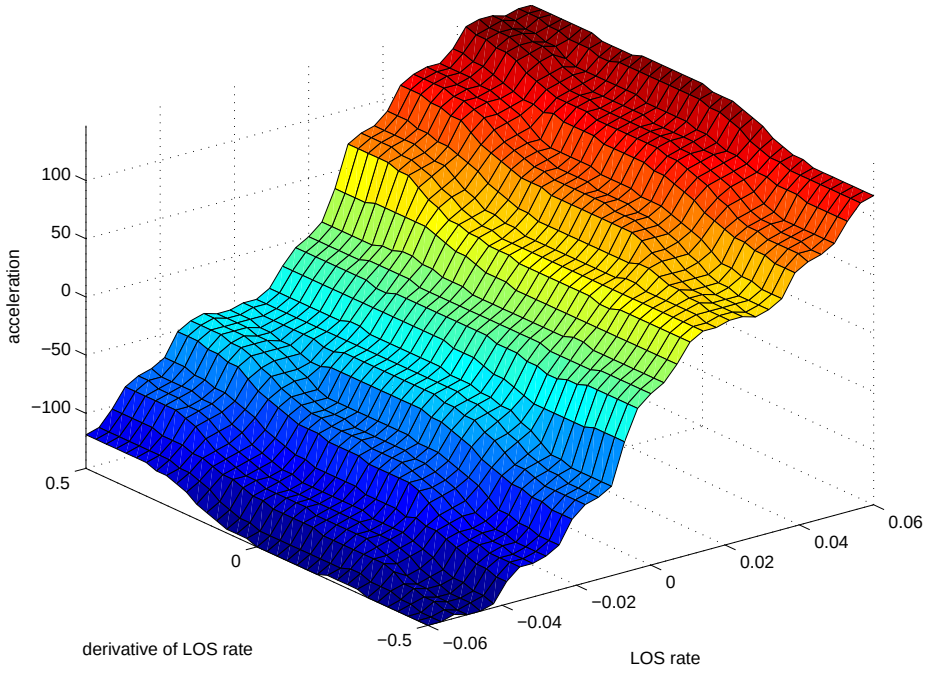

Figure 4.16 Output surface for FPIDG at τ 0 rad.

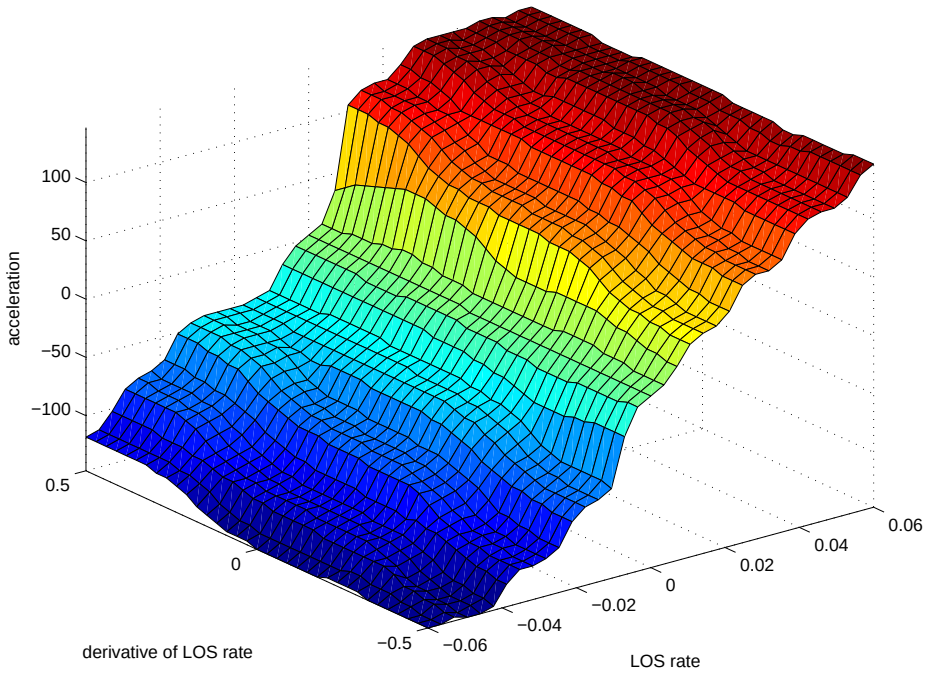

Figure 4.17 Output surface for FPIDG at τ 0.01 rad.

CHAPTER 5

SIMULATIONS

The six degree of freedom simulations are done for the PNG and the four fuzzy logic guidance systems designed in CHAPTER 4 for different types of targets. The simulations are performed with a model formed on Matrix-X, Systembuild the block diagram of which is given in Figure 5.1.

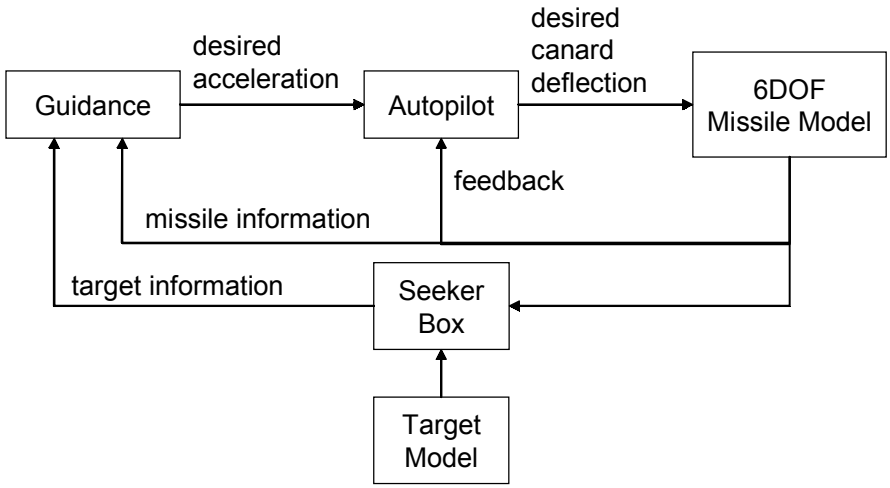

Figure 5.1 Block diagram of the model formed

During the simulations, missile is assumed to have saturation limits described in APPENDIX A. The target models used are explained in detail in APPENDIX B, and the seeker box is explained in detail in APPENDIX C.

The performances of the guidance systems are compared in this chapter. The main performance parameter is the hit/miss result of the simulation. The secondary performance parameters are hit/miss distance, time of flight (TOF) until hit/miss, and the control effort used. The control effort is defined as [13],

$$\Delta V = \int_0^{TOF} \left| a_{ref}(t) \right| dt \tag{5.1}$$

where ΔV is the cumulative velocity increment and a_{ref} is the reference acceleration command.

Simulations results are given in subsections as position plots, acceleration plots, canard deflection plots, and performance table. Position plots are the superimposed X vs. Y and X vs. Z plots for the target and the missile guided with the five guidance methods. Acceleration plots are the superimposed plots of reference acceleration commands vs. time for five guidance methods. Canard deflection commands are the superimposed plots of δ_r vs. time and δ_e vs. time for five guidance methods. And the performance table is the tabulated form of the performance results of the guidance methods for the simulated target type.

5.1 Simulation Results for Target One

Target one is a target moving horizontally with a constant speed, which is also known as classical proportional navigation target (see APPENDIX B.1 for details).

5.1.1 Position plots

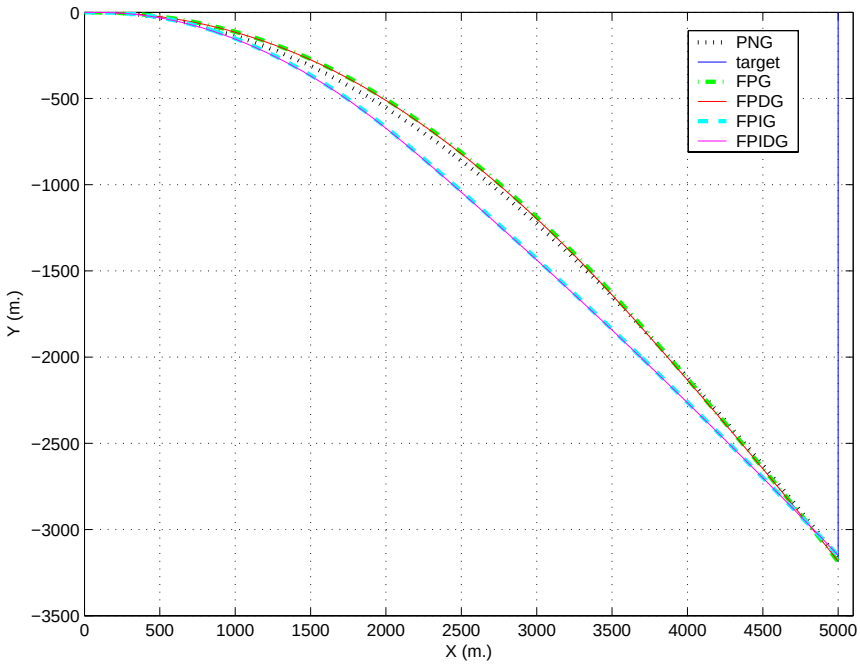

Figure 5.2 X vs. Y for target one

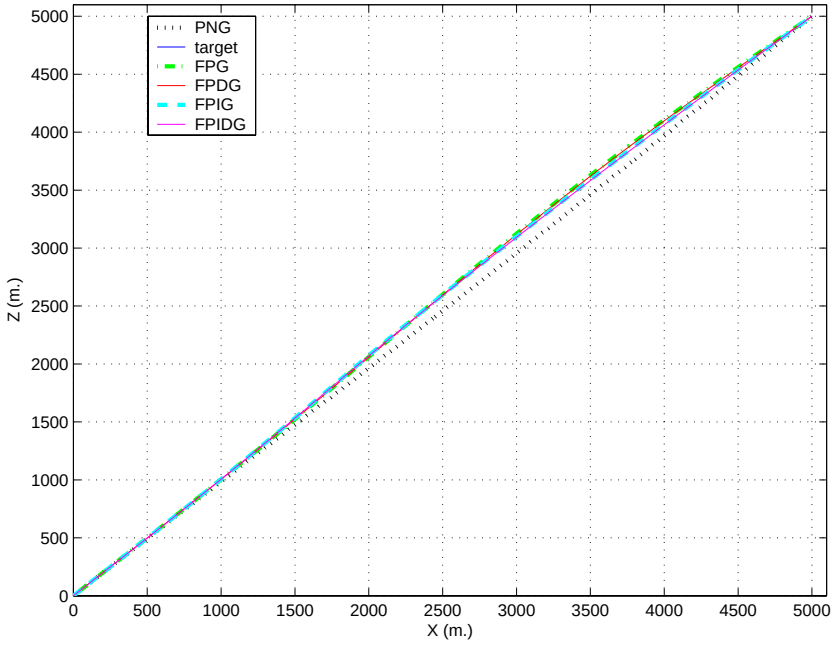

Figure 5.3 X vs. Z for target one

5.1.2 Acceleration plots

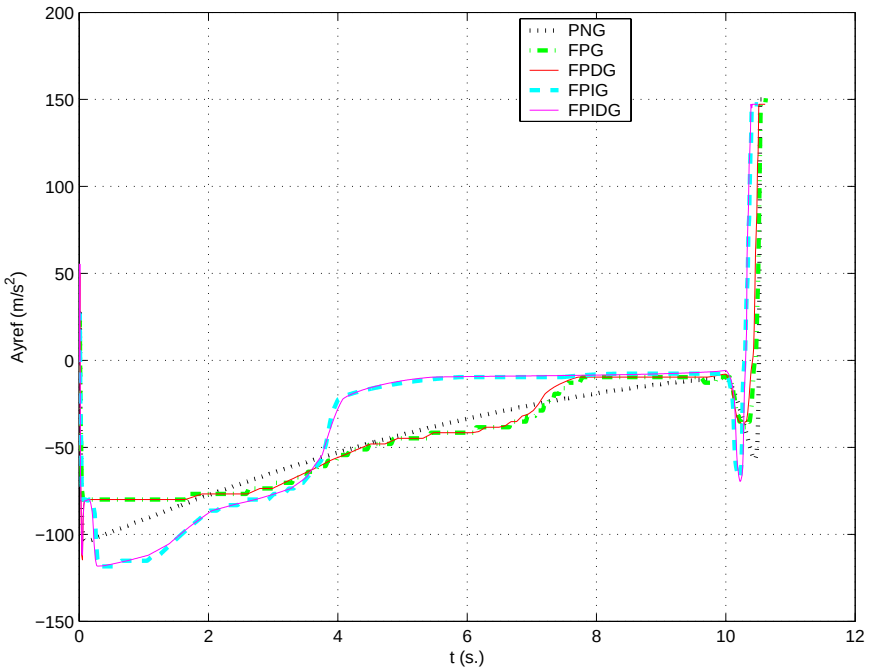

Figure 5.4 Ayref vs. t for target one

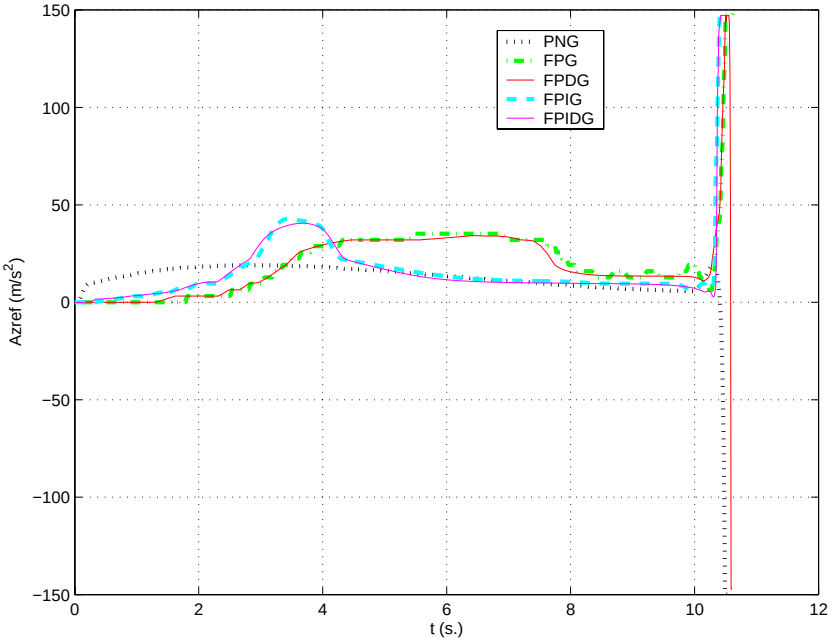

Figure 5.5 Azref vs. t for target one

5.1.3 Canard deflection plots

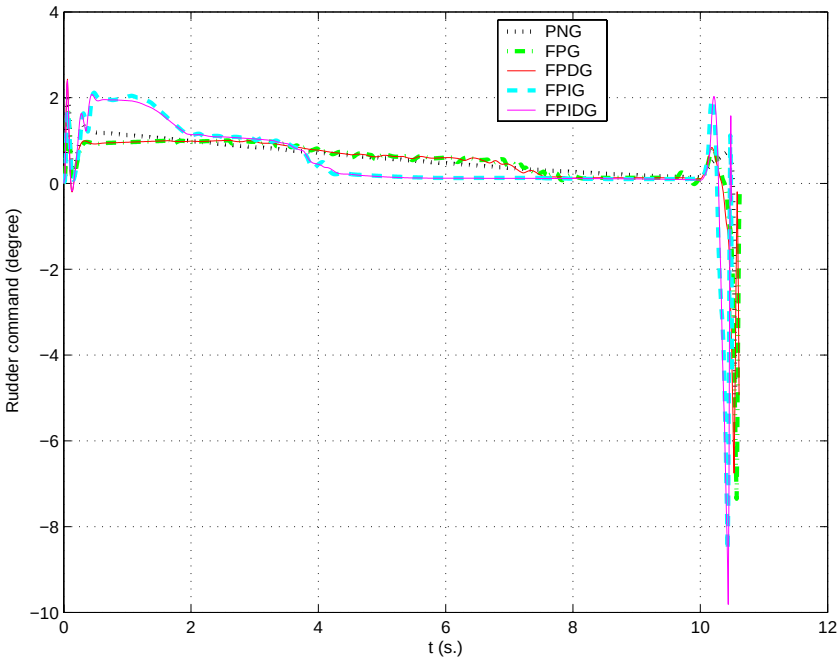

Figure 5.6 Rudder command vs. t for target one

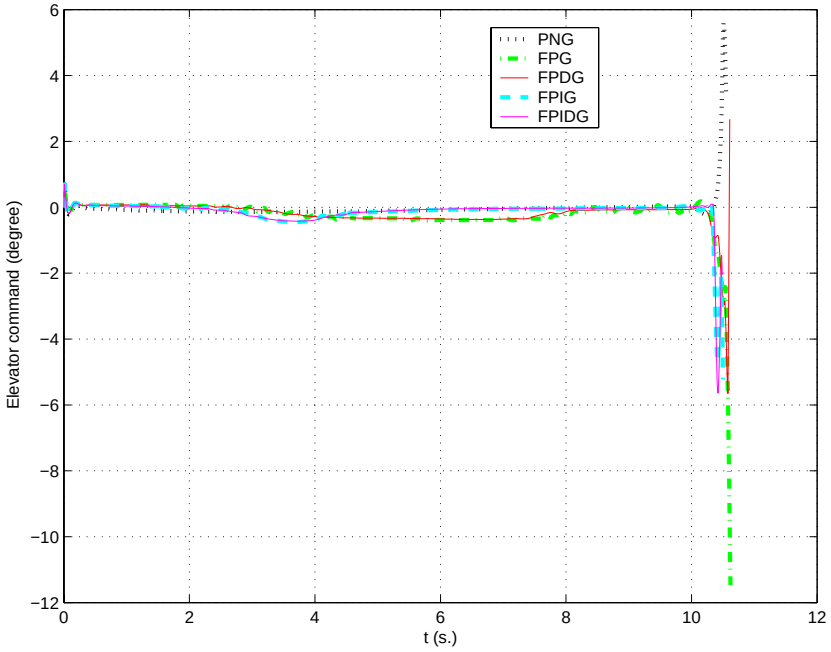

Figure 5.7 Elevator command vs. t for target one

5.1.4 Performance table

Table 5.1 Performance table for target one

Guidance method	hit/miss	Min. distance (m.)	TOF (s.)	Control effort (m/s)		
				A_{yref}	A_{zref}	Total
PNG	hit	***0.211***	10.552	487.542	***138.075***	625.617
FPG	hit	1.092	10.618	478.067	202.824	680.891
FPDG	hit	1.008	10.61	476.475	197.888	674.363
FPIG	hit	1.150	10.498	427.192	150.047	577.239
FPIDG	hit	0.884	***10.494***	***423.428***	143.906	***567.334***

All of the guidance methods hit the target. The minimum result in a column is printed in bold italic.

5.2 Simulation Results for Target Two Variation One

Target two is a target accelerating parabolically in XY plane. It is trying to pass over the missile. Simulation results in this section are given for target two with variation one (see APPENDIX B.2 for details).

5.2.1 Position plots

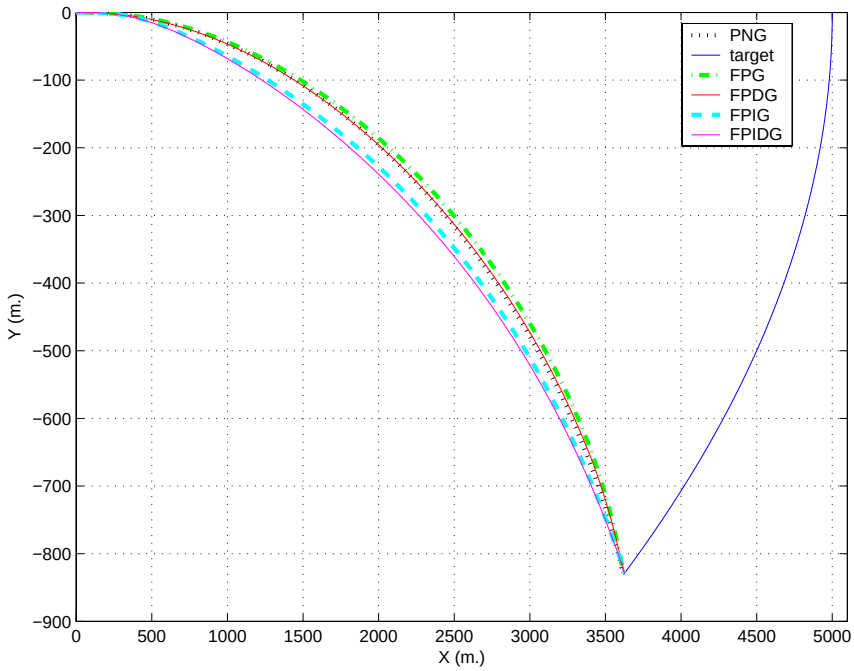

Figure 5.8 X vs. Y for target two with variation one

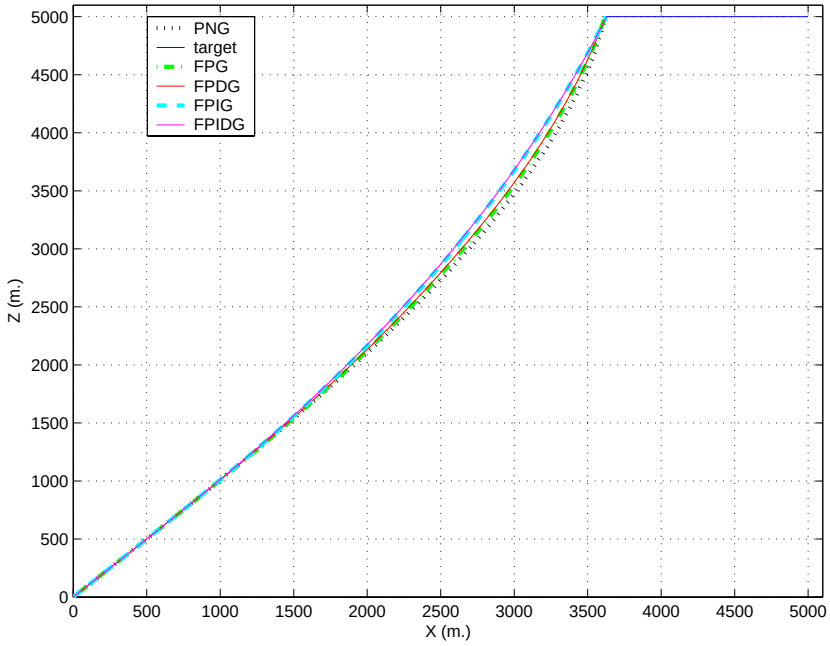

Figure 5.9 X vs. Z for target two with variation one

5.2.2 Acceleration plots

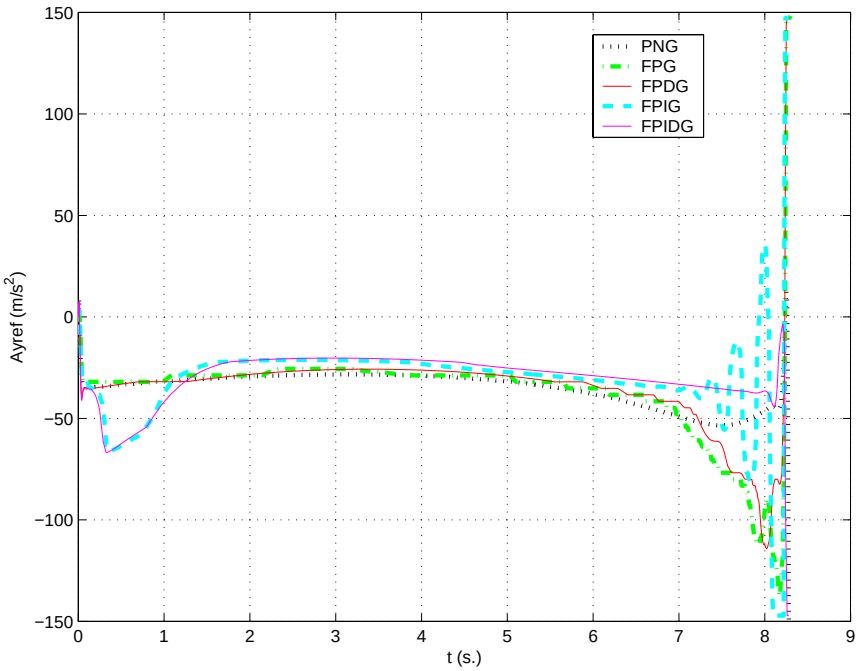

Figure 5.10 Ayref vs. t for target two with variation one

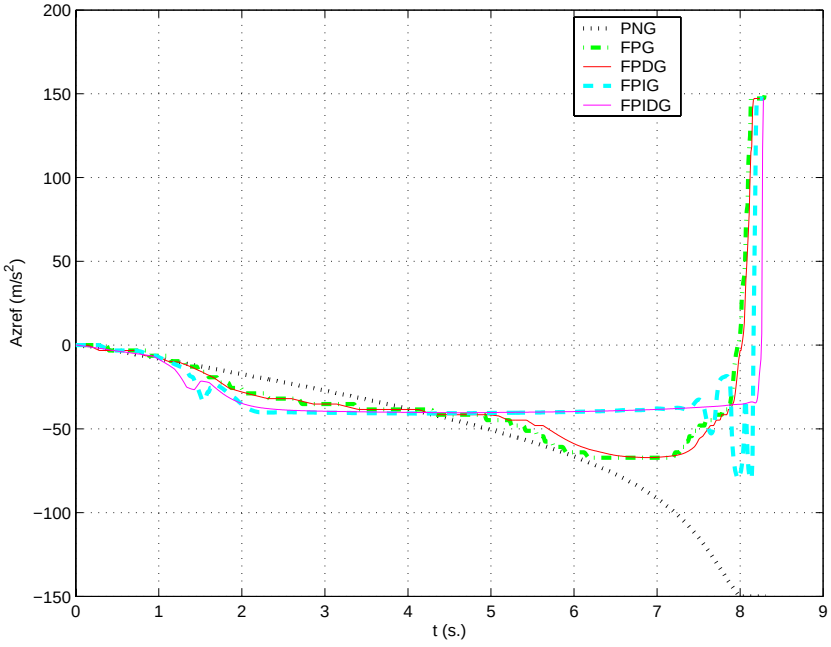

Figure 5.11 Azref vs. t for target two with variation one

5.2.3 Canard deflection plots

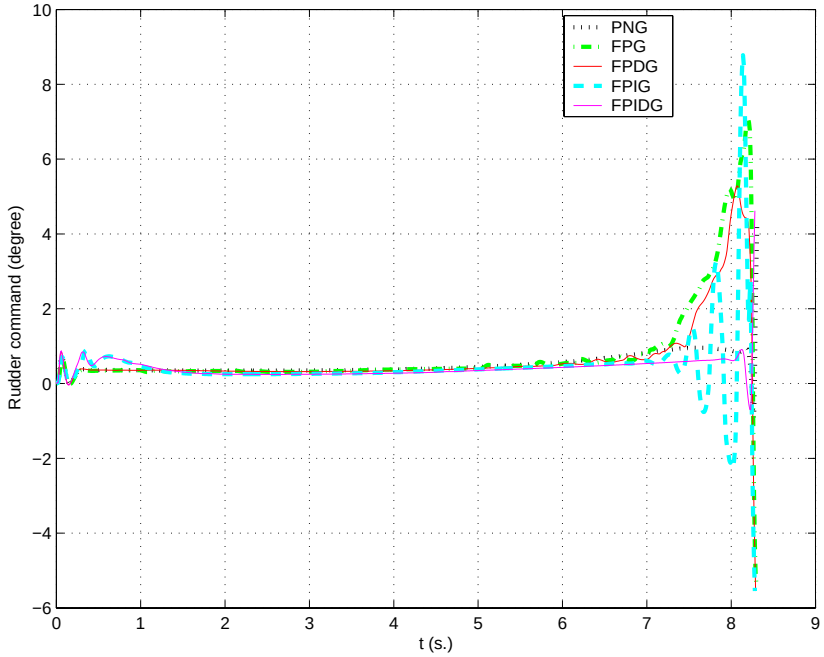

Figure 5.12 Rudder command vs. t for target two with variation one

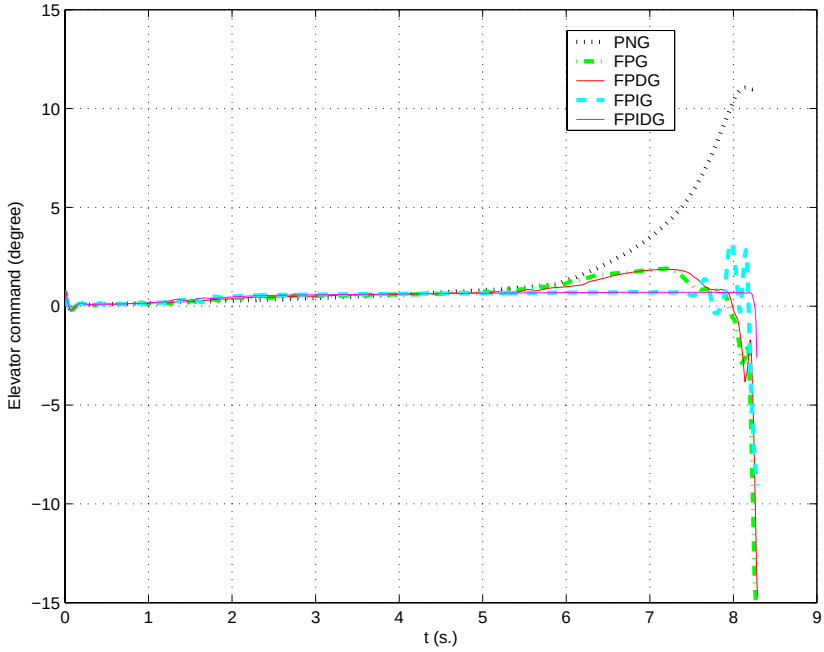

Figure 5.13 Elevator command vs. t for target two with variation one

5.2.4 Performance table

Table 5.2 Performance table for target two with variation one

Guidance method	hit/miss	Min. distance (m.)	TOF (s.)	Control effort (m/s)		
				A_{yref}	A_{zref}	Total
PNG	hit	0.277	8.310	288.531	403.321	691.852
FPG	hit	1.698	8.302	312.209	319.716	631.925
FPDG	hit	1.553	8.298	297.204	311.499	608.703
FPIG	hit	1.326	8.283	255.488	272.761	528.249
FPIDG	hit	***0.061***	***8.282***	***243.393***	***267.712***	***511.105***

All of the guidance methods hit the target. The minimum result in a column is printed in bold italic.

5.3 Simulation Results for Target Two Variation Two

Target two is a target accelerating parabolically in XY plane. It is trying to pass over the missile. Simulation results in this section are given for target two with variation two (see APPENDIX B.2 for details).

5.3.1 Position plots

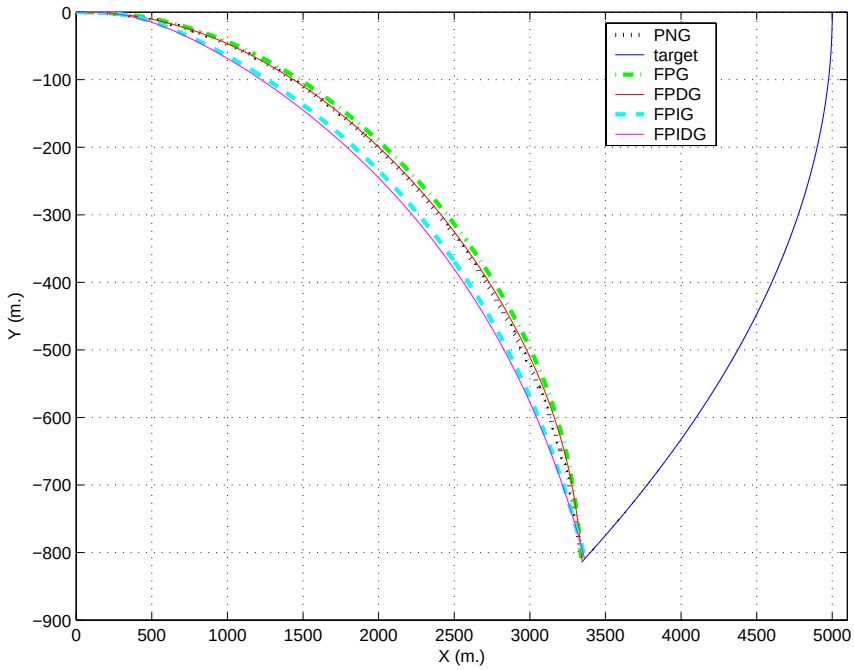

Figure 5.14 X vs. Y for target two with variation two

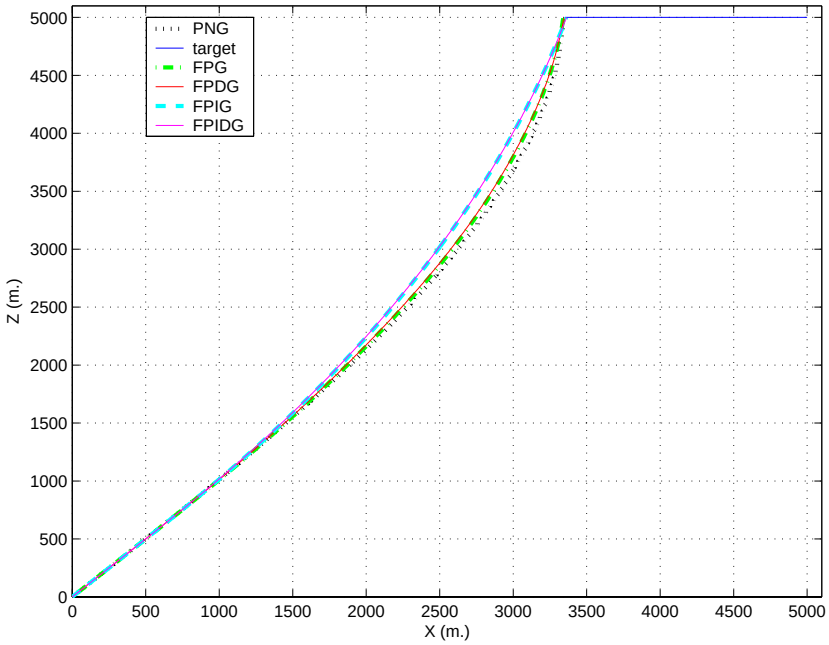

Figure 5.15 X vs. Z for target two with variation two

5.3.2 Acceleration plots

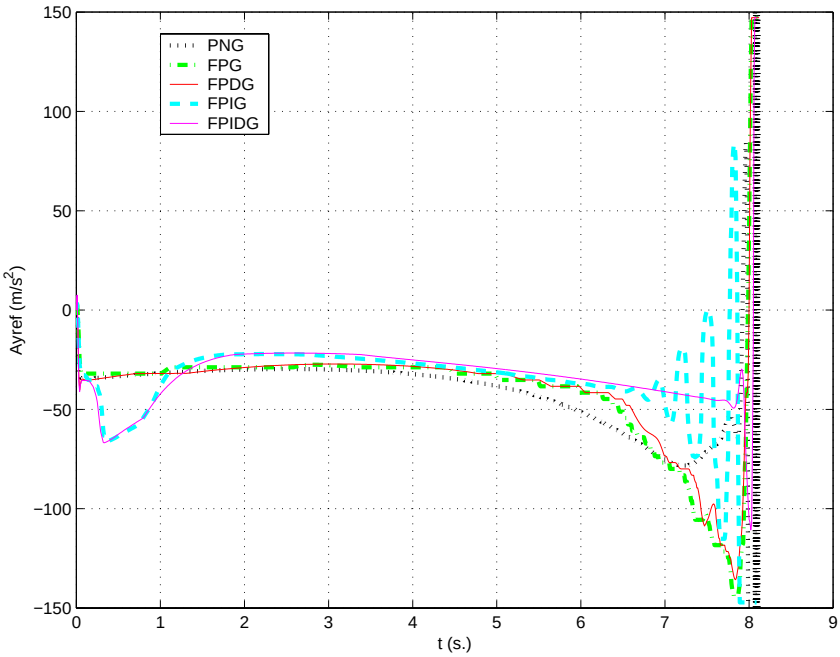

Figure 5.16 Ayref vs. t for target two with variation two

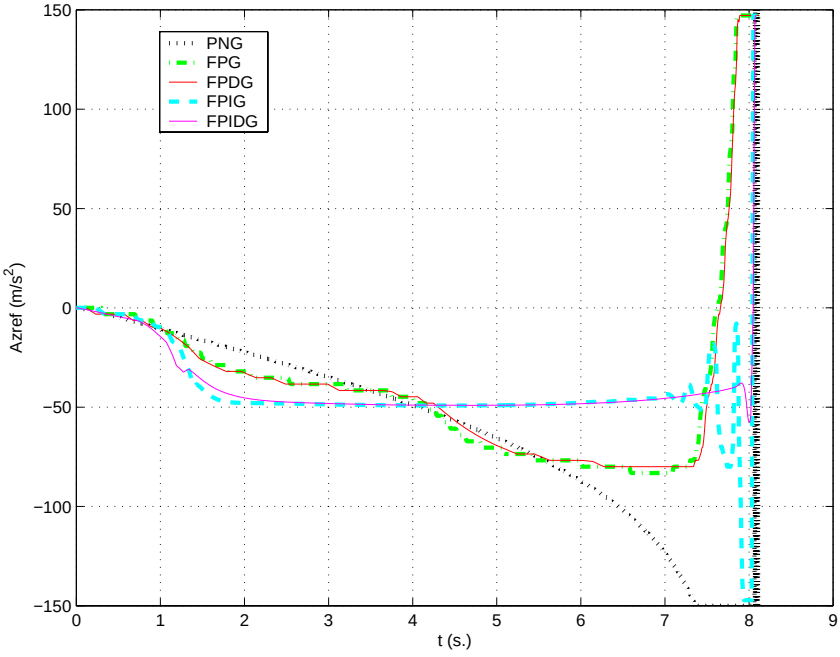

Figure 5.17 Azref vs. t for target two with variation two

5.3.3 Canard deflection plots

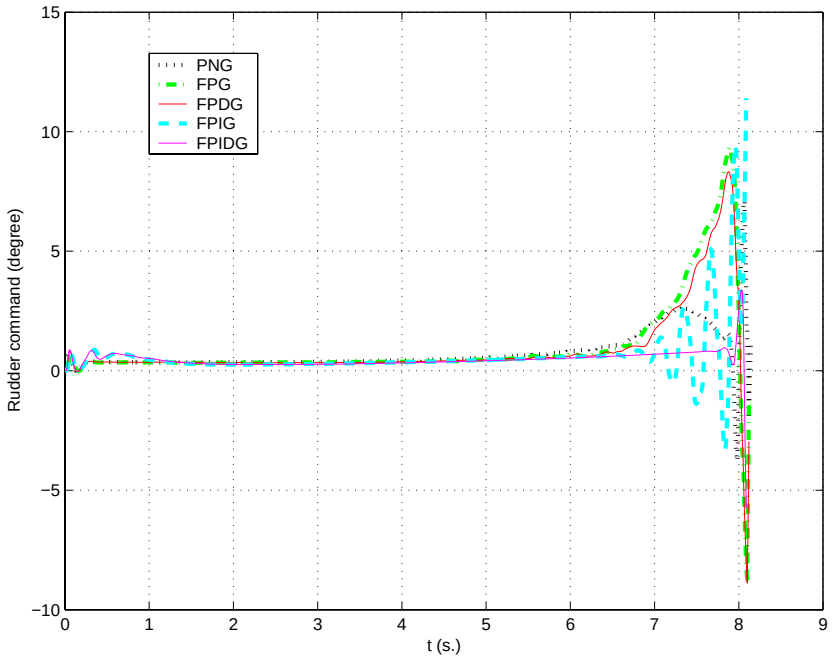

Figure 5.18 Rudder command vs. t for target two with variation two

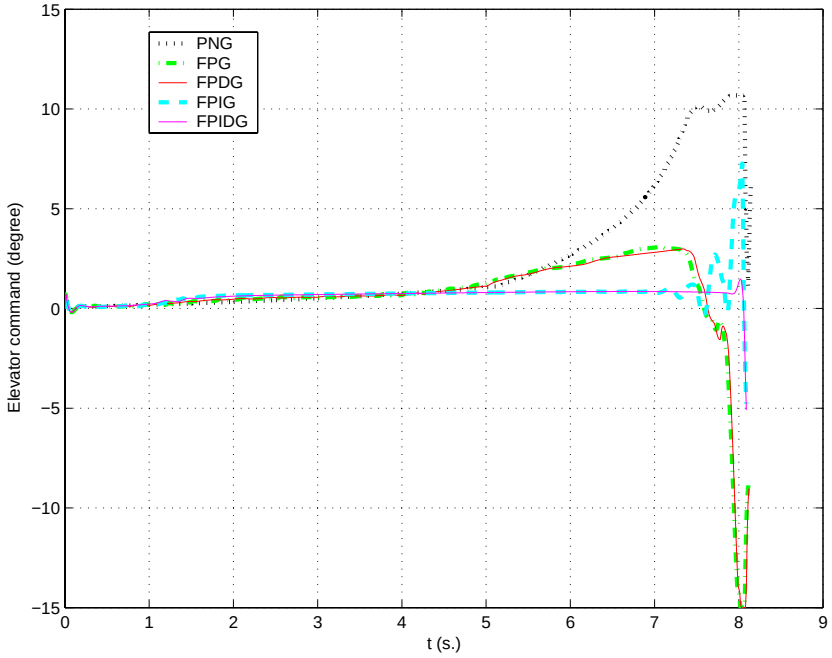

Figure 5.19 Elevator command vs. t for target two with variation two

5.3.4 Performance table

Table 5.3 Performance table for target two with variation two

Guidance method	hit/miss	Min. distance (m.)	TOF (s.)	Control effort (m/s)		
				A_{yref}	A_{zref}	Total
PNG	miss	18.941	8.142	333.683	479.812	813.495
FPG	miss	8.098	8.127	342.234	406.531	748.765
FPDG	miss	6.255	8.122	331.107	404.046	735.153
FPIG	hit	1.962	8.094	277.059	335.334	612.393
FPIDG	hit	***0.261***	***8.093***	***266.254***	***323.346***	***589.600***

The guidance methods FPIG and FPIDG hit the target. The minimum result in a column is printed in bold italic.

5.4 Simulation Results for Target Two Variation Three

Target two is a target accelerating parabolically in XY plane. It is trying to pass over the missile. Simulation results in this section are given for target two with variation three (see APPENDIX B.2 for details).

5.4.1 Position plots

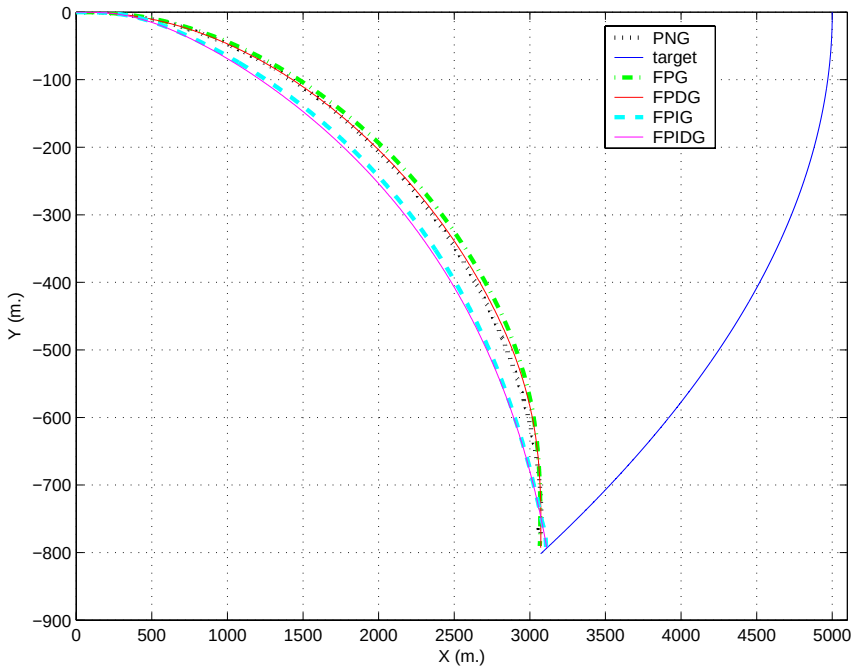

Figure 5.20 X vs. Y for target two with variation three

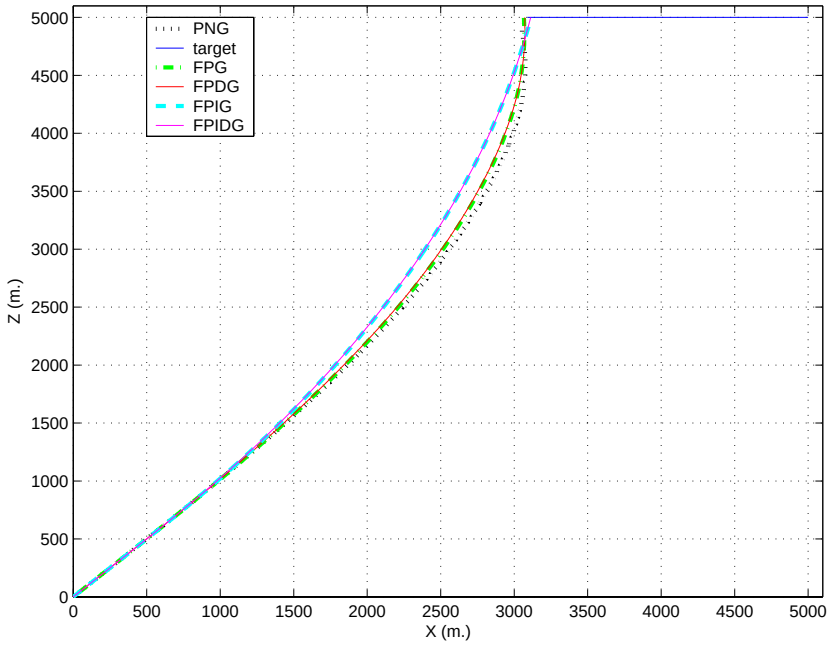

Figure 5.21 X vs. Z for target two with variation three

5.4.2 Acceleration plots

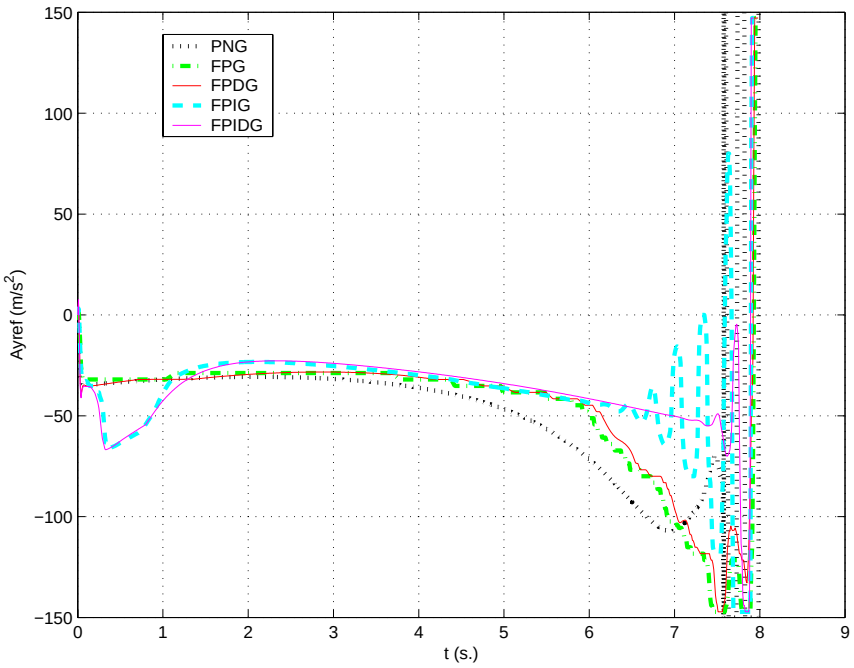

Figure 5.22 Ayref vs. t for target two with variation three

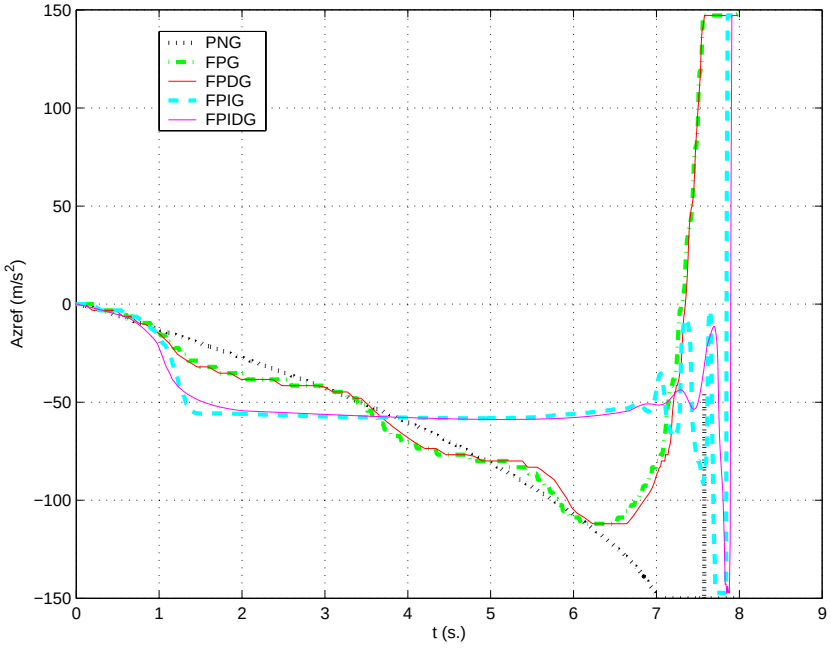

Figure 5.23 Azref vs. t for target two with variation three

5.4.3 Canard deflection plots

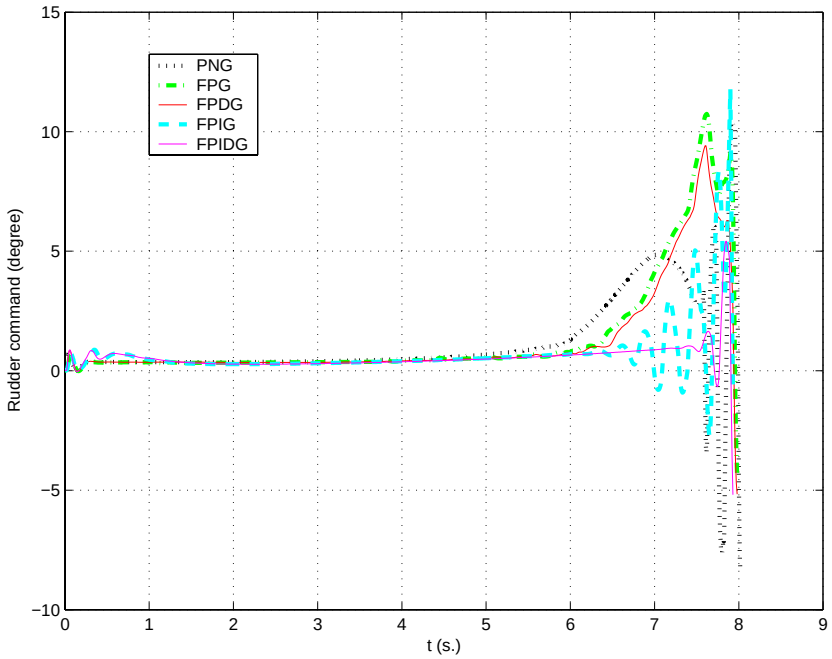

Figure 5.24 Rudder command vs. t for target two with variation three

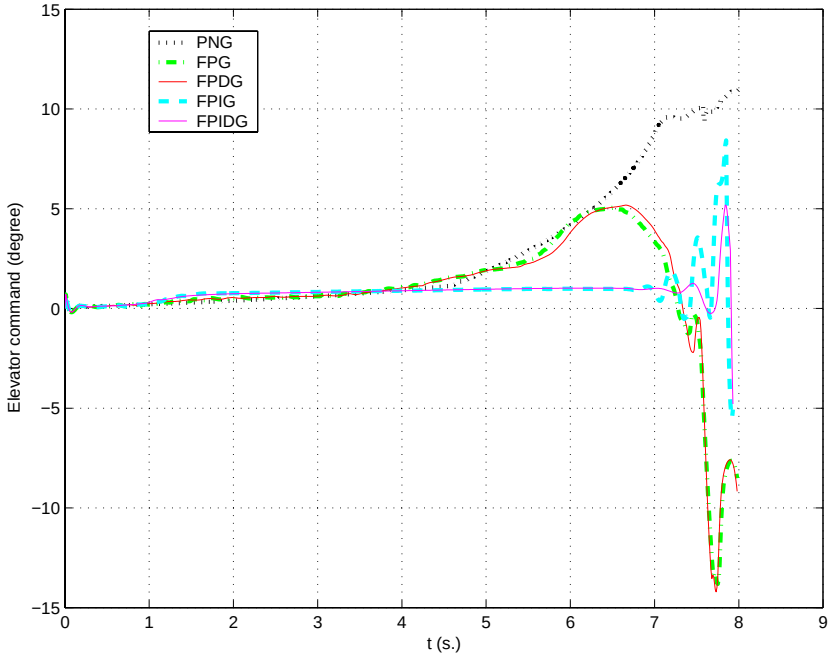

Figure 5.25 Elevator command vs. t for target two with variation three

5.4.4 Performance table

Table 5.4 Performance table for target two with variation three

Guidance method	hit/miss	Min. distance (m.)	TOF (s.)	Control effort (m/s)		
				A_{yref}	A_{zref}	Total
PNG	miss	41.781	8.017	382.584	541.761	924.345
FPG	miss	21.390	7.987	381.448	480.826	862.274
FPDG	miss	17.336	7.982	365.336	482.592	847.928
FPIG	miss	5.123	***7.932***	304.057	389.854	693.911
FPIDG	hit	***0.743***	***7.932***	***290.606***	***375.535***	***666.141***

Only FPIDG guidance method hits the target. The minimum result in a column is printed in bold italic.

5.5 Simulation Results for Target Two Variation Four

Target two is a target accelerating parabolically in XY plane. It is trying to pass over the missile. Simulation results in this section are given for target two with variation four (see APPENDIX B.2 for details).

5.5.1 Position plots

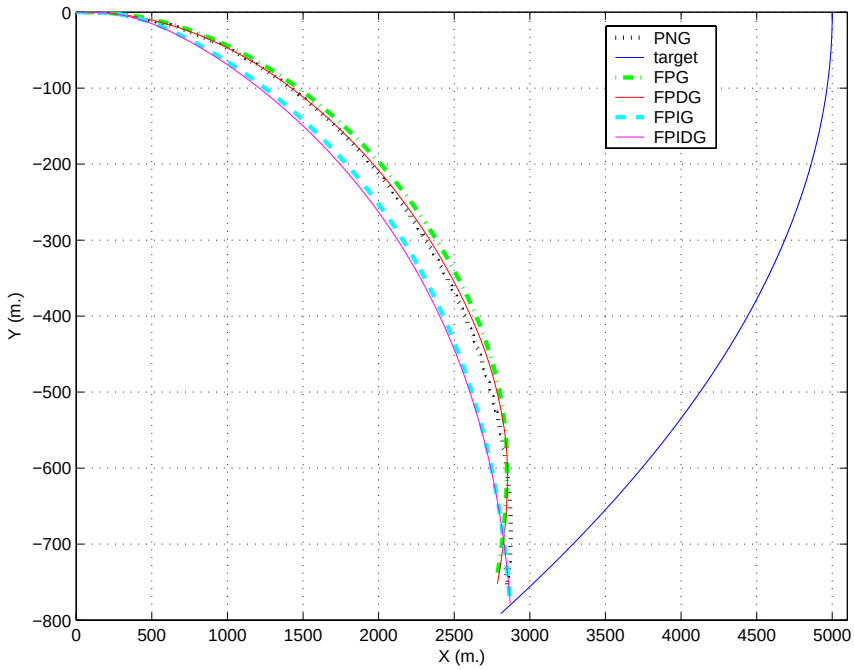

Figure 5.26 X vs. Y for target two with variation four

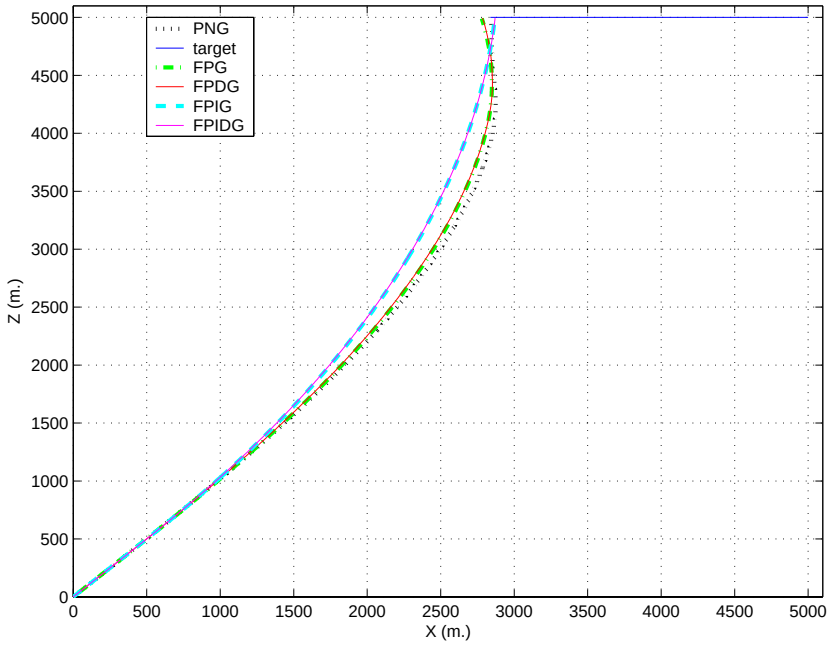

Figure 5.27 X vs. Z for target two with variation four

5.5.2 Acceleration plots

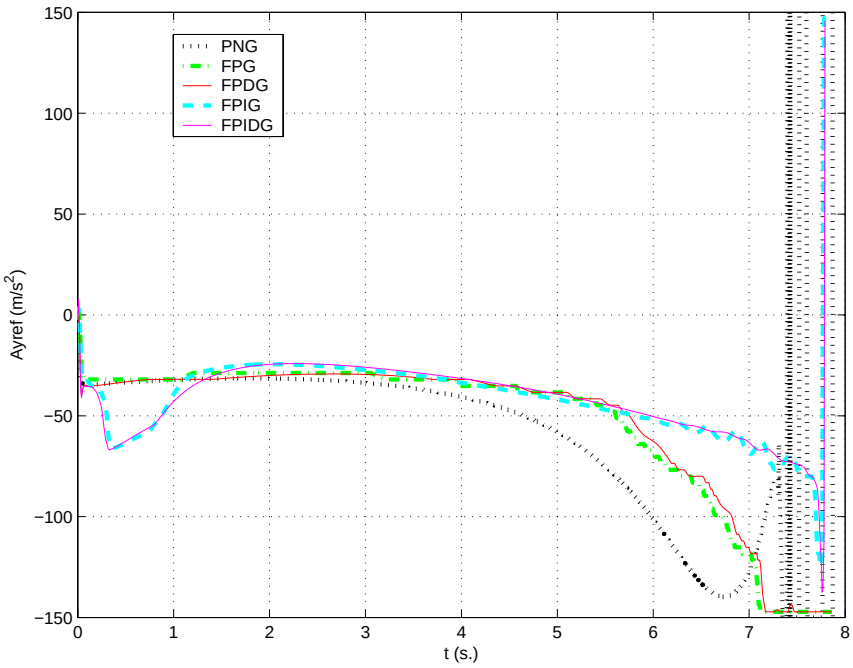

Figure 5.28 Ayref vs. t for target two with variation four

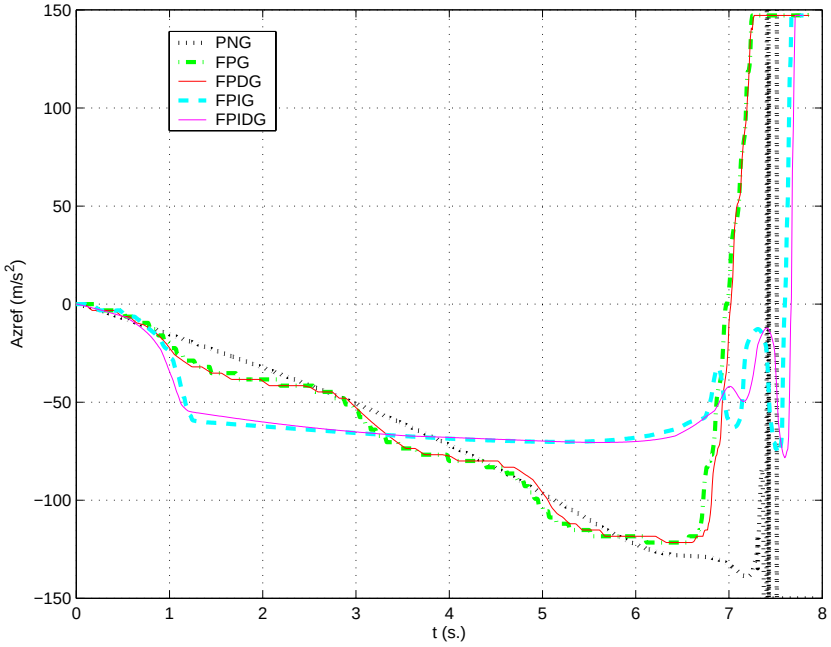

Figure 5.29 Azref vs. t for target two with variation four

5.5.3 Canard deflection plots

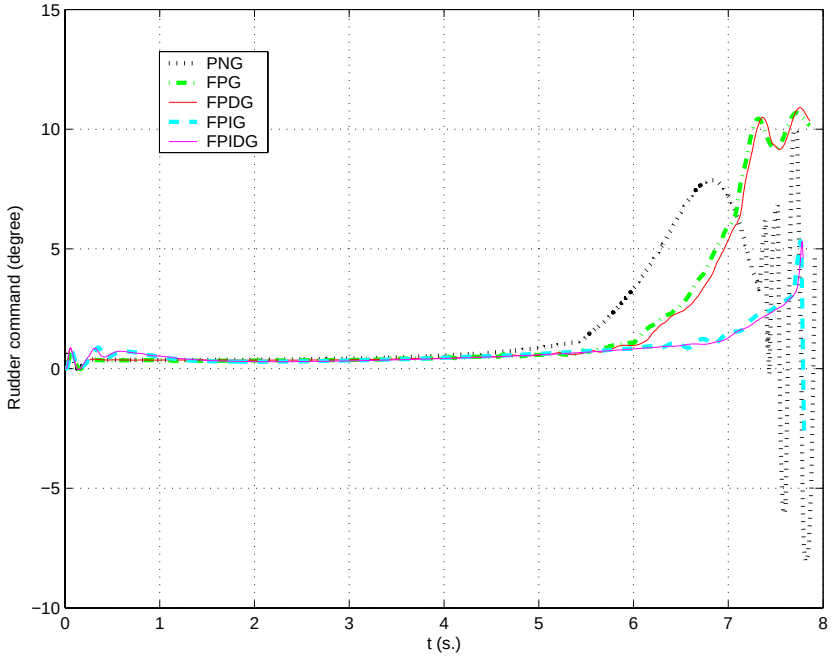

Figure 5.30 Rudder command vs. t for target two with variation four

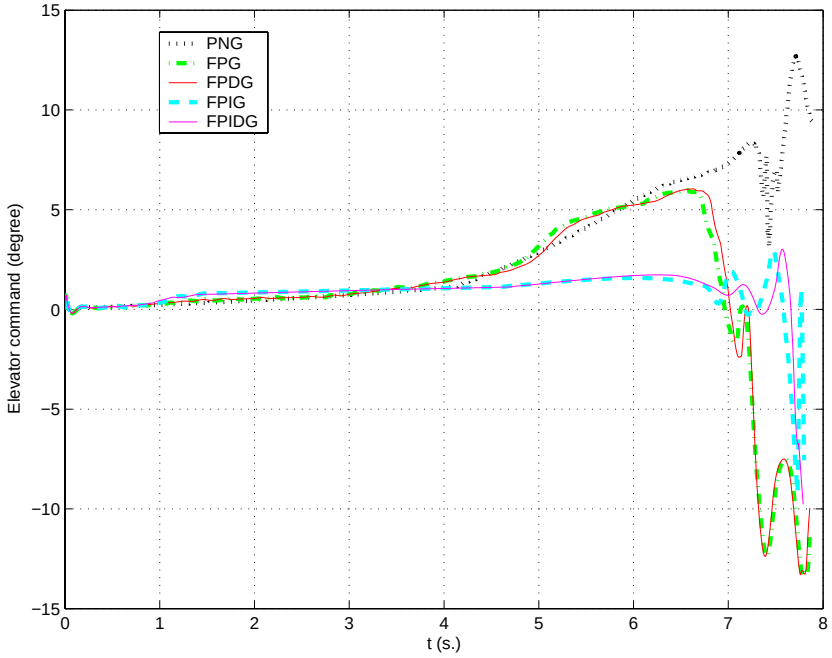

Figure 5.31 Elevator command vs. t for target two with variation four

5.5.4 Performance table

Table 5.5 Performance table for target two with variation four

Guidance method	hit/miss	Min. distance (m.)	TOF (s.)	Control effort (m/s)		
				A_{yref}	A_{zref}	Total
PNG	miss	68.853	7.913	447.091	568.280	1015.4
FPG	miss	67.898	7.868	410.708	556.617	967.325
FPDG	miss	62.152	7.862	403.090	558.540	961.630
FPIG	hit	1.617	7.801	327.125	422.787	749.912
FPIDG	hit	***1.242***	***7.798***	***320.723***	***420.864***	***741.587***

The guidance methods FPIG FPIDG hit the target. The minimum result in a column is printed in bold italic.

5.6 Simulation Results for Target Three Variation One

Target three is a target making a constant speed sine wave in the XY plane. It is weaving to escape from the missile (see APPENDIX B.3 for details).

5.6.1 Position plots

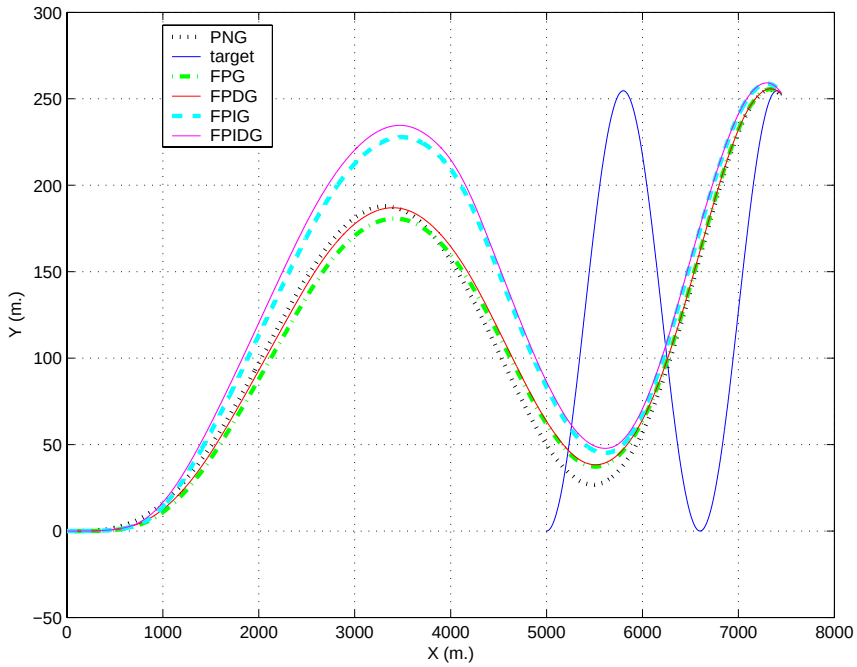

Figure 5.32 X vs. Y for target three with variation one

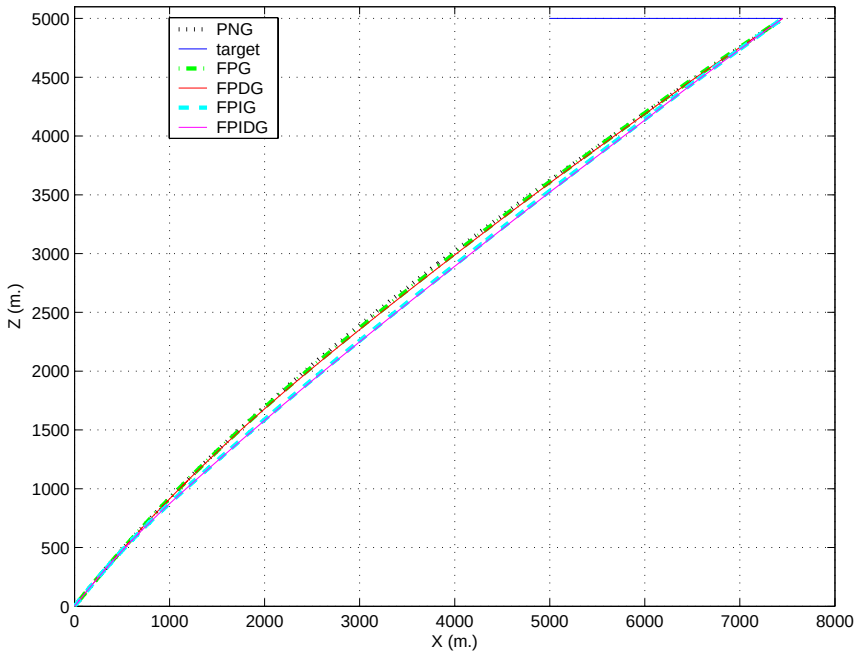

Figure 5.33 X vs. Z for target three with variation one

5.6.2 Acceleration plots

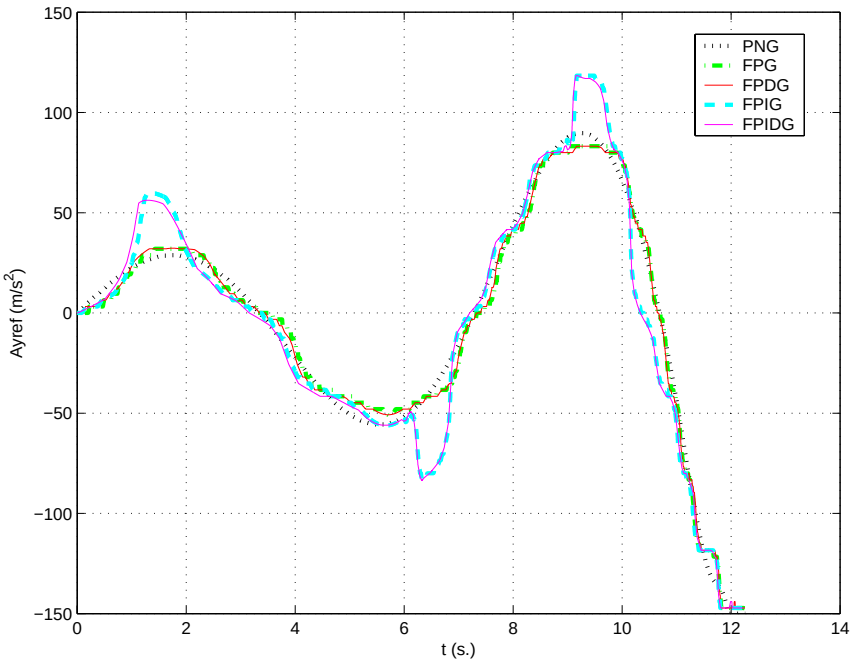

Figure 5.34 Ayref vs. t for target three with variation one

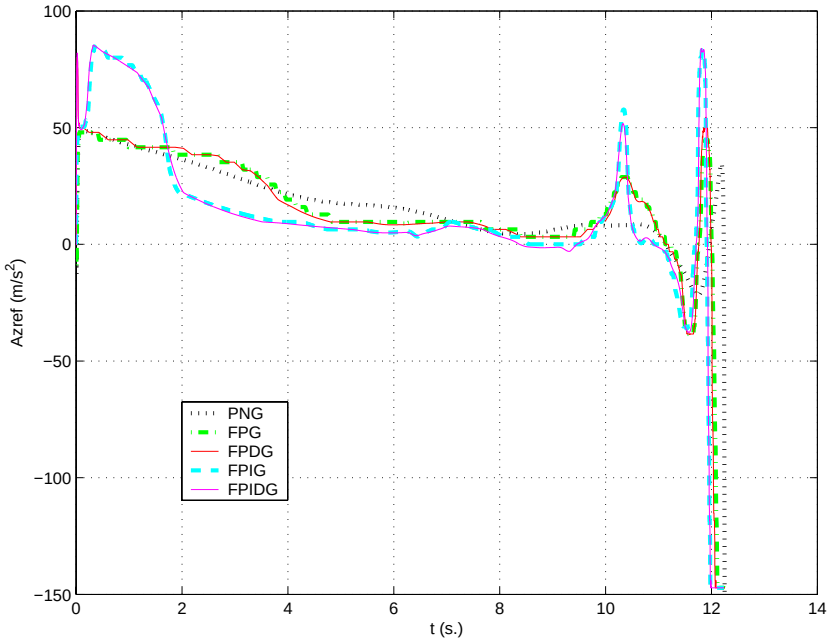

Figure 5.35 Azref vs. t for target three with variation one

5.6.3 Canard deflection plots

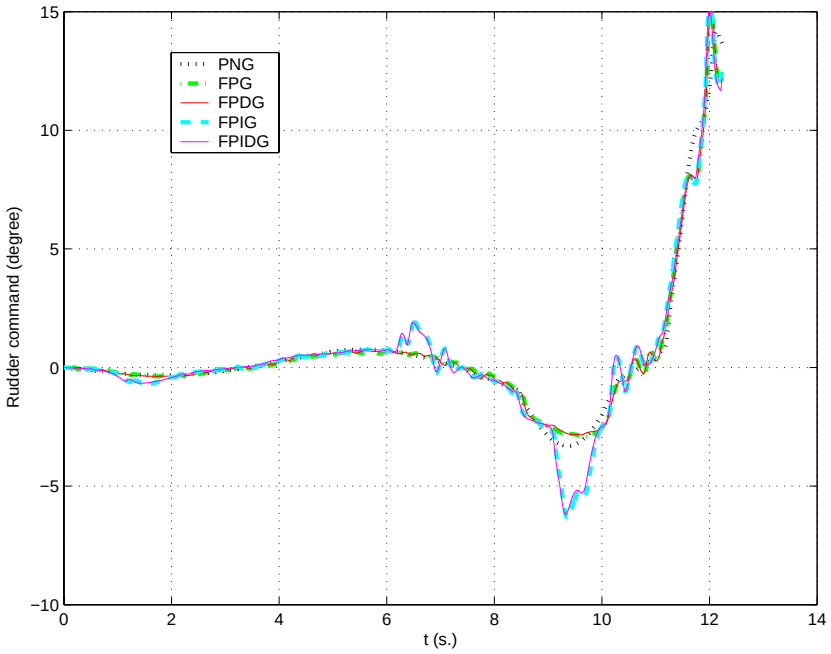

Figure 5.36 Rudder command vs. t for target three with variation one

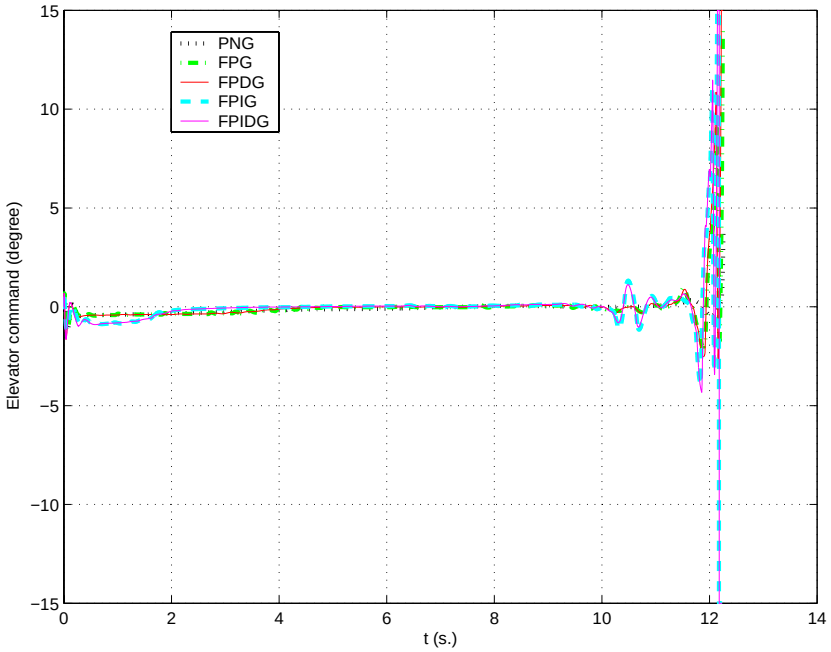

Figure 5.37 Elevator command vs. t for target three with variation one

5.6.4 Performance table

Table 5.6 Performance table for target three with variation one

Guidance method	hit/miss	Min. distance (m.)	TOF (s.)	Control effort (m/s)		
				A_{yref}	A_{zref}	Total
PNG	hit	***0.268***	12.268	535.327	***232.534***	767.861
FPG	hit	0.620	12.258	***512.780***	251.594	***764.374***
FPDG	hit	0.613	12.255	522.661	255.049	777.710
FPIG	hit	1.052	12.235	587.702	248.229	835.931
FPIDG	hit	1.096	***12.234***	594.400	246.293	840.693

All of the guidance methods hit the target. The minimum result in a column is printed in bold italic.

5.7 Simulation Results for Target Three Variation Two

Target three is a target making a constant speed sine wave in the XY plane. It is weaving to pass over the missile (see APPENDIX B.3 for details).

5.7.1 Position plots

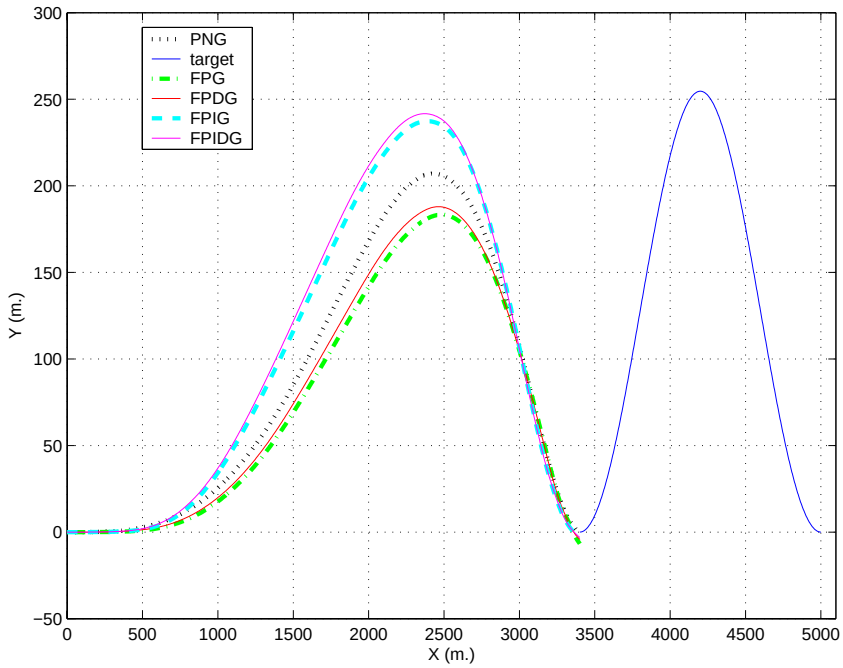

Figure 5.38 X vs. Y for target three with variation two

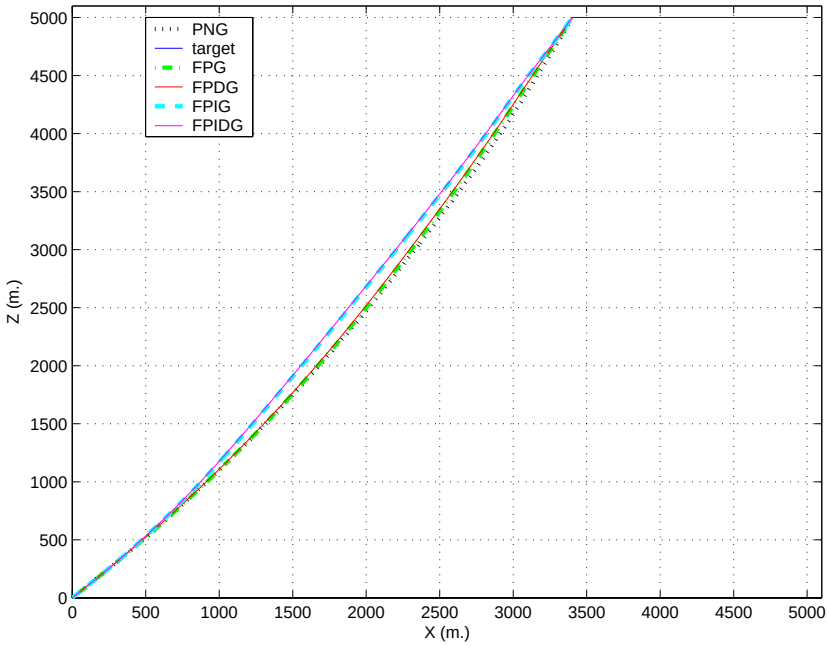

Figure 5.39 X vs. Z for target three with variation two

5.7.2 Acceleration plots

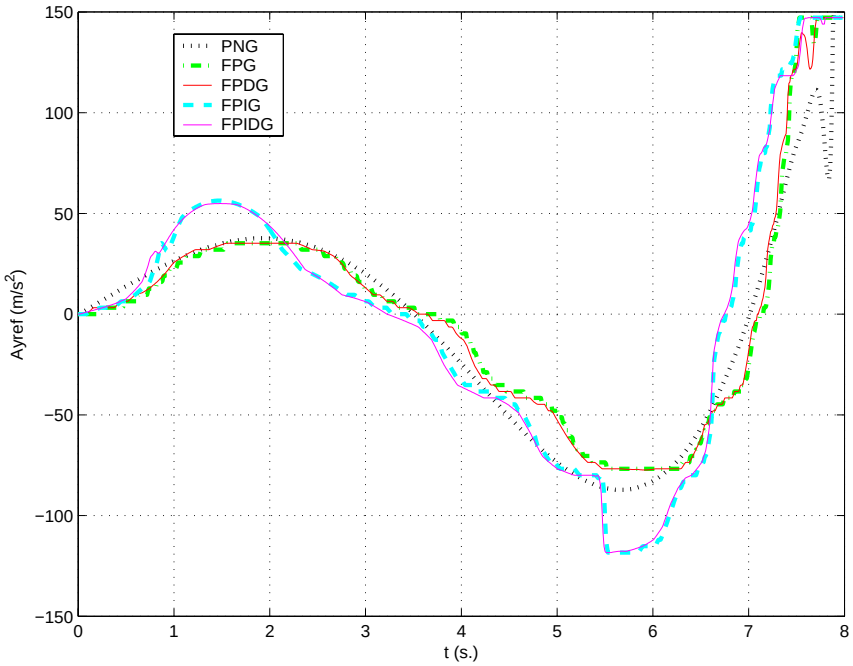

Figure 5.40 Ayref vs. t for target three with variation two

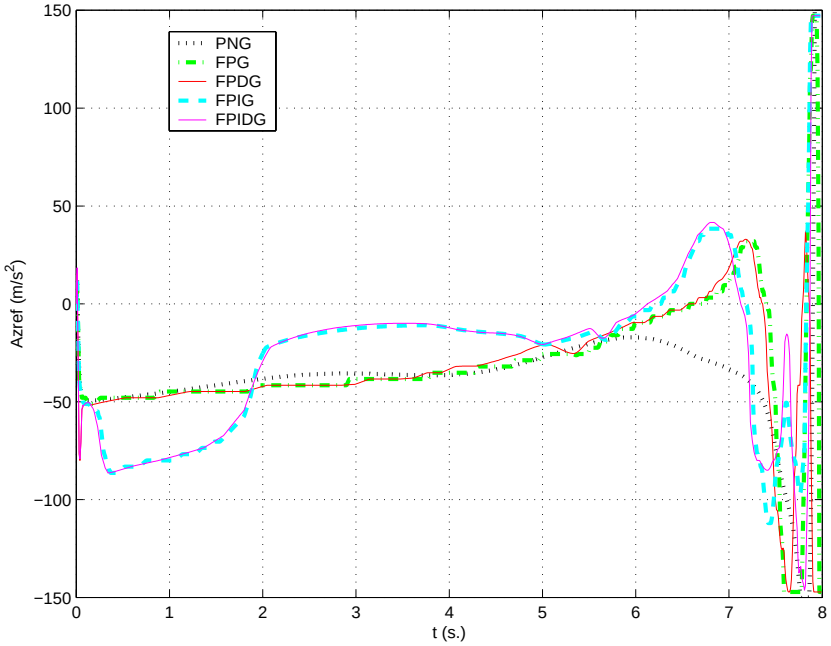

Figure 5.41 Azref vs. t for target three with variation two

5.7.3 Canard deflection plots

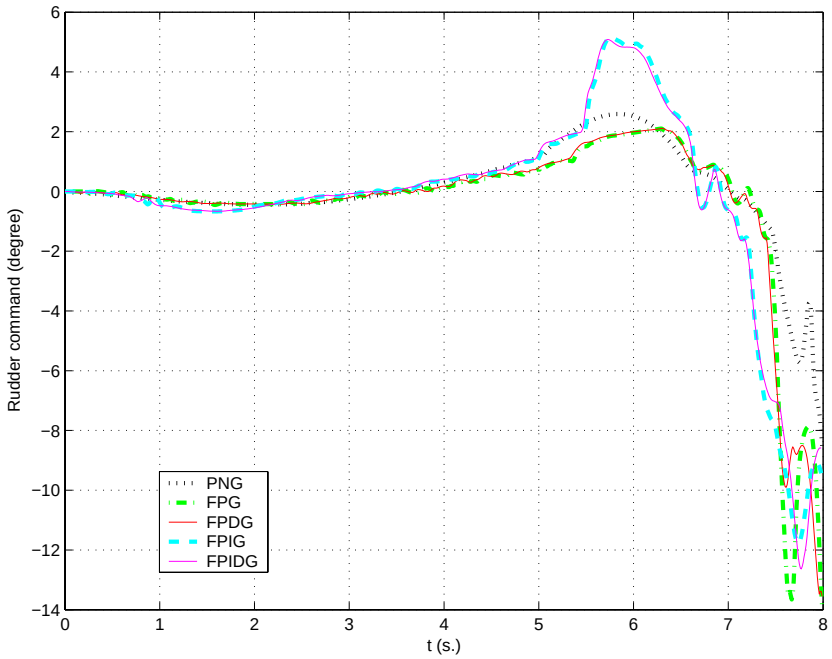

Figure 5.42 Rudder command vs. t for target three with variation two

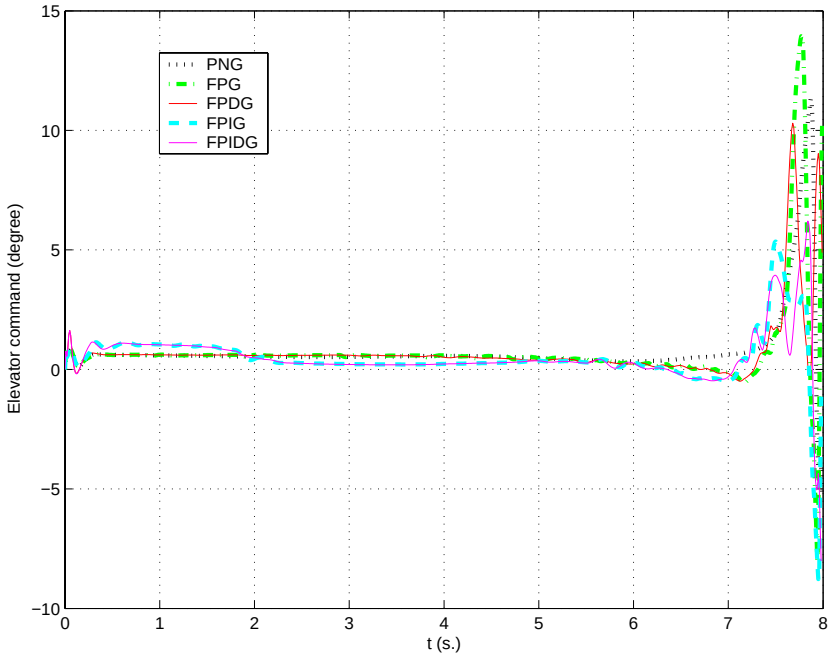

Figure 5.43 Elevator command vs. t for target three with variation two

5.7.4 Performance table

Table 5.7 Performance table for target three with variation two

Guidance method	hit/miss	Min. distance (m.)	TOF (s.)	Control effort (m/s)		
				A_{yref}	A_{zref}	Total
PNG	hit	***0.950***	7.998	335.782	305.568	641.350
FPG	miss	6.769	7.991	***319.543***	283.793	603.336
FPDG	miss	4.311	7.990	329.766	273.021	***602.787***
FPIG	miss	3.547	***7.984***	410.754	***266.532***	677.286
FPIDG	miss	3.425	***7.984***	416.945	269.906	686.851

Only the PNG law hits the target. The minimum result in a column is printed in bold italic.

5.8 Simulation Results for Target Four

Target four is a target maneuvering towards the missile at a point that missile is close enough. It is trying to get inside the missile turning diameter to escape from the missile (see APPENDIX B.4 for details).

5.8.1 Position plots

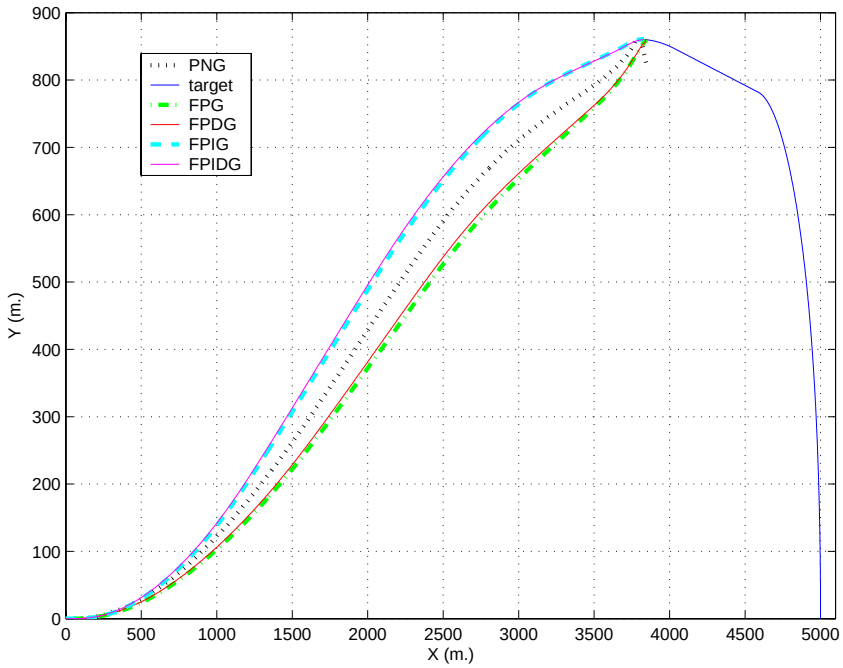

Figure 5.44 X vs. Y for target four

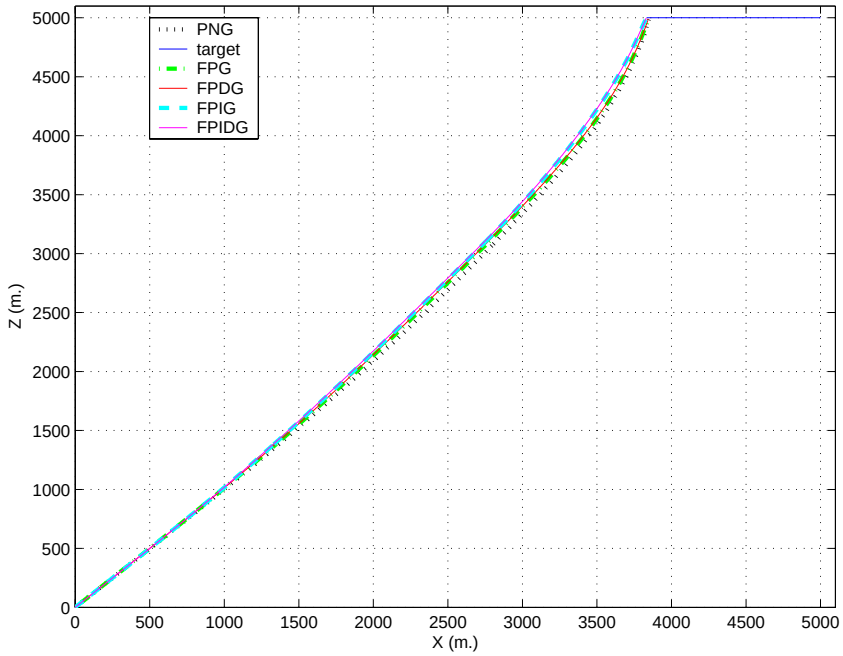

Figure 5.45 X vs. Z for target four

5.8.2 Acceleration plots

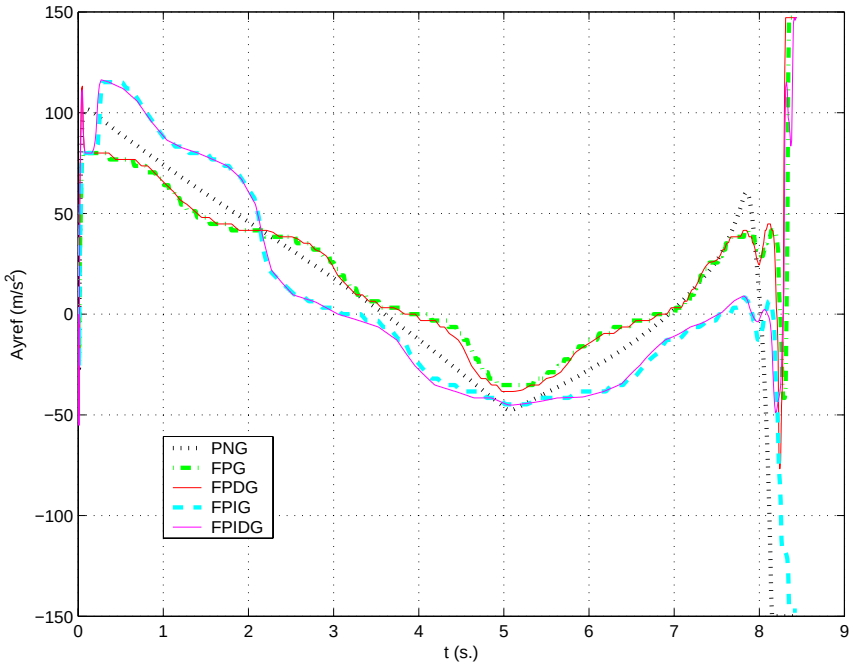

Figure 5.46 Ayref vs. t for target four

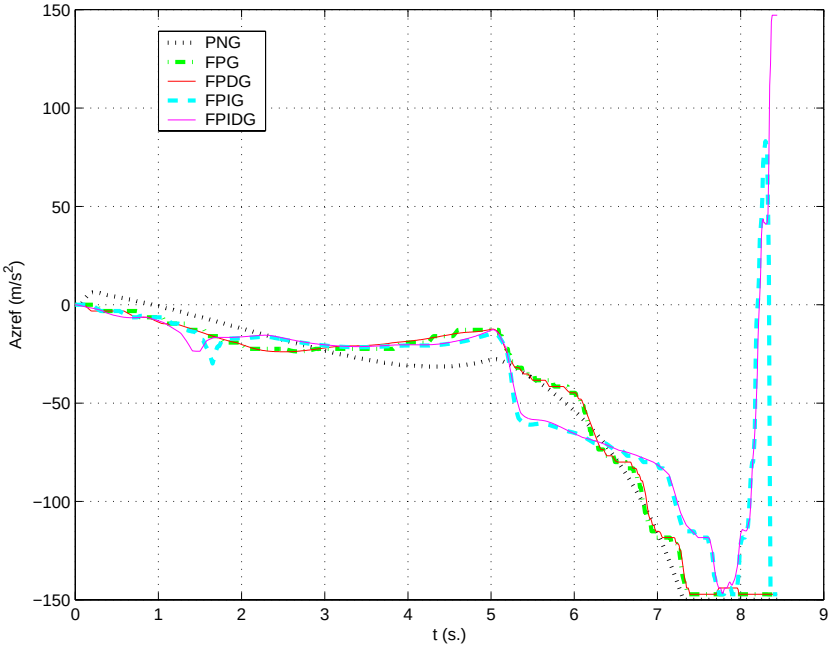

Figure 5.47 Azref vs. t for target four

5.8.3 Canard deflection plots

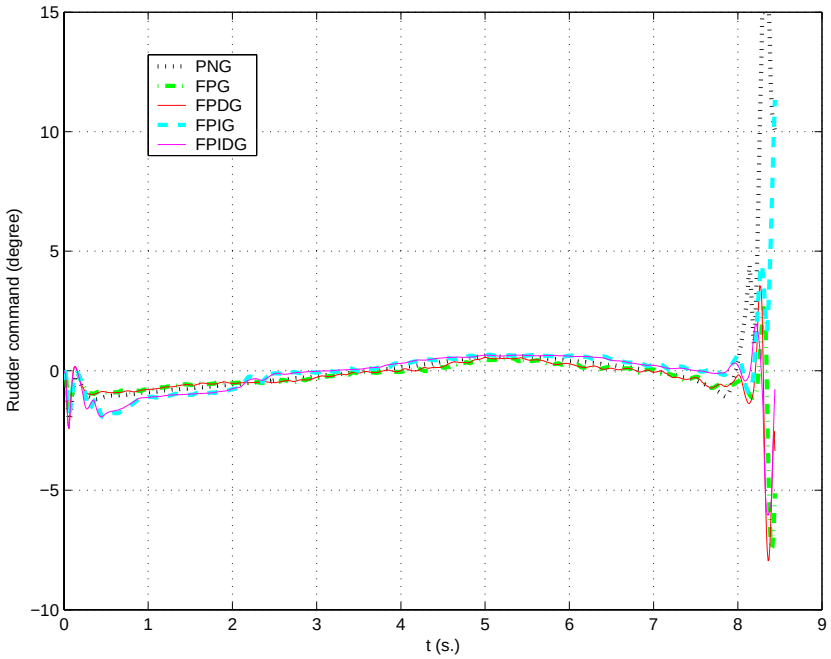

Figure 5.48 Rudder command vs. t for target four

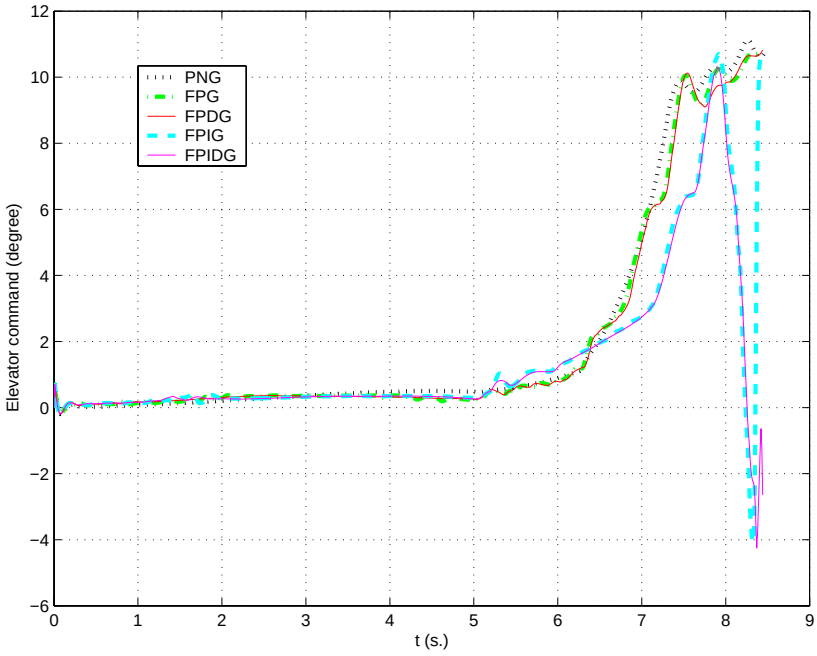

Figure 5.49 Elevator command vs. t for target four

5.8.4 Performance table

Table 5.8 Performance table for target four

Guidance method	hit/miss	Min. distance (m.)	TOF (s.)	Control effort (m/s)		
				A_{yref}	A_{zref}	Total
PNG	miss	46.338	8.461	341.193	405.895	747.088
FPG	miss	15.668	8.449	***249.327***	381.963	***631.290***
FPDG	miss	15.872	8.448	259.284	378.708	637.992
FPIG	hit	1.326	8.445	327.914	341.044	668.958
FPIDG	hit	***0.604***	***8.444***	323.392	***339.190***	662.582

The guidance methods FPIG and FPIDG hit the target. The minimum result in a column is printed in bold italic.

5.9 Simulation Results for Target Five

Target five is a ballistic missile. The guidance methods try to hit the missile before it completes its mission (see APPENDIX B.5 for details).

5.9.1 Position plots

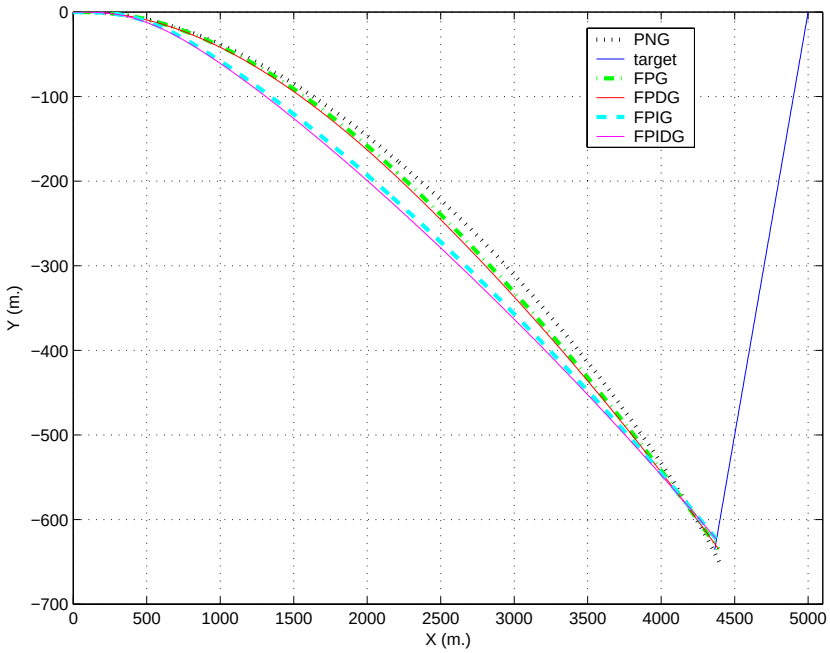

Figure 5.50 X vs. Y for target five

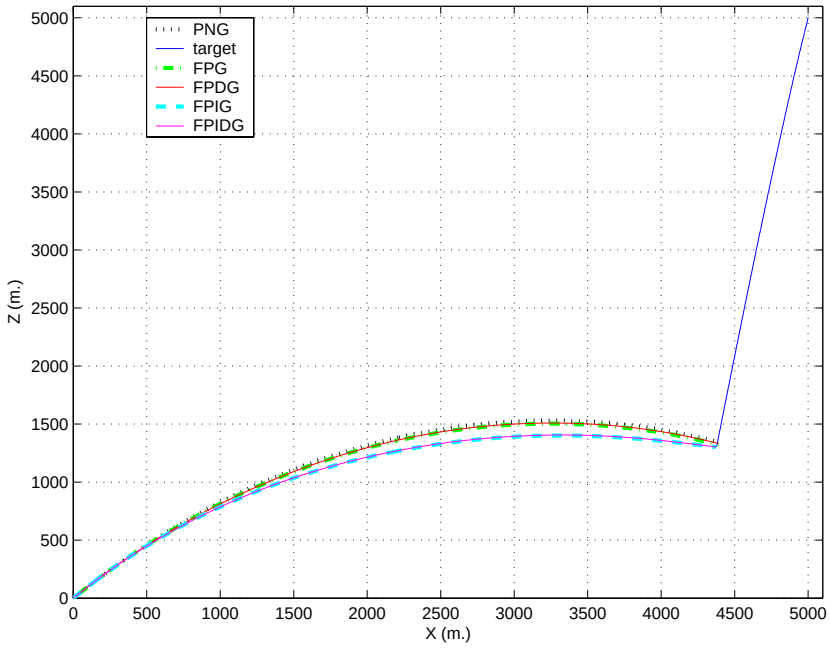

Figure 5.51 X vs. Z for target five

5.9.2 Acceleration plots

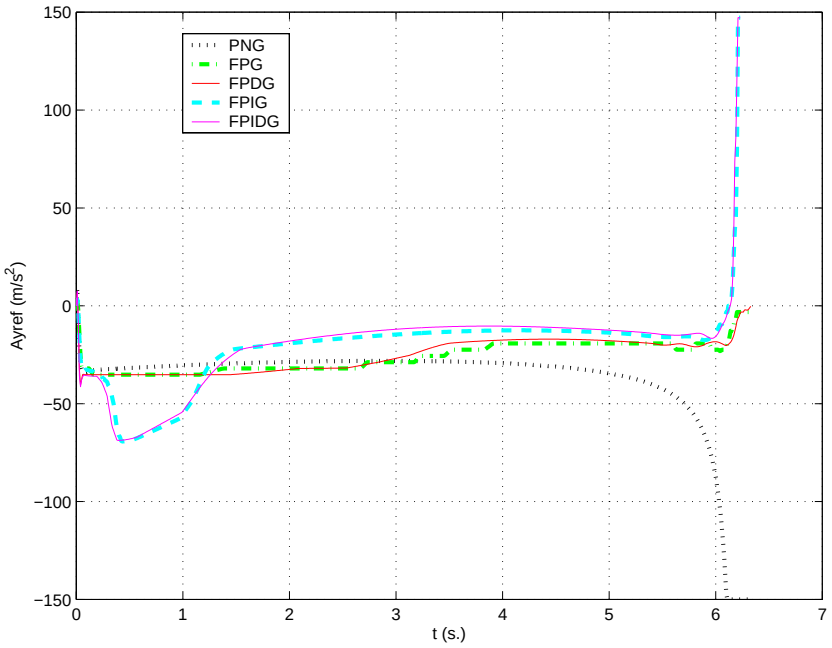

Figure 5.52 Ayref vs. t for target five

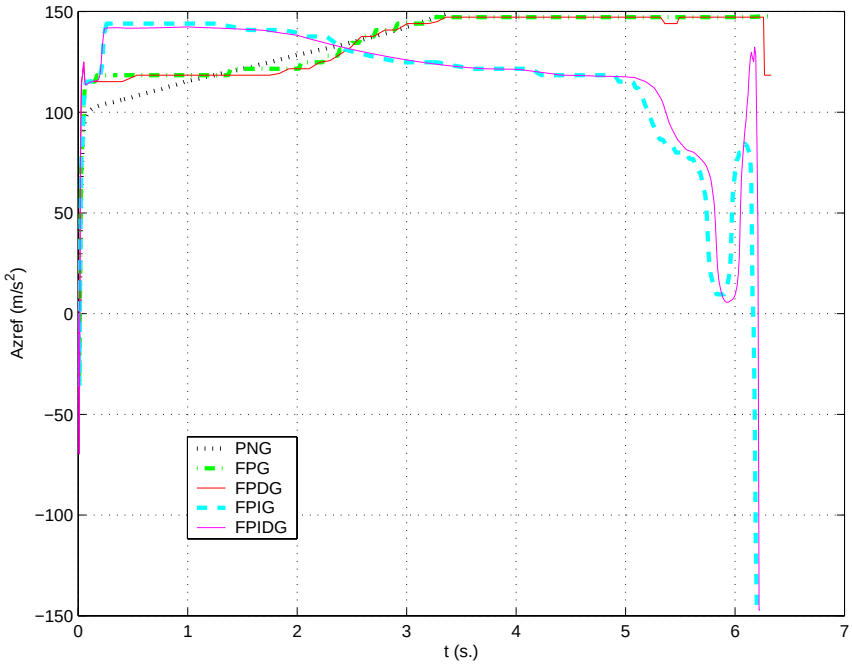

Figure 5.53 Azref vs. t for target five

5.9.3 Canard deflection plots

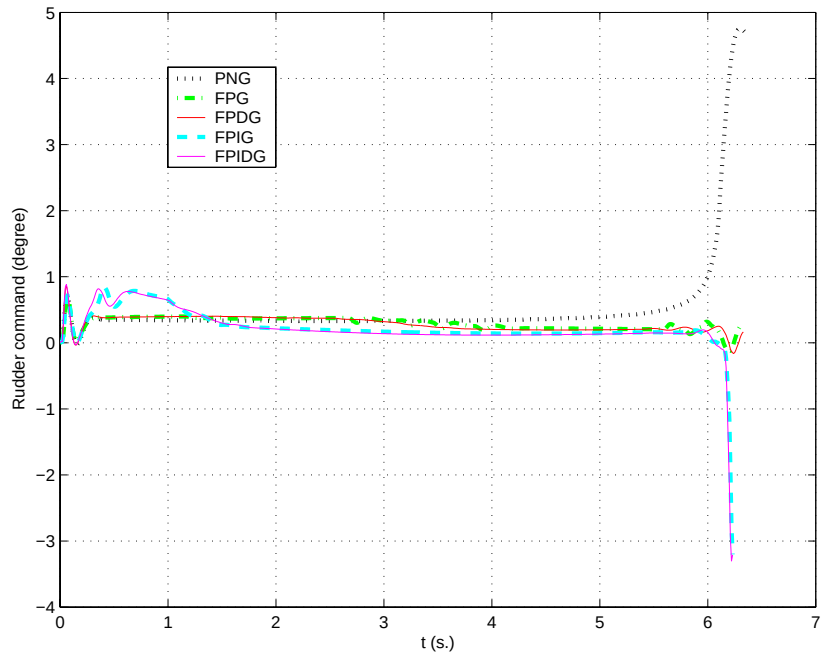

Figure 5.54 Rudder command vs. t for target five

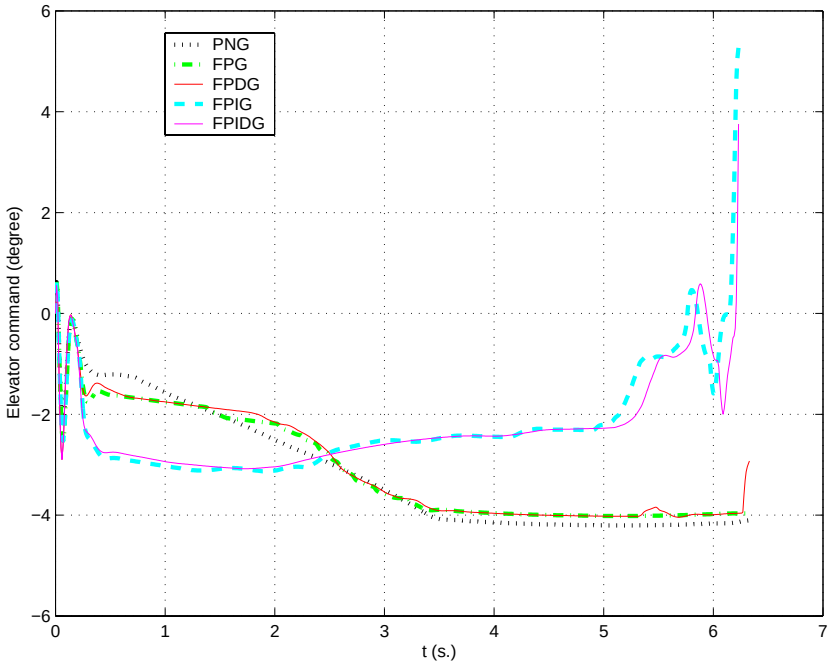

Figure 5.55 Elevator command vs. t for target five

5.9.4 Performance table

Table 5.9 Performance table for target five

Guidance method	hit/miss	Min. distance (m.)	TOF (s.)	Control effort (m/s)		
				A_{yref}	A_{zref}	Total
PNG	miss	127.363	6.365	232.640	851.105	1083.7
FPG	miss	83.681	6.330	164.577	845.092	1009.7
FPDG	miss	94.352	6.333	160.579	841.908	1002.5
FPIG	hit	0.660	***6.231***	139.887	***730.334***	***870.221***
FPIDG	hit	***0.571***	6.232	***135.174***	736.762	871.936

The guidance methods FPIG and FPIDG hit the target. The minimum result in a column is printed in bold italic.

CHAPTER 6

CONCLUSION

This thesis shows that fuzzy logic can be implemented as guidance law.

In order to compare with the famous and commonly used guidance law PNG, fuzzy logic guidance systems are designed to use the information available for PNG. Using the same available information, they resulted in better performance results.

In this thesis, a lateral and a longitudinal autopilot, and four fuzzy logic guidance systems are designed. The designed guidance systems are tested in a canard controlled surface to air missile against five different target types with some variations.

The decoupled dynamics of the missile is assumed to be maintained by a roll autopilot, which is keeping the missile at zero roll angle with a satisfactorily fast response.

During the simulations it is assumed that there is no noise on the measurements of the sensors, seeker, and the process of taking the numeric derivative of the LOS rate. Especially the process of taking the numeric derivative of the LOS rate would multiply the noise on the measured signal if there were any. But, this would also be eliminated by the fuzzy logic, which is highly capable of noise rejection.

In all of the simulations, the PNG is plotted by a dotted line and behaves apparently different than the fuzzy logic guidance systems. The FPG is plotted by a dash-dotted line and has characteristics that are very close to the FPDG which is plotted by a straight line. So in the plots, plots of FPG and FPDG appear very close to each other. The FPIG is plotted by a dashed line and has characteristics that are generally very close to the FPIDG which is plotted by a straight line, So in the plots, plots of FPIG and FPIDG appear very close to each other.

In the simulation results against target one, which is the classical proportional navigation target, PNG provides the most precise hit, and it behaves better than the FPG and FPDG. But, the X vs. Y trajectories (Figure 5.2) and Ayref of the FPIG and FPIDG (Figure 5.4) are better than PNG, and they hit at a smaller TOF with less control effort. The acceleration commands demonstrate the behavior explained in 4.3 Fuzzy Logic Guidance. Target one seems as a point mass in X-Z plane in Figure 5.3. In this plane, trajectory of PNG is nearly a straight line but the fuzzy logic guidance systems make a smooth parabola to the target. That behavior is due to the gravitational acceleration in this plane. Fuzzy guidance systems try to output

more acceleration against disturbances and target maneuvers, which cause the parabola in the plot.

In the simulation results against target two with variation one, FPIDG gives the best results in all of the performance parameters. All of the guidance methods hit the target but FPIDG hits the target with the smoothest control performance plotted in Figure 5.10 and Figure 5.11. In the same figures, FPIG shows an oscillatory behavior in the terminal phase of the flight, which also exists in Figure 5.12 and Figure 5.13.

Simulation results for target two with variation two gives similar behavior to the simulation results for target two with variation one. But in this variation, three guidance methods, PNG, FPG and FPDG, miss the target while FPIG and FPIDG hit the target. FPIDG gives the best results in all of the performance parameters. Figure 5.16 and Figure 5.17 shows the reasons of the miss for the three guidance laws. PNG, FPG, and FPDG reach the saturation limit for Azref. In Ayref, PNG shows a bang-bang behavior in the terminal phase. Oscillatory behavior of the FPIG still exists although it hits the target.

Simulation results for target two with variation three gives similar behavior to the simulation results for target two with previous variations. In this variation only FPIDG hits the target, which gives the best results in all of the performance parameters. PNG, FPG, and FPDG saturate in Ayref and Azref in Figure 5.22 and

Figure 5.23. FPIG misses the target most probably due to the high oscillation in Ayref and Azref.

Surprisingly in simulation results for target two with variation four, both FPIG and FPIDG hit the target. It is surprising for FPIG to hit this variation since it accelerates faster than the previous one and FPIG missed the previous variation. FPIDG gives the best results in all of the performance parameters. PNG, FPG, and FPDG saturate in Ayref and Azref in Figure 5.28 and Figure 5.29. The reason for FPIG to hit this time can be understood from Ayref and Azref behavior. In this variation FPIG does not make oscillations in the terminal phase of the flight.

All of the guidance systems hit the target three with variation one. PNG makes the most precise hit and FPIDG makes the hit in minimum TOF. FPIG and FPIDG make more control effort on this target. That is why this target is making sine wave, and the fuzzy guidance systems are still trying to increase the control output to get to in front of the target. So they could hit the target by applying a greater control effort.

All of the fuzzy guidance systems miss the target three with variation two. Only PNG could hit this target. This situation can be counted as a hit/miss by chance. That can be explained by the performance results. The fuzzy logic guidance systems reach the target at an earlier time, when the target is just about to turn the peak of the sine wave. When target turns the peak of the sine wave, fuzzy logic guidance systems can not take that much turn to get to the target. But PNG reaches

the target at a later time when the target has already made the turn of the sine wave peak. And also PNG did not make much overshoots in the trajectory to get in front of the target. So when target turns the peak it comes just in front of the PNG missile. This explains the hit/miss by chance.

In the simulation results for the target four, FPIG and FPIDG hit the target. The reason for the other guidance methods to miss the target can be understood by Figure 5.46 and Figure 5.47. PNG, FPG and FPDG seem to saturate in Ayref in the last few ten milliseconds of the flight, but they saturate in Azref for about one second, which tells that the guidance systems missed the target mostly in X-Z plane.

In the simulation results for target five, FPID and FPIDG hit the target. The reason for the other guidance methods to miss the target can be understood by Figure 5.52 and Figure 5.53. Ayref seems to be normal for all guidance methods, but PNG, FPG and FPDG are saturated in Azref most of the time in the flight. That is why they miss the target.

By the results of the simulations it can be concluded that all of the fuzzy guidance systems afford to increase the output acceleration to get to the front of the target, which is the design objective of the fuzzy logic guidance systems.

Fuzzy logic guidance systems are considerably effective for accelerating and high speed targets. That is due to the design objective of the fuzzy logic guidance systems.

FPG is the fuzzy logic guidance system which is the most closer to PNG. Addition of $\ddot{\lambda}$ input to FPG, which results in FPDG, does not make much contribution to FPG. The results for both of them are very close to each other during the simulations. But addition of τ input to FPG, which results in FPIG, makes considerable contribution to the guidance law. Addition of $\ddot{\lambda}$ to FPIG, which results in FPIDG, generally does not make considerable contribution to the guidance law. But in the results of the simulation for target two in all variations, it is seen more clearly that addition of $\ddot{\lambda}$ input eliminates the oscillatory behavior of the output in the terminal phase of the flight. Thus, FPIDG can be told to be the best guidance system considered in this study.

REFERENCES

[1] KrishnaKumar, K., Gonsalves, P., Satyadas, A., and Zacharias, G., "Hybrid Fuzzy Logic Controller Synthesis via Pilot Modelling", Journal of Guidance, Control and Dynamics, Vol. 18, No. 5, September-October 1995

[2] Tseng, H. C. and Chi, C. W., "Aircraft Antilock Brake System with Neural Networks and Fuzzy Logic", Journal of Guidance, Control and Dynamics, Vol. 18, No. 5, September-October 1995

[3] Geng, Z. J. and McCullough, C. L., "Missile Control Using Fuzzy Cerebellar Model Arithmetic Computer Neural Networks", Journal of Guidance, Control and Dynamics, Vol. 20, No. 3, May-June 1997

[4] Mishra, K., Sarma, I. G., and Swamy, K. N., "Performance Evaluation of Two Fuzzy Logic Based Homing Guidance Schemes", Journal of Guidance, Control and Dynamics, Vol. 17, No. 6, November-December 1994

[5] Rahbar, N. and Menhaj, M. B., "Fuzzy Logic Based Closed Loop Optimal Law for Homing Missiles Guidance", Journal of Guidance, Control and Dynamics, Vol. 20, No. 3, May-June 2000

[6] Lin, C. L. and Chen, Y. Y., “Design of Fuzzy Logic Guidance Law Against High Speed Target”, Journal of Guidance, Control and Dynamics, Vol. 23, No. 1, January-February 2000

[7] Fernandez-Montesinos, M. A., Schram, G., Vingerhoeds, R. A., Verbruggen, H. B., and Mulder, J. A., “Windshear Recovery Using Fuzzy Logic Guidance and Control”, Journal of Guidance, Control and Dynamics, Vol. 22, No. 1, January-February 1999

[8] Lin, C. L. and Su, H. W., “Adaptive Fuzzy Gain Scheduling in Guidance System Design”, Journal of Guidance, Control and Dynamics, Vol. 24, No. 4, July-August 2001

[9] Lin, C. M. and Hsu, C. F., “Guidance Law Design by Adaptive Fuzzy Sliding Mode Control”, Journal of Guidance, Control and Dynamics, Vol. 25, No. 2, March-April 2002

[10] Passino, K. M. and Yurkovich, S., “Fuzzy Control”, Addison Wesley Longman Inc., 1998

[11] Nesline, F. W. and Zarchan, P., “A New Look at Classical versus Modern Homing Missile Guidance”, AIAA Guidance and Control Conference Proceedings, pp. 230-242, 1979

[12] Shukla, U. S. and Mahapatra, P. R., “The Proportional Navigation Dilemma – Pure or True?”, IEEE Transactions on Aerospace and Electronic Systems Vol. 26 No. 2, pp. 382-392, March 1990

[13] Shukla, U. S. and Mahapatra, P. R., “Optimization of Biased Proportional Navigation”, IEEE Transactions on Aerospace and Electronic Systems Vol. AES-25 No. 1, pp. 382-392, January 1989

[14] Zarchan, P., “Tactical and Strategic Missile Guidance”, Progress in Astronautics and Aeronautics Vol. 176, AIAA Tactical Missile Series, 1997

[15] Lin, C. F., “Modern Navigation Guidance, and Control Processing”, Prentice Hall Series in Advanced Navigation, Guidance, and Control, and Their Applications, Prentice-Hall Inc. A Simon & Schuster Company Englewood Cliffs, New Jersey, 1991

[16] Ateşoğlu, Ö., “Different Autopilot Designs and Their Performance Comparison for Guided Missiles”, M.S. Thesis, Aeronautical Engineering Department, METU, Ankara, December 1996

[17] McLean, D., “Automatic Flight Control Systems”, Prentice Hall International (UK) Ltd., 1990

[18] Blake, W.B., “Missile DATCOM User’s Manual”, AFRL-VA-WP-TR-1998-3009, Wright Patterson Air Force Base, Ohio USA, February 1997

APPENDIX A

PROPERTIES OF THE MISSILE

A.1 Missile Geometry

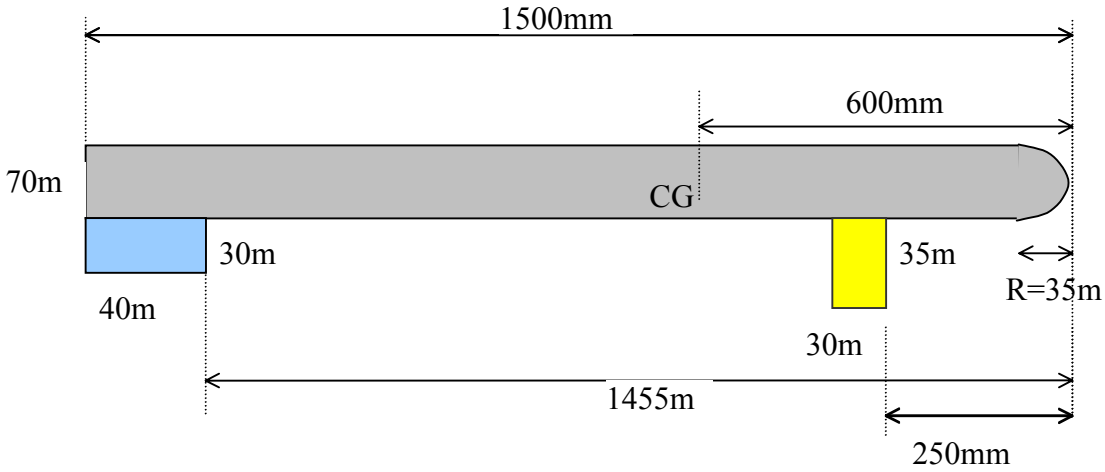

CANARD FIN CROSS-SECTION

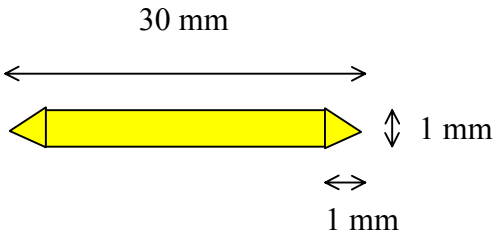

TAIL FIN CROSS-SECTION

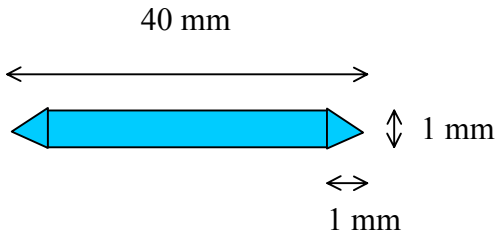

There are four canard and tail fins distributed uniformly at angles 0º, 90º, 180º, and 270º.

A.2 Physical Properties of Missile

Mass = 9 kg

I_{yy} = 1.7 kg.m^2

S_{ref} = 0.0038465 m^2

L_{ref} = 0.07 m

A.3 Velocity Profile

The effects of the forces caused by axial thrust and axial drag are assumed to cause the axial velocity profile below,

Table A.1 Missile velocity profile

t (s.)	0	10	20
U (m/s)	800	700	400

A.4 Saturation Limits of the Missile

Missile saturation limits on some control parameters. These are the canard deflections and the acceleration command outputs of the guidance systems. The saturation limits on the canard deflection represent a physical limit on the turn angle of the canards. The saturation limits on the acceleration command outputs of the guidance system are required by the structural acceleration limits that the missile may experience.

Saturation limits for the canard deflections are, ±15°.

Saturation limits for the acceleration command outputs of the guidance systems are ±150 m/s^2.

APPENDIX B

TARGET MODELS

B.1 Target One

Target one is a target moving horizontally with a constant speed, which is also known as a classical proportional navigation target. The position of target one can be evaluated as,

$$X_t = 5000 \tag{B.1}$$

$$Y_t = -300t \tag{B.2}$$

$$Z_t = -5000 \tag{B.3}$$

B.2 Target Two

Target two is a target accelerating parabolically in XY plane. The position of the target can be evaluated as,

$$X_t = 5000 - \text{vart2}.t^2 \tag{B.4}$$

$$Y_t = -100t \quad \text{(B.5)}$$

$$Z_t = -5000 \quad \text{(B.6)}$$

vart2 is a variation parameter used to change the acceleration of the target. Its value changes as below,

Table B.1 Variations of target two

Variation:	variation one	variation two	variation three	variation four
vart2	-20	-25	-30	-35

B.3 Target Three

Target three is a target making a constant speed sine wave in the XY plane. The position of the target can be evaluated as,

$$X_t = 5000 + \text{vart3}*200t \quad \text{(B.7)}$$

$$Y_t = \int 100 \sin\left(\frac{\pi}{4} t\right) dt \quad \text{(B.8)}$$

$$Z_t = -5000 \quad \text{(B.9)}$$

Variation one of vart3 = 1 and variation two of vart3 = –1

B.4 Target Four

Target four is a target maneuvering towards the missile at a point that missile is close enough. The parameters ka and an change with time as in the given table.

Table B.2 Parameter changes for target four

t (s.)	0	5	5.1	7.8	7.9	20
ka	–0.2	–0.2	0.4	0.4	0	0
an	–50	–50	0	0	–50	–50

$$\text{utarg} = \text{ka} \cdot \left(300 + \int \text{ka}(t)dt\right) \tag{B.10}$$

where utarg is a saturated value outside the range [–300 300].

$$X_t = \text{ka} \cdot \left(300 + \int \text{ka}(t)dt\right) \cdot \sin\left(\int \text{an}(t) \cdot \text{utarg}(t)dt\right) \tag{B.11}$$

$$Y_t = \text{ka} \cdot \left(300 + \int \text{ka}(t)dt\right) \cdot \cos\left(\int \text{an}(t) \cdot \text{utarg}(t)dt\right) \tag{B.12}$$

$$Z_t = -5000 \tag{B.13}$$

B.5 Target Five

Target five is a ballistic missile. The target represents the last portion of the trajectory of the ballistic missile threat.

Table B.3 Z axes velocity profile for target five

t (s.)	0	1	2	3	4	5	8
$\dot{Z}_t$	500	550	580	600	620	630	650

$$X_t = 5000 - 100t \quad \text{(B.14)}$$

$$Y_t = -100t \quad \text{(B.15)}$$

$$Z_t = -5000 + \int \dot{Z}_t(t)dt \quad \text{(B.16)}$$

APPENDIX C

SEEKER BOX

Seeker is the component of the missile which detects target and supplies information on target.

The seeker box used in the simulation is not an actual seeker model but is a series of functions that supply the information that the seeker would supply during the flight of the missile. The information supplied by the seeker box are τ, $\dot{\lambda}$, and $\ddot{\lambda}$ separately for pitch and yaw plane. These information are calculated as,

$$\vec{\dot{\lambda}} = \frac{\vec{R} \times \dot{\vec{R}}}{\left|\vec{R}\right|^2} \tag{C.1}$$

$$\ddot{\lambda}(t) = \frac{d\dot{\lambda}(t)}{dt} \tag{C.2}$$

$$\tau = \sigma_T - \sigma_M \tag{C.3}$$

where τ, σ_T and σ_M are the angles explained in Figure 4.2. $\vec{R}$ is the vector formed by connecting the line MT in Figure 4.2.